Heliyon 7 (2021) e07408

Contents lists available at ScienceDirect

Heliyon

journal homepage: www.cell.com/heliyon

Review article

Evolution of anodised titanium for implant applications

J. Alipal [a], T.C. Lee [b,*], P. Koshy [c], H.Z. Abdullah [d], M.I. Idris [d]

[a] Department of Chemical Engineering Technology, Faculty of Engineering Technology, Universiti Tun Hussein Onn Malaysia (UTHM), Pagoh Higher Education Hub, 84600 Muar, Johor, Malaysia
[b] Department of Production and Operation Management, Faculty of Technology Management and Business, UTHM Parit Raja 86400, Batu Pahat, Johor, Malaysia
[c] School of Materials Science and Engineering, UNSW Sydney, Sydney, NSW 2052, Australia
[d] Department of Manufacturing Engineering, Faculty of Mechanical and Manufacturing Engineering, UTHM Parit Raja 86400, Batu Pahat, Johor, Malaysia

ARTICLE INFO

Keywords:
Anodised titanium
Anodic oxidation
Anodic layer
Titanium nanotube
Implant coating
Surface modification
Anodization
TiO_2
Coating template stencil

ABSTRACT

Anodised titanium has a long history as a coating structure for implants due to its bioactive and ossified surface, which promotes rapid bone integration. In response to the growing literature on anodised titanium, this article is the first to revisit the evolution of anodised titanium as an implant coating. The review reports the process and mechanisms for the engineering of distinctive anodised titanium structures, the significant factors influencing the mechanisms of its formation, bioactivity, as well as recent pre- and post-surface treatments proposed to improve the performance of anodised titanium. The review then broadens the discussion to include future functional trends of anodised titanium, ranging from the provision of higher surface energy interactions in the design of biocomposite coatings (template stencil interface for mechanical interlock) to techniques for measuring the bone-to-implant contact (BIC), each with their own challenges. Overall, this paper provides up-to-date information on the impacts of the structure and function of anodised titanium as an implant coating *in vitro* and *in/ex vivo* tests, as well as the four key future challenges that are important for its clinical translations, namely (i) techniques to enhance the mechanical stability and (ii) testing techniques to measure the mechanical stability of anodised titanium, (iii) real-time/*in-situ* detection methods for surface reactions, and (iv) cost-effectiveness for anodised titanium and its safety as a bone implant coating.

1. Introduction

In the 1950s, Brånemark discovered that titanium could permanently incorporate with bone and introduced the term "osseointegration", which describes the stable fixation of titanium to bone tissues [1, 2]. Since then, numerous studies have been conducted to obtain a better understanding of the benefits of osseointegration in implants [3, 4]. In most of their reported findings, in order to guarantee that an implant is well integrated into the body's bone-like structures over a long period of time, it surface must be bioactive [5, 6]. Thus, the porous, rough and crystalline surface of anodised titanium with higher surface energy, hydrophilicity, and crystallinity has been recognised as possessing the ideal bioactive coating properties for osseointegration of implants [7, 8].

A passive thin film of titanium dioxide (TiO_2) occurs naturally on the surface of a titanium, with a thickness of ~2–5 nm in atmospheric conditions. This passive layer naturally protects the bulk titanium metal from corrosion [9]. Titania (TiO_2) exists as three crystallographic phases namely, anatase, brookite, and rutile. Among these phases, rutile is the most common and stable form, and in the industry, only rutile and anatase are manufactured on a large scale. Both anatase and brookite structure are based on cubic packing of oxygen atoms with octahedral coordination. On the other hand, rutile structure is based on a slightly distorted hexagonal close-packing of oxygen with the titanium atoms occupying half of the octahedral interstices [10]. Moreover, anatase and rutile exhibit negative surface charge in physiological solutions. These materials are biocompatible, corrosion-resistant and show good photocatalytic performance [11]. Owing to these properties, a combination of both structures has been widely used in biomedical applications [12, 13, 14, 15].

Commercially pure titanium (cp-Ti) and Ti-6Al-4V alloys are the most prominent titanium alloys used for biomedical applications [4, 16]. These materials are widely used due to their high Young's modulus (compared to human bone [15]), eminent biocompatibility, machinability, formability, compatibility, corrosion, and crack resistance, as well as their remarkable bending and fatigue strength [17, 18]. These properties make titanium and its alloys ideal for bone and joint or

* Corresponding author.
E-mail address: tclee@uthm.edu.my (T.C. Lee).

https://doi.org/10.1016/j.heliyon.2021.e07408
Received 30 November 2020; Received in revised form 15 April 2021; Accepted 23 June 2021

cochlear replacements, orthodontic surgery screw parts, tooth fixation dental implants, artificial heart valves, and surgical instruments [19, 20].

However, owing to its bio-inertness, insignificant bone apposition of titanium occurs after implantation [21, 22, 23]. This apposition response results in major clinical issues, such as high rate of implant failure [24, 25] and bacterial infections [26, 27, 28], which then requires some extra systemic treatments [29]. Titanium and its alloy also have low hardness, wear and abrasion resistance. These properties can cause a reduction in the implant service life [30]. Therefore, to overcome the drawbacks, different surface coating methods have been trialled including sol-gel [31], plasma spraying [32], biomimetic coating [18], gel oxidation [33], chemical vapour deposition [34], and anodic oxidation [35]. These methods have produced coatings with excellent physicochemical and mechanical properties and importantly created a bioactive surface on titanium substrates. Among these surface modification techniques, anodic oxidation (AO) has earned substantial attention due to its simplicity, cost-effectiveness, and high clinical success rates [4].

Work of anodic oxidation of titanium started in the 1950s [36]. Anodic oxidation is an electrochemical method used to oxidise the titanium substrates into forming ceramic TiO_2 layers of thicknesses varying from hundreds of nanometres to hundreds of micrometres [37, 38]. In the electrolytic oxidation process, tailoring the electrochemical parameters such as applied voltage, electrolyte composition and concentration, and current density will drive the formation of the ceramic TiO_2 layer (anodised titanium) with distinctive properties [39, 40]. In some cases, calcium phosphate (CaP) containing compounds and titanate compounds could be incorporated or doped on the titanium surface when the substrate is anodised in CaP containing electrolytes [40, 41, 42, 43, 44, 45]. At present, titanium-based devices doped with CaP compounds have been applied clinically for dental and orthopaedic implants [3, 4], for instance, in intramedullary nails and rods, bone plates and screws, spine cages, and spinal surgery [20].

In addition, recently the fabrication of anodised titanium topography has focussed on the growth of self-ordered nanotubes (TNTs) [46, 47, 48, 49, 50], which has allowed their use as a structure with good osseointegration capabilities [51, 52, 53] to drug nanocontainers for localised therapeutics [46, 47, 54, 55]. Such diverse possibilities for the use of anodised titanium as implant coating material has motivated this current review. The review focusses on the following key aspects: (i) emerging trends in the fabrication of anodised titanium, (ii) mechanism for the formation of anodic oxide layers (anodised TiO_2), (iii) factors affecting the formation of the layers, (iv) recent surface treatments to enhance the coating performances, (v) current challenges of anodised titanium as bone implant coating as well as its applications. In relation to its applications, this review paper also emphasises that the anodised titanium has recently been used as a template stencil for other biomaterial elements to be incorporated such that it forms a biocomposite surface (based on mechanical interlock mechanism between material interfaces) either in micro- and/or nano-structured forms [56, 57, 58, 59, 60, 61].

2. Anodic oxidation

In general, anodised titanium is an oxide coating engineered on titanium surface using a surface modification technique (i.e., anodic oxidation). This surface modification technique is an *in-situ* electrochemical method for depositing an oxide layer on the anode surface of a metal substrate by using an electrical field to aid the ionisation of elements in the aqueous electrolyte and their diffusion to the metal [17]. The deposited oxide (anodic layer) has been produced by the oxidation of the metal base, and varies in thickness from tenth of nanometres to hundreds of micrometres depending on the parameters used in the anodic oxidation cell (AO cell) and the processing parameters. The common setup for an AO cell consists of anode, cathode, electrolyte bath, power supply, magnetic stirring bar, thermometer, and cooling system as shown in Figure 1 [62]. The anodisation is typically combined with essential pre-processing such as acid activation, polishing, alkaline cleaning, electrolyte formulation and sample drying. Generally, nitric acid, hydrofluoric acid, and acetone are all used for polishing, alkaline cleaning, and acid activation. One of the ultimate functions of these processes is to remove the native oxide layer and contaminants that are present on the titanium substrate when it was exposed to air at room temperature [63, 64, 65, 66, 67, 68].

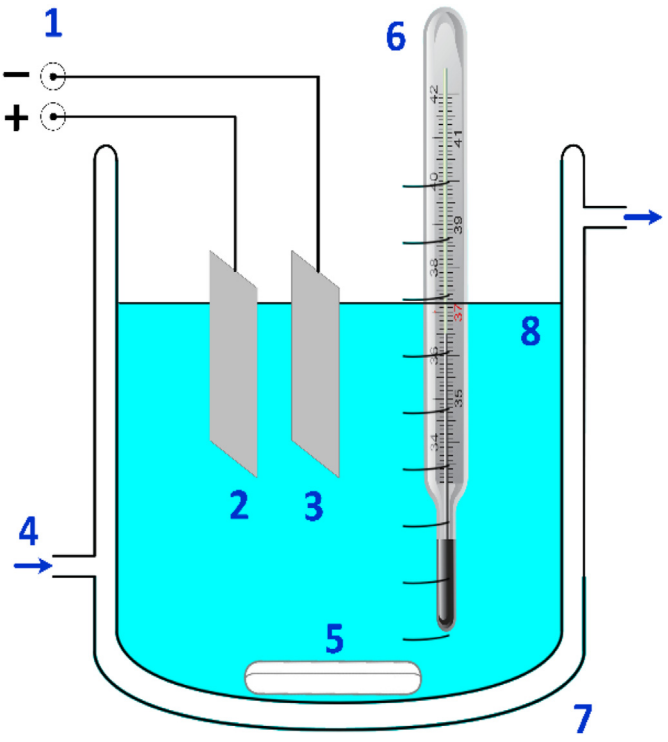

Figure 1. Schematic diagram of anodic oxidation, AO electrochemical cell: (1) power supply, (2) anode (3) cathode (4) cooling water (5) magnetic stirrer bar (6) thermometer, (7) jacketed beaker, (8) electrolyte (redrawn with permission from [62]).

Over the last decades, anodic oxidation has become popular in the surface modification of titanium for biomedical applications due to its significant advantages, i.e. (i) simple processing method and cost-effectiveness [2, 69, 70], (ii) capability to improve coating adhesion, interfacial bonding and corrosion resistance with easily tuneable properties [71, 72, 73, 74, 75, 76, 78, 79], (iii) as well as enhanced mechanical compatibility of the coating via the creation of porous structure with excellent potential for cell colonisation [17, 35, 80, 81]. The anodising variables that influence the characteristics of the oxide layer are: (i) process parameters i.e. applied voltage, current density, anodising time, ultrasonic and stirring effect, bath temperature, types and concentration of electrolytes; (ii) alloying elements of titanium substrate; (iii) pre- and/or post-treatment such as acid/alkaline treatment [45, 82], hydrothermal [83, 84, 85], heat [86, 87, 88], ultraviolet irradiation or photocatalytic [18, 87], ultrasonic [50, 89], microwave [44, 90] also two-step oxidation [91, 93].

2.1. Types of anodic oxidation

Anodic oxidation (AO) can be categorised into two types of processes: galvanostatic and potentiostatic [81]. The differences between the two processes are as follows:

- Potentiostatic process [94]: The anodic oxidation is carried out at constant voltage while the current changes.
- Galvanostatic process [95]: The anodic oxidation is carried out at constant current while the voltage changes.

At low applied voltage (lower than the dielectric breakdown limit), the current-voltage characteristics of the power supplied vary according to the Ohm's law. Hence, a thin and compact oxide layer is produced. At this stage, the anodic oxidation is carried out in a potentiostatic process [62]. Meanwhile, visible sparking, cracking noise, gas evolution, localised melting and voltage oscillations occur if the voltage is higher than the dielectric breakdown limit, and this stage of reactions is found in the galvanostatic process. As a result, oxide layers that are thick, less uniform, more porous, slightly cracked, and of complex are produced. This type of anodic oxidation can be labelled in different manners as micro-arc oxidation (MAO) [90], anodic spark deposition (ASD) [96], plasma electrolytic oxidation (PEO) [97] or plasma electrolytic saturation (PES) [95], microplasma oxidation (MPO) [98], micro-arc discharge oxidation (MDO) [99], or anodic plasma-chemical process (APC) [100].

Moreover, in galvanostatic AO, the applied voltage usually in the range of 150 V–1000 V, depending on several parameters, including electrolyte type and concentration, pH, and temperature. In the anodic and cathodic half circle, the voltage is usually in the range of 150–1000 V and 0–100 V, respectively [17]. Electrical arcing is commonly associated with galvanostatic AO; Arcing is a luminous discharge of electrical current crossing the gap between two electrodes. The arcing can only be achieved by the use of sufficiently high current, temperature, and pressure (from the applied electrical fields) during anodic oxidation. For instance, the local temperature and pressure in the discharge channel during MAO can increase up to 10,000 K and several hundred bars, respectively. Usually, the coating produced via MAO consists of three layers: (i) a porous and thick outer layer with numerous cavities and cracks, (ii) an inner layer which acts as a barrier, and (iii) a thin interlayer between the dense layer and titanium substrate [17]. The cracks are observed owing to the thermal stress gradients established during and after arcing [62]. Ultimately, high quality coatings with good adhesive strength and wear resistance of the oxide layer can be feasibly produced by MAO [101].

2.2. Formation of the TiO_2 layer

As the redox process take place in an AO cell (Figure 1) in either acidic, alkaline, or CaP-based electrolytes, the oxidation occurs on the substrate functioning as the anode, whereas reduction takes place at the cathode. Eqs. (1), (2), (3), and (4) show the main reactions leading to the oxidation at the anode surface [17, 81];

At the Ti/TiO_2 interface:

$$Ti \rightarrow Ti^{2+} + 2e^{-} \quad (1)$$

At the TiO_2/electrolyte interface:

$$2H_2O \rightarrow 2O^{2-} + 4H^{+}$$
(oxygen ions react with titanium to form TiO_2) (2)

$$2H_2O \rightarrow O_2\ (gas) + 4H^{+} + 4e^{-}$$
(oxygen gas evolves and is generally lost to the atmosphere or adheres to the electrode-electrolyte interface) (3)

Thus, at both the interfaces:

$$Ti^{2+} + 2O^{2-} \rightarrow TiO_2 + 2e^{-} \quad (4)$$

On the other hand, at high voltage, the anodised TiO_2 layer is formed due to the inward migration of O^{2-} ions from the electrolyte to the metal/film interface and the outward migration of Ti^{4+} ions from metal substrate to film/electrolyte interface. Delplancke et al. [102] explained that the growth of an anodic film on titanium surface occurs through the following steps:

natural continuous formation of Ti-oxide film → growth of the TiO_2 crystals → possible formation of a discontinuous film; thickening and coalescence of the TiO_2 film → oxygen evolution → dissolutions of the film in electrolyte.

The growth of the final TiO_2 coating by anodic oxidation shows a linear relationship with the applied voltage, and the correlation factor is known as the growth constant [103]. The relationship of final TiO_2 thickness and applied voltage can be represented by Eq. (5) [17, 81].

$$d = \alpha U \quad (5)$$

where,

d = Final oxide thickness
α = A constant within the range 1–3 nm/V, but most often around 2 nm/V
U = Applied voltage

The growth rate is strongly dependent on the process parameters of anodic oxidation. However, this relationship is invalid if the oxide layer formation increases to a thickness value that causes the dielectric breakdown limit of the TiO_2, depending on the process conditions of the anodic oxidation (discussed in section 3). This is due to the fact that the TiO_2 layers will no longer be resistive enough when the applied voltage reaches the dielectric breakdown limit [17].

On the other hand, the formation of TiO_2 nanotubes (TNTs) is slightly different from the above anodic oxidation. In general, the formation of TNTs starts when Ti is oxidised to Ti^{4+} and forms a compact TiO_2 layer through the reactions shown by Eqs. (6) and (7). Further, the fluoride ions chemically dissolve TiO_2 or react with Ti^{4+} with at the oxide-electrolyte interface and lead to the formation of water-soluble $[TiF_6]^{2-}$ (Eqs. (8) and (9)). As a result, the compact TiO_2 layer transforms to TiO_2 nanotubes [49, 104, 105].

$$Ti \rightarrow Ti^{4+} + 4e^{-} \quad (6)$$

$$Ti + 2H_2O \rightarrow TiO_2 + 4H^{+} + 4e^{-} \quad (7)$$

$$TiO_2 + 6HF \rightarrow [TiF_6]^{2-} + 2H_2O + 2H^{+} \quad (8)$$

$$Ti^{4+} + 6F^{-} \rightarrow [TiF_6]^{2-} \quad (9)$$

Moreover, Allam and Grimes [105] described the possible formation mechanism of TNTs produced by anodising in chloride based electrolytes (Eqs. (10), (11), and (12)).

$$TiO_2 + H^{+} + Cl^{-} \rightarrow TiO(OH)Cl \quad (10)$$

$$TiO(OH)Cl + 3H^{+} + Cl^{-} \rightarrow TiCl_2^{2+} + 2H_2O \quad (11)$$

$$TiCl_2^{2+} + 4Cl^{-} \rightarrow TiCl_6^{2-} \quad (12)$$

2.2.1. Micropore formation mechanism

The formation of micropores in the anodised layers can be described using avalanche theory [38, 76]. Figure 2 illustrates the growth model of micropores produced by MAO. The newly-formed oxide layer on the anode keeps growing until the dielectric breakdown limit is reached during anodic oxidation (Figure 2A). At this stage, the local temperature is increased by over 1000°-3000 °C and this leads to localised melting on the anode surface. Compressive stress of oxide layer increases significantly during the transformation from amorphous oxide layer to crystalline oxide layer. Breakdown of the barrier oxide layer occurs and this results in the formation of pores on the oxide layer (Figure 2B). The potential drop at the weak points exceeds the dielectric limit and causes sparking to occur. However, a new oxide layer immediately covers the areas where electrical breakdown occurred and this process is called repassivation (Figure 2C). The process continues with the formation of small pores on the oxide layer due to the breakdown occurring again inside the repassivated regions (Figures 2D and 2E) [106]. The produced oxide layer is not uniform due to the existence of flaws, defects, local stress, and non-uniform oxide thickness [107].

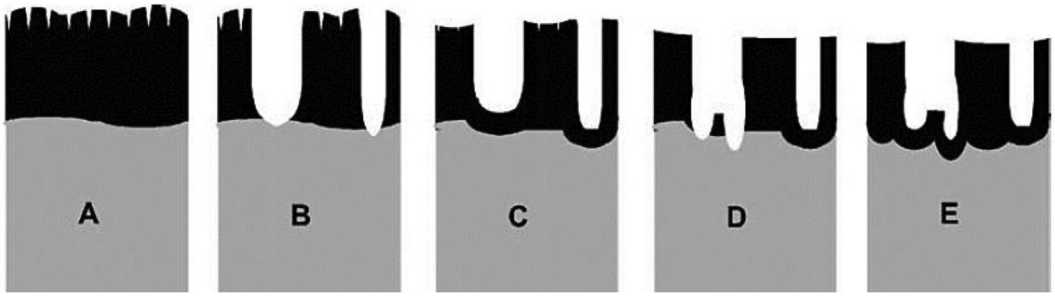

Figure 2. Formation mechanism of oxide layer under MAO: (A) oxide growth at maximum thickness, (B) crystallite (pore formation) revolution of oxide, (C) instant reassignment of the pores, (D) bursting of reassigning oxide, and (E) dissolution and second reconstitution of the formed oxide (taken with permission from [106]).

2.2.2. Nanotube formation mechanism

Unlike MAO, formation of TiO_2 nanotubes (TNTs) usually occurs under potentiostatic mode (<30 V) [94]. Figure 3 shows the growth mechanism of TiO_2 nanotubes; first, the TiO_2 layer is formed on the anode (Figure 3A). Then, fluoride ions react with newly-formed TiO_2 and form TiF_6^{2-}. As a result, irregular pits are formed on the TiO_2 layer (Figure 3B). With an increase in anodising time, the pores are uniformly distributed and orderly structured as the oxide layer (Figure 3C). The depth of the pores increases further due to the effect of electrochemical oxidation and electrochemical corrosion (Figure 3D). Lastly, the TiO_2 nanotubes are formed and length of the nanotubes do not increase any further since both electrochemical oxidation and the electrochemical corrosion are in a dynamic balanced state [108, 109].

Fabrication of TiO_2 nanotubes using fluoride based electrolyte has resulted in many problems arising from its toxicity, time required, corrosion, and environmental pollution [110]. In order to overcome these problems, extensive research has used fluoride free electrolyte to produce nanotubes TiO_2 [111, 112, 113, 114]. Rapid breakdown anodisation (RBA) has been introduced to shorten the anodising time for fabricating TiO_2 nanotubes. In RBA, titanium is transformed into TiO_2 nanotubes within few seconds after applying voltage in chloride, perchlorate, and bromide-based electrolytes. The thin layer of TiO_2 is grown over the applied voltage, which is quickly attacked by halide ions. As a result, localised pits are formed on the TiO_2 layer. Subsequently, water soluble halide ions such as $[TiCl_6]^{2-}$ are formed resulting in the formation of TiO_2 nanotubes [115]. The TiO_2 nanotube formation mechanism for fluoride free electrolyte is almost similar to fluoride-based electrolyte (Figure 3). The only differences are processing time and types of water-soluble ions involved in the process.

2.3. Colourisation in anodised titanium

Visually, anodised titanium may appear in different colours, and this phenomenon is called colourisation. The cause of different colours in anodised titanium depends on the thickness and the crystal structure of the anodic TiO_2 layers. Various colour of coatings such as blue, black, orange, green, silver, grey, brown, yellow, and purple could be easily achieved by tailoring the parameters of anodic oxidation [116]. The colour of anodised titanium can be explained by the multi beam interference theory [102]. According to the theory, interference colours are affected by the non-uniformity of the oxide layer on the titanium substrate. As illustrated in Figure 4, the reflected beams from the oxide surface and surface oxide/titanium substrate interface can produce interference colours. The colour of oxide layer will change due to the increase of oxide thickness. According to Fresnel law, constructive and destructive interference of certain wavelengths results in various colours, depending on thickness of the oxide layer [102, 117]. Apart from that, another explanation of the colour difference of the oxide layer may be ascribed to the differences in crystal structures of the anodic layer. The colour formation can be due to the interference of waves in a crystalline or partly crystalline anodic layers [118]. In general, different colours namely, orange, yellow, blue, green, brown, grey, and purple are produced by anodisation of titanium [119].

2.4. Evolution of methods for anodic oxidation

In early work on coating development via anodic oxidation, dilute acids such as sulphuric acid, acetic acid, and hydrochloric acid, bases such as sodium hydroxide and salts such as sodium sulphate were used as electrolyte to form TiO_2 coating [37]. Nanoporous or microporous compact oxide layer can be formed by using dilute acid or alkaline electrolytes [118]. Traditionally, this compact oxide surface morphology

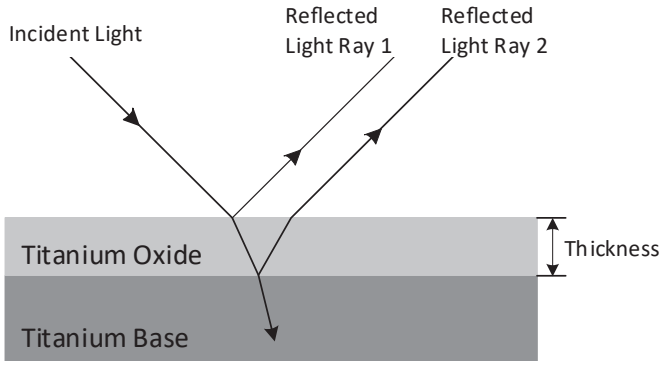

Figure 4. Multi beam interference responsible for colour of anodised titanium (redrawn with permission from [102].

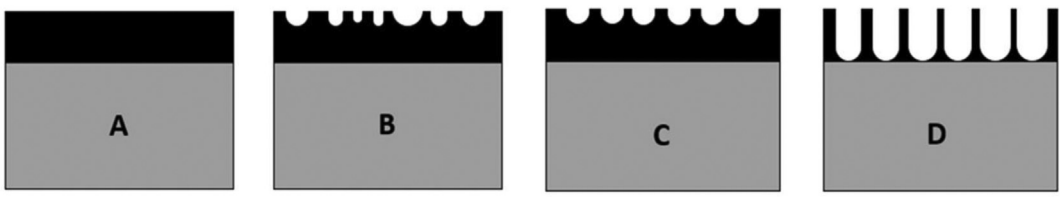

Figure 3. Formation mechanism of TiO_2 nanotubes. The reaction leading to the TNTs' synthesis in Ti (A) begins with the formation of the TiO_2 layer on the metal (B), then this oxide is dissolved with fluoride ions leading to the appearance of nanopores (C) and deepened until the nanophores form an orderly and compact layer of TNTs (D) (redrawn and adapted from [109]).

provides high energy interaction of bone-to-implant contact (BIC) [18, 120]. In 1995, Ishizawa and Ogino introduced the calcium-phosphorous (CaP) based electrolyte which is able to produce microporous TiO_2 and incorporate Ca^{2+} and PO_4^{3-} ions into the oxide layer [51]. The advantages of CaP based electrolyte lies in its ability to form a thick (1–10 μm), rough, and porous oxide layer integrated with calcium and phosphate ions, which have beneficial effects on the growth of bone tissue and enhanced anchorage of the implants to the bone [62]. The presence of CaP ions has been shown to support cell growth, nutrient circulation, and augmented BIC matrix [120].

In 1999, Zwilling et al. fabricated self-ordered TiO_2 nanotubes by anodising titanium substrates in a fluoride based electrolyte [121, 122]. In order to improve the processing time of anodic oxidation, many researchers focus on the fluoride-free electrolyte, such as perchlorate, chloride, and bromide-based electrolytes for fabricating TiO_2 nanotubes [112, 113, 114, 123, 124, 125]. The TiO_2 nanotubes (TNTs) have similar dimensions to the non-stoichiometric component of human bone nanocrystal [4, 15], thus promoting osseointegration, preventing the adhesion of bacteria on implant surface, and enabling local drug release [109]. The ability of TNTs as drug eluting reservoirs was first reported in 2006 by Ayon et al. [46]. Overall, the timeline of electrolyte evolution for anodic oxidation and the development of functionality for the oxide layer is shown schematically in Figure 5. Among other factors in brief, the type of electrolyte will significantly produce TiO_2 layers with differing characteristics, as discussed in section 3. At present, the research is focussed on CaP-based and fluoride based electrolyte [15].

Eaninwene et al. [47] is believed to be the first to suggest the need for investigating the ability of the TNTs to deliver drugs, and Ayon et al. [46] was the first to conduct the required investigation. The core purpose was to fabricate the implant surface that can overcome infection [47] and reduce inflammation [46, 47] while promoting bone ingrowth (hard tissue secretion). Ayon et al. [46] was the first to design anticoagulants, analgesics and antibiotic drugs-eluting implants via TNTs loaded with dexamethasone, while Eaninwene et al. [47] prolonged the TNT drug delivery capacity in preventing infection by coating the TNTs with a combination of dexamethasone and penicillin/streptomycin.

However, until recently, there has been insufficient work on *in vivo* or post-implant studies to verify the feasibility of the proposed mechanism and the stability impact of TNTs as drug-eluting reservoirs on clinical trials. Therefore, there are gaps in the discussion with regard to the following aspects (i) the degradation state of drug-loaded TNTs post-implantation to ensure no toxicity [126], and (ii) the long-term mechanical stability of TNT for load-bearing implants allows for bone fixation [127], are challenges that need to be ascertained through clinical trials [128]. Current progress, challenges and perspectives of TNTs as drug-eluting implants has focussed on enhancing the total dosage of drugs in the TNTs [129, 130], release kinetics during initial burst release (IBR) or the total release (TR) [126, 131] and implementation of different payloads of therapeutics for single load or co/multiple delivery [54, 126, 132, 133]. This physicochemical modification work focused on enhancing the current TNT implant properties to promoting better cell integration and antibacterial capacity to treat patients suffering from a broad range of bone diseases [127, 128, 134].

3. Factor affecting characteristics of TiO_2 layer

Anodisation parameters greatly influence the characteristics of the TiO_2 anodised layer. It is evident that variations in the surface morphologies, mineralogies, topographies, and biocompatibilities of TiO_2 anodic layer can result by tailoring the anodisation parameters. The following section will discuss the effects of the major anodisation parameters on the characteristics of anodised layer.

3.1. Critical parameters in anodisation

3.1.1. Applied voltage

The effect of applied voltage on the characteristics of TiO_2 anodic layer have been investigated. Most studies show that the surface porosity, thickness, roughness, wettability, and crystallinity increased with increase in the applied voltage. This is due to increased electrochemical reactions at higher applied voltage which caused an increase in the thickness and resistance of the oxide layer. Therefore, higher potential

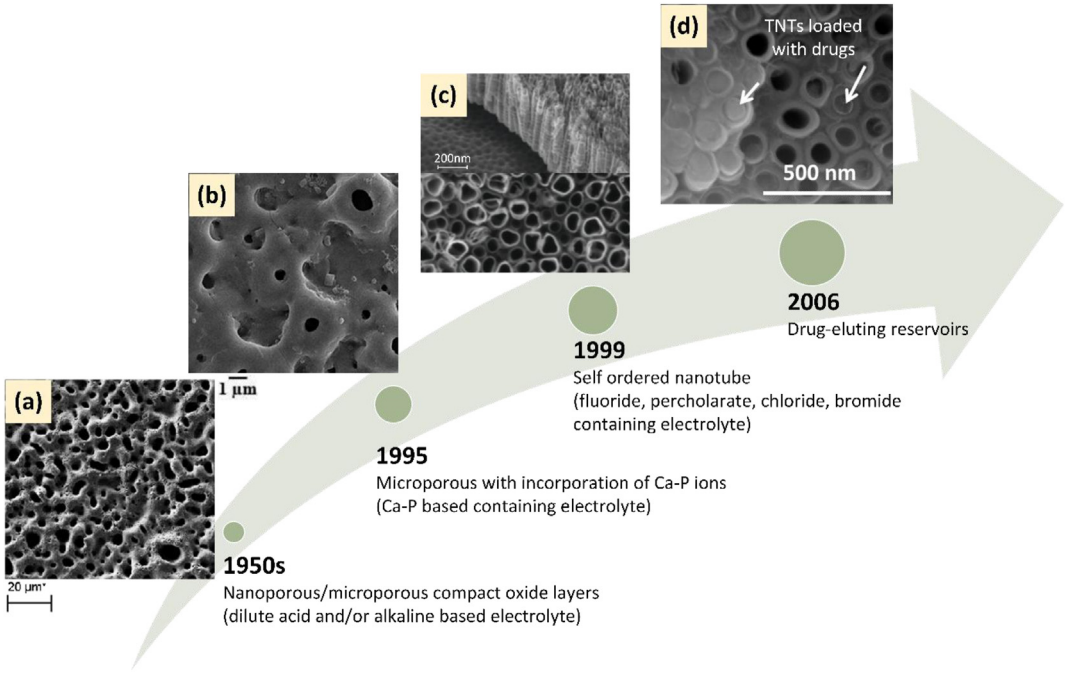

Figure 5. The evolution of (i) electrolytes for anodic oxidation (a–c), (ii) functions of the anodised titanium (a) for high energy interaction of bone-to-implant contact (BIC), (b) to promote cell ingrowth, nutrient circulation, and augmented BIC matrix, (c) to interact with bone nanocrystals and (b & c) enhanced BIC matrix of bone anchorage, and (d) as a drug-eluting reservoir. (micrographs redrawn and adapted with permission from (a) [62], (b) [116], (c) [135] (d) [136]).

energy is required to break down the dielectric layer, leading to the formation of porous surface, increased surface roughness, and improved wettability of the oxide layer [137]. The crystallinity of TiO_2 anodic layer was enhanced at higher voltages owing to the localised heating on the surface of titanium during anodisation [17] leading to melting of the surface and recrystallisation. As a result, higher crystallinity of TiO_2 (anatase and rutile), titanate compounds, and CaP compounds are generally obtained at higher applied voltages. Teng et al. [138] studied the effect of applied voltage on surface characteristics of the oxide layer. High purity titanium foils were anodised in mixtures of H_2SO_4 and H_3PO_4 at varying voltages (100 V, 140 V, 180 V, and 200 V). They found that a more porous, rougher, and higher crystallinity oxide layer was obtained at the applied voltage of 200 V and these results match observations in other studies [19, 28, 64, 66, 67, 68, 69, 70, 71, 72, 73]. In the case of fabrication of TiO_2 nanotubes, low voltages (5–60 V) were applied during anodic oxidation. Hsu et al. [147] performed anodic oxidation at 5 V and 10 V in NH_4F/NaCl electrolyte to produce TiO_2 nanotubes. The diameters of nanotubes increased from 24-30 nm for 5 V to 35–53 nm for 10 V which matches trends in other studies with similar electrolytes [75, 76, 77, 78, 79, 80, 81, 82, 83, 84, 85, 86, 87, 88, 89, 90, 91, 92, 93, 94, 95, 96]. Michalska-Domańska et al. [169] reported that the diameter of nanotubes did not grow linearly with applied voltage when fabrication was done at 30–60 V in ethanol-based electrolyte containing NH_4F and deionised water. The diameters increased linearly from 30 V (88 nm) to 50 V (124 nm) but decreased at 60 V (105 nm). Su and Zhou [170] also observed that the diameter of nanotubes decreased when the applied voltage exceeds a critical value. The diameter of pores and the thickness of the layer grow linearly in an organic electrolyte up to a potential of less than 60 V. When the potential exceeds ~60 V, the pore diameter decreases due to the restriction on the dissociation of water, and this has a detrimental effect on the morphology of the resulting pores [169].

3.1.2. Current density

The current density is defined as amount of current flow through a unit cross-sectional area. In anodic oxidation, the current density also plays a crucial role in tailoring the surface characteristics. Similar to applied voltage, higher current density leads to higher intensity of the spark discharge and results in highly crystalline, porous oxide layers. Quintero et al. [171] used prepared TiO_2 layer on titanium in a mixture of H_2SO_4 and H_3PO_4, employing current densities of 10 mA/cm^2 to 50 mA/cm^2. They found that the porosity and crystallinity increased with current density and less time was required for morphological transition when a higher current density was applied. Other researchers [41, 66, 171, 172, 173] also noticed the same trend. Laurindo et al. [174] investigated the effect of high current density (400, 700, 1000 and 1200 mA/cm^2 for a period of 15 s) on the surface characteristics of oxide layer in CaP-based electrolyte. They noticed that the porosity and rutile content were decreased significantly and cracks were observed at current density values exceeding a threshold of 1000 mA/cm^2. Abdullah et al. [175] explained that the existence of cracks was due to the thermal gradients established during and after arcing. Feschet-Chassot et al. [77] also reported that higher current density of AO in hydrofluoric acid results in greater diameter and higher hydrophilicity of TNTs. Feschet-Chassot et al. discovered that during the initial 70 s of AO, the current density decayed to a local minimum of 10 mA/cm^2 and created local TiO_2 oxide pits with a diameter of 30 nm. After the current density was increased to 12.7 mA/cm^2 at 1000 s, the diameter of the formed TNTs was 85 nm. 20 minutes after that, TNTs arrays with diameters of 100 nm and 105 nm grew to full size. This indicates that the dissolution rate of TNT is greater than its rate of development. As a result, in a steady state, the pore diameter varies regardless of the anodisation time.

3.1.3. Anodisation time

Another important key factor in modifying the surface characteristics of TiO_2 anodic layer is anodisation time. Most of studies reported that prolonged anodisation time results in higher spark discharge intensity which leads to the formation of high-surface area and high crystallinity anodic layer. However, there is also exception to this rule if the anodisation time exceeds the limit which results in unstable discharge sparks [176]. Durdu et al. [177] fabricated the TiO_2 layer in Ca-P based electrolyte at current density of 0.123 A/cm^2 for 5, 10, 20, 40, 60 and 90 min. The coating thickness and density were enhanced with increasing anodisation time. Moreover, Li et al. [178] studied the effect of anodisation time on the formation of TiO_2 nanotubes at 10 V for 10 min, 30 min, 1 h, and 4 h in 1 M NaF. The pore diameters and surface roughness increased with anodisation time. The array of nanotubes clumped together as the anodisation time increased, lowering the surface free energy due to the increased tubular length. As the oxide film thickens near the wall over time, the field intensity increases, causing the tube to widen [78, 178]. Overall, the effect of anodisation time on surface characteristics of TiO_2 anodic layer also has been intensively reported in other works [78, 144, 145, 179, 180, 181, 182, 183, 184, 185, 186, 187, 188, 189]. These studies showed when the anodising time was increased from hundreds of seconds to hundreds of minutes, which increased the thickness of the TiO_2 anodic layer as well as pore diameter, surface roughness, and hydrophilicity.

3.1.4. Ultrasonic agitation and stirring effects

Ultrasonic and magnetic stirring have been employed by researchers to facilitate the formation of highly crystalline porous oxide layer during anodisation. Neupane et al. [65] investigated the effects of ultrasonic intensity on the fabrication of TiO_2 on titanium substrate anodised in CaP-based electrolyte. Different ultrasonic intensities (180, 250 and 350 W) were applied during anodic oxidation. They found than the porosity, surface roughness and crystallinity of the oxide layer increased with ultrasonic intensity. They explained that ultrasonic waves increase the anodisation reaction rates. Moreover, these results indicated that ultrasonic condition resulted in uniform mass transfer and higher homogeneity in electrolyte compositions. As a result, more nucleation sites are produced during the anodic oxidation for the pore formation on the oxide layer. Under different intensities of UV illumination (0.8–4.7 mW/cm^2), Liu et al. [157] demonstrated that with the assistance of ultrasonic wave irradiation, highly order TiO_2 nanotubes can be produced. However, tube length of the wall thickness of TiO_2 nanotubes decreased due to the ultrasonic irradiation. To investigate the effect of stirring speed on surface characteristics of anodic layer, Lee et al. [190] prepared TiO_2 layer by anodising in Ca-P based electrolyte at different agitation speeds (300–1500 rpm). They observed the same trend as Neupane et al. [65] after applying higher agitation speeds. They explained that gas bubbles attached on the anode surface during anodic oxidation will decrease the surface area of the anode for electrochemical reactions. By applying higher agitation speeds during anodic oxidation, the attached gas bubbles could be removed which enhanced the electron transfer from the film/electrolyte interface to the metal substrate. Consequently, the surface of the anodised titanium became more porous and highly crystalline. Furthermore, Syrek et al. [191] and Liu et al. [192] concluded that when the stirring speed exceeded the critical value (300 rpm), it will result in the reduction of TiO_2 nanotube pores size and breakage of nanotubes structure. This is owing to the occurrence of turbulent flow at stirring speed more than 300 rpm which inhibits the efficient equilibration of electrochemical reaction rates.

3.1.5. Bath temperature

The bath temperature is an essential factor in determining the surface characteristics of TiO_2 anodic layer. Huang & Liu [193] prepared TiO_2 layer on pure titanium foils in 2 M NaOH in different bath temperatures and found worm-like nanostructures after anodising at 20 °C, while short nanowire-like nanostructures were formed at 40 °C and 60 °C. Increased temperature increased the photoelectrochemical property of titanium oxide and this was attributed to the presence of sub-oxide species from the heated alkaline electrolyte causing nanotube growth to slow and thus structure on the surface became more compact, and this resulted in

Table 1. Summary of surface morphology and mineralogy of anodised titanium produced from different electrolytes.

Electrolyte composition	Surface morphology (pore diameter)	XRD detected phase(s)	Ref.
Sulphuric acid	Open pores (0.1–0.5 μm)	Ti, anatase, rutile	[143, 173, 198]
Acetic acid	Pores with small white substrates (1 μm)	Ti, anatase	[199]
Phosphoric acid	Open pores (0.3–1 μm) and flowery pattern	Ti, anatase	[200, 201, 202, 203]
Hydrochloric acid	Open pores (10 μm)	Ti, anatase, rutile	[204]
Sodium sulphate	Gel-like pore structure	Ti, anatase, rutile	[72, 143, 205]
Sodium hydroxide	Nanorod, nanowire, nanoleaf, and nanoflower porous structure	Ti	[193, 206, 207]
Potassium hydroxide	Open pores (150 nm)	Ti	[207, 208]
Sulphuric acid + Phosphoric acid	Open pores (0.5–1.6 μm)	Ti, anatase, rutile	[138, 171, 209]
Potassium hydroxide + Potassium silicate	Large open pores (5–6 μm)	Ti, anatase	[210]
Chromic acid + hydrogen fluorine	Rose-like irregular pore	Ti, anatase	[142]
Sodium hydroxide + Na-tartrate + EDTA + Sodium silicate	Open pores (1 μm)	Ti, anatase, rutile	[211]
Tetraborate electrolytes; lithium, sodium and potassium tetraborate	Cortex-like structure	Ti, anatase, rutile, amorphous B_2O_3	[91]
Ca-P based electrolyte			
• calcium acetate + calcium glycerophosphate or β- glycerophosphate	Donut-shape pore (1 μm)	Ti, anatase, rutile, $Ca_2Ti_5O_{12}$, β-$Ca_2P_2O_7$, α-$Ca_3(PO_4)_2$, $CaTiO_3$	[66, 139, 142, 174, 177, 182, 192, 212, 213, 214, 215]
• calcium acetate + β- glycerophosphate + sodium hydroxide	Nanoflower-like structure	Ti, anatase, rutile, $Na_2Ti_3O_7$	[43]
• calcium acetate + β- glycerophosphate + sulphuric acid	Need-like structure	Ti, anatase, rutile, HAp	[216]
• calcium acetate + monosodiumorthophosphate	Petaling-like structure	Ti, anatase, rutile, HAp	[40]
Fluorine based electrolyte			
• NH_4F + NaCl			[148]
• H_2O + glycerol + NH_4F			[14, 217, 218, 219, 220, 221, 222]
• H_3PO_4 + NaF			[223, 224]
• NaF			[160]
• Na_2SO_4 + NaF			[158]
• H_2SO_4 + NaF			[180]
• H_3PO_4 + HF			[225]
• H_3PO_4 + NH_4F			[226]
• Glycerol + H_3PO_4 + HF	Nanotubes, TNTs	Ti	[162]
Non-fluorine based electrolyte			
• $NaClO_4$ + NaCl + H_2O + C_2H_5OH			[123]
• NaCl + H_2O + glycerol			[124]
• KBr + H_2O + glycerol			[112]
• $HClO_4$ + $NaClO_4$			[112]

higher photocurrent. Lee et al. [42] revealed that higher bath temperature will inhibit the formation of porous oxide layer since it favours the reactants during the anodic oxidation. Thereby, porous oxide layer will not be formed on the titanium anodised at higher bath temperature. Yetim [194] and Traid et al [195] also found that higher bath temperature leads to the reduction of porosity and thickness of TiO_2 anodic layer. Similarly, lower bath temperature also induces the formation of TiO_2 nanotubes with ideal packed hexagonal prisms. Lazarouk et al. [196] demonstrated that highly self-ordered TiO_2 nanotubes with a structure close to packed hexagonal prisms and smooth tubular morphology were formed at the bath temperature <0 °C. They explained that lower bath temperature results in higher gas solubility and reduces the gas bubbles which periodically block the continuity of the electrochemical process. Furthermore, Peighambardoust et al. [79] reported that higher tube wall thickness to tube diameter ratio could be achieved by anodising in low bath temperature (0 °C). This behaviour is consistent with that found by other researchers [162, 163, 197], who also noted that the decrease in bath temperature leads to formation of TiO_2 nanotubes with packed hexagonal prism structure.

3.1.6. *Type of electrolytes*

As listed in Table 1, the choice of electrolyte had an impact on the properties of the oxide layer produced, whereas Figure 6 depicts the more common AO morphologies from different electrolytes. The electrolyte could change the properties of the final coating, leading to surface structures, morphology, and mineralogy being tailored to fit different biomedical applications.

Throughout Table 1 and Figure 6, it clearly can be seen that various patterns of microporous and highly crystalline TiO_2 anodic layer could be obtained by anodising in acidic electrolyte (sulphuric acid, acetic acid, phosphoric acid, and hydrochloric acid) and neutral electrolyte (sodium sulphate). In contrast to acidic and neutral electrolyte, nanoporous amorphous TiO_2 anodic layer is formed by anodising in alkaline electrolyte (potassium hydroxide and sodium hydroxide). These contradictory surface characteristics are due to the acidic and neutral electrolyte having higher electrical conductivity compared to alkaline electrolytes. As a results, the driver force for arcing and dielectric breakdown is enhanced by the higher electrical conductivity of electrolyte, consequently increasing the oxidation rate [62].

An interesting application could result from anodising a metal in CaP-based electrolyte. For example, $Ca_2Ti_5O_{12}$, β-$Ca_2P_2O_7$, α-$Ca_3(PO_4)_2$, $CaTiO_3$, and HAp can possibly be formed by anodising titanium in Ca-P based electrolyte. The formation of Ca and CaP compounds is owing to the calcium ions and phosphate ions which are ionically contained on the oxides surface of titanium during anodic oxidation. It is believed that the Ti-OH groups which are produced during anodic oxidation induced the precipitation of Ca and Ca-P compounds by reacting with calcium and phosphate ions [41, 216]. The nanoflower sodium titanate on titanium substrate was firstly reported by Lee et al. [43] by anodising cp-Ti in mixture of calcium acetate, β-glycerophosphate, and sodium hydroxide. They claimed that NaOH promotes the dissolution of titanate precursor and results in anisotropic growth of sodium titanate. Meanwhile, TiO_2 nanotubes could be obtained through anodising in fluorine based or non-fluorine-based electrolyte. Fluorine based electrolytes are commonly used to achieve self-organised highly ordered TiO_2 nanotubes, however, it is time consuming and non-environmental compliance. Hence, non-fluorine-based electrolytes are introduced to overcome these drawbacks. Yet to date, uniformity in sizes and lengths of TiO_2 nanotubes remains a major challenge.

3.1.7. Electrolyte concentration

The electrolyte concentration is one of the important parameters that influence the surface characteristics of the TiO_2 layer formed by anodisation. Previous research has shown that there is a positive correlation between the electrolyte concentration and surface characteristics. The increase in electrolyte concentration increases the surface porosity, thickness, roughness, and crystallinity. This is owing to the higher concentration of O_2 bubbles evolved from the reactions enhancing the arcing intensity and crystallisation of the coating [228, 229]. Alves et al. [230] investigated the effect of calcium acetate concentration on surface characteristics of anodised titanium. The concentration of calcium acetate was varied from 0.15 mol/L to 0.35 mol/L. The results showed that an increase in electrolyte concentration resulted in higher pore diameters. The pores size for 0.15 mol/L to 0.35 mol/L were 0.5–1 μm and 1.5–2 μm, respectively. Moreover, rutile TiO_2 was formed when 0.35 mol/L of calcium acetate was employed. A similar trend of results was also observed by using higher concentration of tricalcium phosphate [213], acetic acid [199], and sulphuric acid [231]. Table 2 summarises the variations in the pore sizes as seen present this study.

On the other hand, the surface characteristics of TNTs are strongly link to the concentration of the following species:

- **Fluorine:** The optimal concentration of fluorine ions required to produce highly homogeneous TiO_2 nanotubes is in the range of 0.5–1 wt % owing to the sufficiently slow etching rate. Higher concentration of fluorine ions (>1 wt%) results in fast chemical etching which will prevent the formation of nanotubes.
- **Aqueous solvent:** The pore sizes, lengths, and diameters of TiO_2 nanotubes increase with increasing amount of water owing to the

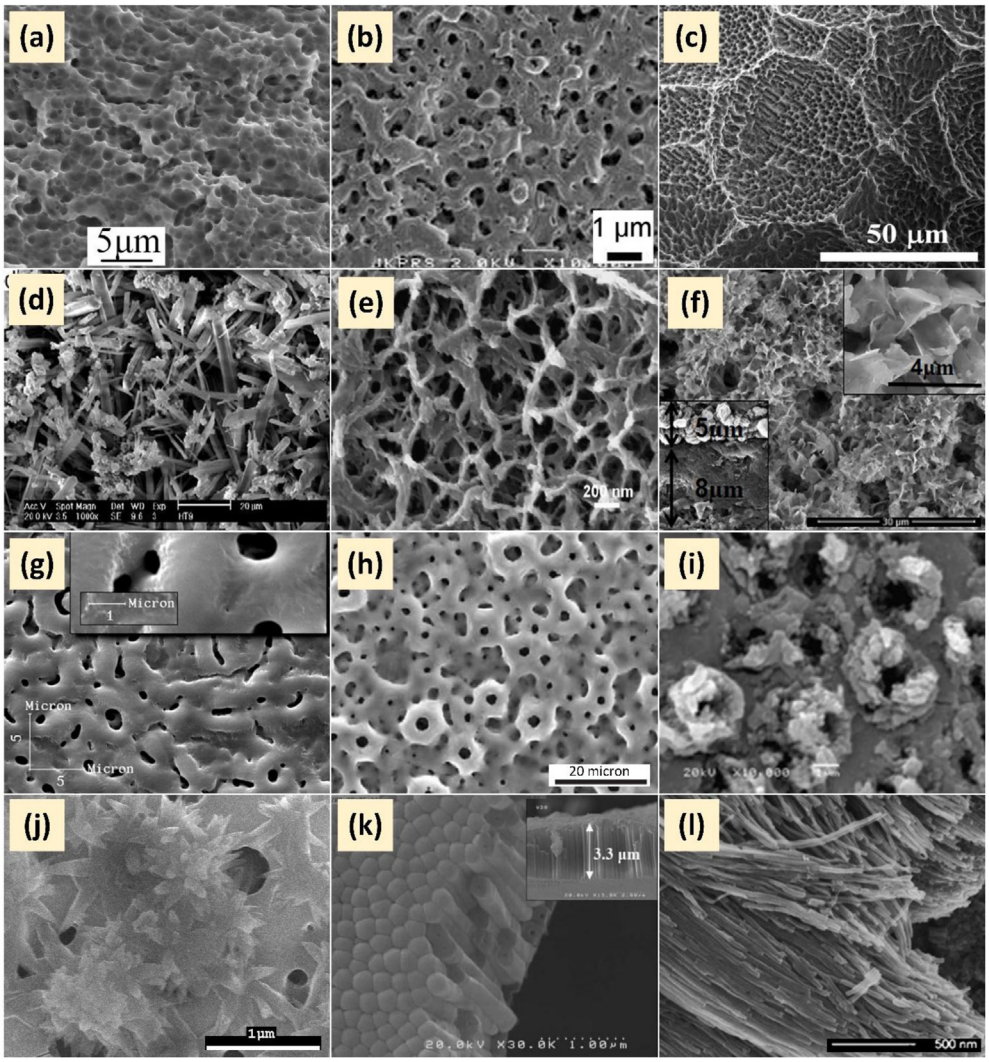

Figure 6. FESEM micrographs of different morphologies of anodised titanium produced in different type of electrolytes; (a) Ti alloy anodised in NaTESi electrolyte, containing 300 g/L sodium hydroxide, 65 g/L Na-tartrate, 30 g/L Ethylenediaminetetraacetic acid (EDTA) and 6 g/L Na_2SiO_3 [211]; (b) Ti alloy anodised in 1 M Sulphuric Acid, H_2SO_4 [173]; (c) Micro/nano-textured Ti surface anodised in electrolyte consisting of 0.95 mol dm^{-3} NaCl and 1.2 mol dm^{-3} HF [206]; (d) Needle-like structure of HAp on Ti anodised in 0.0105 mol/L $Ca(NO_3)_2$, 0.0063 mol/L $NH_4H_2PO_4$ co-deposited with TiO_2 under an influence of 200 °C hydrothermal bath [227]; (e) Network of nanowire on Ti substrate anodised in 80 °C of 4 M NaOH [193]; (f) MAO Petaling-like structure anodised in 0.2 mol/L calcium acetate ($(CH_3COO)_2Ca•H_2O$) and 0.1 mol/L monosodiumorthophosphate ($NaH_2PO_4•2H_2O$) [40]; (g) Cortex-like structure on cp-Ti surface anodised in 1.4 M H_3PO_4 electrolyte [200]; (h) Donut-shape like on Ti substrate anodised in 0.04 mol/l β-glycerophosphate disodium salt pentahydrate ($C_3H_7Na_2O_6P•5H2O$) and 0.4 mol/l calcium acetate monohydrate ($(CH_3COO)_2Ca•H_2O$) [41]; (i) Rose-like irregular pore on Ti substrate anodised in 0.5 M chromic acid solution with 1.7 wt% HF electrolyte [142]; (j) Nanoflower-like structure on cp-Ti anodised in 0.04 M β-glycerophosphate, 0.4 M calcium acetate (CA), and 1.0 M sodium hydroxide (NaOH) [43]; (k) TNT anodised in ethylene glycol + 4wt% H_3PO_4 + 0.25wt% HF [162]; (l) TNT anodised in nonfluorine based electrolyte, 50/50 water–ethylene glycol mixture containing 0.3M NaCl or 0.3 M KBr [124]. All micrographs redrawn and adapted with permission form the cited literatures.

lower diffusivity of the electrolyte [232]. Lei et al. [166] suggested that the optimal water content for formation of uniform circular TiO_2 nanotubes was 0.75 wt%. The nanotubes possess regular circular pores when the water content is low (<0.75 wt%). Lei et al. discovered that the top view of nanotube morphology is not circular but an irregular polygon at higher water concentrations (2–10 wt%). These findings suggest that adding different amounts of water to the electrolyte can influence the diffusivity and relative concentrations of the ions. As the water content in the solution increases, the ionic strength of the solution decreases, potentially resulting in lower diffusivity. As a result, an irregular hollow polygonal morphology is observed at higher water contents owing to the slow diffusion of F^{--} anions to the Ti metal from the electrolyte.

- **Non aqueous solvent:** Song et al. [233] reported that the pore sizes and diameters of TiO_2 nanotubes increase with increasing concentrations of ethylene glycol. Similar to effect of aqueous solvent, higher concentration of ethylene glycol leads to a reduction of diffusivity of electrolyte and promote the formation of tube-like structure. Moreover, they suggested that the optimal concentration of ethylene glycol in mixtures of 0.15 mol/L NH_4F and 0.11 mol/L citric acid to form uniform TiO_2 nanotubes was 60%.
- **Acidic electrolyte:** Due to its ability to form barrier type TiO_2 films, H_3PO_4 is most commonly used in conjunction with fluorine-based electrolytes. As the oxide film thickens and its resistance increases, acidic elements from the phosphoric acid film act as a barrier to the flow of ions and electrons, slowing and eventually ceasing the oxidation process. The presence of a poreless barrier layer limits the final thickness of the oxide to a few hundred nanometres, resulting in compact nanotubular structures [234]. Chen et al. [226] and Zhang et al. [76] concluded that the addition of H_3PO_4 significantly decreased the pore sizes and length while increasing the diameter of TiO_2 nanotubes. Both of them reported that the structure of nanotubes was not formed if the concentration of H_3PO_4 was $\geq$10 wt%. This is owing to the inhibiting effect of PO_4^{3-} anions on the migration of F^- anions, O^{2-} ions, and Ti^{4+} ions for the formation of nanotubes.

3.2. Alloying elements of titanium

Among the Ti-alloys commonly used for biomedical applications, Cp-Ti, Ti-6Al-4V, Ti-6Al-7Nb, Ti-13Nb-13Zr, and Ti-12Mo-6Zr have been widely used for implants and hard tissue replacement [235]. The effect of alloying elements of titanium substrates on the surface characteristics of oxide layer is well known. Ou et al. [236] compared the surface characteristics of anodised cp-Ti and Ti-30Nb-1Fe-1Hf. The crystallinity of anodic oxidation film on cp-Ti was higher although identical anodising conditions were used. The authors claimed that Nb in Ti-Nb suppresses the transition from amorphous to crystalline state during the anodic oxidation. Similar results were obtained by Roman et al. [161] who found that highly crystalline TiO_2 nanotubes were successfully coated on the cp-Ti and Ti-6Al-4V, but not on Ti-6Al-7Nb which formed an amorphous inhomogeneous nanotube structure. Furthermore, Yu et al. [211] investigated the surface characteristics and adhesive strength to epoxy of three different types of titanium alloys anodised in NaTESi electrolyte, namely TA15 (Ti–6Al–2Zr–1Mo–1V), TB8 (Ti–15Mo–3Al–2.7Nb–0.2Si), and TC4 (Ti–6Al–4V). After anodising at 20 V, on the TA15 samples, a uniform, dense oxide film formed, while on the TB8 samples, micro-protrusions were seen on a porous oxide film, and on the TC4 samples, an easily dissolved oxide film with large-scale pits were formed. At 20 V, 15 V, and 10 V, the maximal shear strengths were 15.5 MPa (TA15), 19.2 MPa (TB8), and 17.6 MPa (TC4). These differences are attributed to the variations in potential responses under constant current anodisation. Overall, Yu et al. [211] concluded that after anodisation, TiO_2 roughness increased noticeably, and this was owing to the changes in the surface features and phase composition of the films, which are alloying element dependent. The cohesive failure of TB8, a near-beta titanium alloy, confirms that it can achieve a better surface topography for adhesion.

4. Surface treatments to enhance the anodised titanium coating performances

It has been a typical practice that, prior to AO, most samples are ultrasonically cleaned with acetone to remove foreign substances from its polished surface. In conjunction, pre- or post-treatment is performed to improve the bioactivity and mechanical compatibility of the AO coating in the biological environment by providing actives sites for radical nucleation species inside the film [18], subsequently increasing or maintaining the coating integrity [237, 238, 239, 240]. The treatments are either two-step AO [93, 241] or a combination of AO with other methods such as chemical, or thermal; these approaches are implemented before and/or after the process to enhance the ability to form a biomimetic structure on the coating [69, 242]. The pros and cons of pre-/post-treatment of anodised titanium have been addressed several times [4, 15, 81, 239, 243, 244], and this current review study highlights recent pre- or post-treatment advances that enhance the anodised titanium coating performances.

In order to design a hierarchical micro and nanoporous anodised titanium substrate, Lin et al. [45] initiated pre-treatment on titanium substrate using hydrogen fluoride (HF) polarisation to enrich nano-γ-TiH dissolution on the coating layer during NaOH anodisation. As a result, in just 1 day, the MG-63 cells were able to be cultured on this coating structure resulting in enhanced cell adhesion and the presence of multiple filopodias proliferating on the hierarchical micro/nanoporous surface. This pre-treatment verified that hydrogen fluoride reacts as a catalyst to increase hydrogen reaction and/or diffusion during AO, which triggers the formation of dense nanostructures on the micro-phase of Ti hydrides on the final coating structure. Thus, this latest pre-treatment appears to be a necessary and promising procedure for further investigation [45].

Other post-treatment methods on the other hand provided final anodised coating morphologies with a mixture of nanostructured and micron-sized features resulting in an extremely rough, porous and hydrophilic surface [18, 44, 45, 50, 83, 90, 93, 245]. Meanwhile, ultraviolet-assisted post-treatments developed by Lee at al [18] are intended to resolve concerns that the Ca-P micro-arc anodised coatings does not enable rapid nucleation to precipitate bone-like apatite on the surface. This particular post procedure successfully promotes the intensive deposition of Ti-OH on the anodised surface, resulting in a continuous biomimetic layer of thicker, denser and crystalline deposition of bone-like apatites on the anodised Ca-P titania in just 7 days. These

Table 2. Pore size variations of micropores in relation to electrolyte concentrations.

Electrolyte	Low Concentrations	Pore Sizes	High Concentration	Pore Size	Ref.
$Ca_3(PO_4)_2$					
• 3 min PEO, pulsed wave 400–600 V, 50Hz, 400 A/m^2	2 and 4 g/L	~1 μm^2	6–10 g/L	some nm^2 up to 9 μm^2	[213]
CH_3COOH					
• 30 min MAO, 210 V at 200 mA	0.01 and 0.1 M	order of 1 μm Ø	0.5 M	10 μm Ø, but some were small ~1 μm Ø	[199]
H_2SO_4					
• 0.5 h MAO, 210 V at 50 mA/cm^2	0.1 M	tens of nano to micrometres	1.2 M	~50 μm	[231]

Ca-P biomimetic structures showed similar stoichiometry to hydroxyapatite (HAp) found by Song et al. [41] and have recently been engineered by He et al. [83] on top of needle-like Hap structures. He et al. conducted hydrothermal-electrochemical deposition treatment on acid-based anodised titanium for 120 min at 120 °C in an autoclave (the solvent was a mixture of 0.138 mol/L NaCl, 0.016 mol/L $K_2HPO_4{\cdot}3H_2O$ and 0.02 mol/L $CaCl_2$) [83]. The researchers created a bilayer HAp structure with hexagonal edges, which grew in a perpendicular direction to the microporous substrate. As the underlying needle-like HAp layer expanded to a certain level, a large extent of nucleation was seen to develop further into another layer at the top of the needle-like HAp, and this was identified as cotton-like HAp. Owing to the high crystal density of the needle-like HAp precipitated during the first stage of the hydrothermal process, cotton-like HAp was formed after the second process in an AO hybrid with the hydrothermal process.

More complex post-treatment procedures have been carried out by Lin et al. [44, 90]. This is intended to create a highly biocompatible heterogeneous nano-micro Ca/P coating structure. Three Ca/P-based micro-arc anodised titanium samples were prepared in XP-1500 vessels, all of which were immersed in a solution containing 50 mL double-distilled water +0.05 mM calcium hydroxide and 0.03 mM ammonium dihydrogen phosphate. The sample immersed at pH of 6.7 was labelled as MWCP, with the one immersed in pH of 9 was MWCP9 and in pH 11 was MWCP11. The samples were then irradiated with a MARS-5 8 microwave reaction system at 2.45 GHz and 400 W. The maximal temperature was set at 200 °C with a heating rate of 10 °C/min and the temperature was kept at 200 °C for 1 min. In just 7 days, the cell viabilities in the proposed samples were substantially higher than that of anodised titanium treated with hydrothermal alone. The highest alkaline phosphatase activity was expressed on the surface of MWCP11 (highest Ca and P content) after 7 days and 14 days of cultured MG63 cells compared to the other groups. This experiment showed that the rapid microwaved nano-scale surface modification on micro-arc anodised titanium was advantageous in; (i) promoting early cell differentiation via its nanostructured anatase containing calcium and phosphorus on the surface; and (ii) producing heterogenic surfaces that adsorb more proteins by positively charged divalent ion-mediated or terminal OH radical-mediated mechanisms. Such functional surfaces have shown that the microwave process can be a useful method for altering both the nanoscale topography roughness and the micropore surface potential of the anodised surface, thereby improving the differentiation of the attached osteoprogenitor stem cell.

Another complex yet worth noting is Zang et al.'s hybrid post-treatment [246] which tested *in vivo* by Li et al. [245]. The novel Fe-doped hydroxyapatite nanotubes which showed magnetic characteristics on micro-arc oxidised titanium were successfully developed for drug loading application as shown in Figure 7. The micro-arc Ca-P-based anodised titanium (Figure 7(a)) was treated hydrothermally at 110 °C for 24 h to form the top layers of hydroxyapatite (HAp) nanotubes (Figure 7(b)), which were then electrochemically treated with 0.01 M NaCl-adjusted to pH 1.9 by 1.0 M HCl, resulting a local dissolution on basal planes of HAp nanorods that transformed to nanotubes (Figure 7(c)). This hybrid post treatment produced ferromagnetic HA/TiO_2-matrix coatings in the form of tubular nanotubes on top of micropores. As the acidic electrochemical processing time lasted from 2 to 4 min, the premature nanotube would undergo corrosion from the outside to the base plane leading to collapse into nanoslices at 6 min. This magnetic HAp/TiO_2-matrix coating surface is super hydrophilic with a high adhesion strength to the substrate and improved osteoblast response in terms of adhesion, proliferation, differentiation and extracellular matrix mineralisation *in vitro* [245, 246] and new bone formation *in vivo* [245].

Anodised HAp nanotubes have demonstrated the ability to bind tightly to the Ti substrate, while being extremely hydrophilic and capable of improving the osteoblast response [246, 247, 248]. Previous studies have shown that nanorods TiO_2 could be transformed into nanotubes via hydrothermal process [245, 246]. Generally, hexagonal nanorods have positively charged Ca-rich prism-faceted planes and negatively charged OH and P-rich basal-faceted planes. Due to different charges of the crystallographic planes of nanorods, it is believed that selective dissolution on the basal planes of nanorods may form magnetic nanotubes on Ti substrate [245, 246, 249]. Based on studies performed by Peng et al. [250] and Park et al. [251], the recent study by Zhang et al. hypothesised that the Fe-doped HAp nanotubes can exhibit reasonable drug loading and release kinetic properties due to its magnetic nanotopography compared to HAp nanotubes or nanopores [246]. Li et al. [245] proves that micromagnetism provided by Fe-HAp nanotubes further enhances cell response, but up to this date their potential as drug-eluting reservoirs has never been investigated.

As for TNTs, Mansoorianfar et al. [50] have recently engineered tuneable TNTs using sonoelectrochemical process. The composition of the anodising solution is NH_4F (0.3 M), water (2 vol%) in ethylene glycol. They performed anodisation for 2 h such that after 45 min, the substrates were treated with ultrasonication for 15 min. This step is critical to be taken before the next hour of AO, as it allows TNTs to form uniformly on the final coating. Then the final coating is again treated with light ultrasonic for 30 s in ethanol to remove the damaged nanotubes and clean the surface. The first hour of AO created a low-order nanotube on the surface, where all preformed nanotubes were removed by sonication at the next hour, and the fresh surface acts as a template to promote the construction of a clean, open-hole nanostructure.

The goal of this post procedure is to design scalable TNTs that can improve the ability of the structure to elude dopant drugs. Throughout this experiment, it was found that the drug release mechanism of the constructed tuneable TNTs demonstrated four synchronised drug eluding steps: (i) lower initial burst release, (ii) controlled semi-steady release, (iii) specific release, and (iv) sustained steady release [50]. Li et al. [49] addressed the stability of TNTs in detail based on comprehensive work done by others and clogging contaminants, lower crystallisation, uneven tube density, structural degradation, and inadequate sterilisation were identified as key challenges in *in vivo* and clinical implementation of TNTs [49].

For the Ca-P doped microporous anodised titanium, current trends suggest a design of hybrid morphology such as cortex-like [91, 92], petaling-like [40], or nanoflower-like [43] structures to enhance the bioactivity and biocompatibility of the formed micro-arc anodised titanium (MAT) coatings. However, the *in vivo* or clinical complexities of these structures have not yet been identified and their mechanical stability as implant materials is still unknown. Although most Ti-based implants have a MAT biomimetic surface, the concept is still constrained by technology or clinical studies to determine whether the mechanical stability of the proposed surface is adequate for implant coating [136, 252, 253].

5. Current challenges in using TiO_2 anodic layer

The fundamental research on titanium implants has garnered many reviews, addressing the challenges to the proposed implant and its modified surfaces [3, 4, 254, 255, 257, 258]. As far as the biological response is concerned, recent findings state that the anodised titanium has an ability to reduce the risk of haemolysis [259, 260]. The anodised titanium, even in its amorphous phase [259] is capable of regulating the distance and contact osteogenesis of cells for bone healing [261]. As for its physical structure, the microporous surface of anodised titanium had the ability to retain red blood cells. The cells were observed to be attached to micropores and have the correct shape and form of acanthocytes, which were well distributed on the top of the anodised structure and within the micropores [259]. This observation shows that the anodised titanium has an effective topography for cell attachments, and consequently could provide synergetic effects to the bone reconstruction [261, 262].

Despite the promising biological response, concerns remain over its mechanical stability [240, 257, 263]. In a wide range of perspectives,

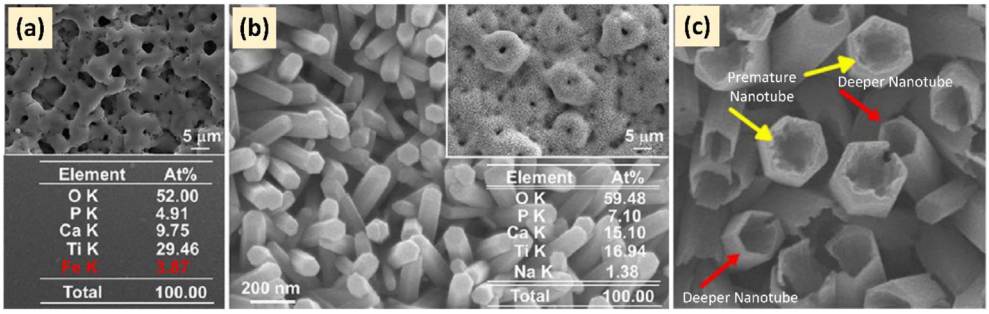

Figure 7. Magnetic HAp formed on top of micro-arc CaP-based anodised titanium (a), whereas its hydrothermal treated nanorods surface (b), transformed into magnetic nanotubes (c), using electrochemical post treatment (taken with permission from [245, 246]).

several studies have alluded to the mechanical stability of anodised titanium as bone implant coatings. Thus, in addition to the existing literature [39, 257, 263, 264], this review covers the following relevant discussion gaps; (i) techniques to enhance mechanical stability and (ii) testing methods to measure the mechanical stability of anodised titanium, (iii) real-time/*in-situ* detection methods for the surface reactions, and (iv) cost-effectiveness for anodised titanium and safety for use as a bone implant coating.

Previous studies have intensively reviewed the mechanical stability of anodised titanium as a bone implant coating [240, 263, 264] particularly the manner in which the mechanical properties of an implant differ from its surface coating. Implants, as bulk or as porous as scaffolds were structurally subjected to aseptic loosening, fatigue structure, fracture toughness, fretting fatigue strength and stress shielding effects once in contact with the implanted environment [16, 240, 257, 265]. In the case of titanium, incorporation of aluminium-vanadium, nickel, and zirconium have been traditionally the most promising alloying elements to enhance the mechanical stability of Ti-implant [257]. The consensus is that the majority of the current Ti alloy surfaces have inadequate comparative studies of their mechanical surface properties along with tissue responses. Typically, surface properties are studied only when they bear relevance to surface treatment. Therefore, there should be a wider scope of testing in order to find out how alloying constituents affect the surface mechanical stability of Ti alloys side-by-side, which could influence the material's cellular response *in vitro* or *in vivo*.

Nitinol [266, 267] is an example of a Ti alloy with advanced functionality. These nickel titanium alloys (TiNi, NiTi, or Nitinol) exhibit distinct characteristics such as increased pseudoelasticity and memory effect (superelasticity) [266]. The Young's modulus of the NiTi porous alloy, in particular, ranges from 1.8 to 14.7 GPa. These values are closest to those of human bone (17.6–31.2 GPa), and they are also the lowest among other Ti alloys [268]. NiTi's mechanical properties may reduce implant stress shielding and, as a result, postoperative complications [269]. Wong et al. [270], on the other hand, discovered a potential risk to the safety application of NiTi *in vivo* that requires further investigation. A higher surface nickel concentration may disrupt the implant-bone osseointegration process [270].

An analogous to this alloying technique, the doping and/or infusing of different types of materials in a coating structure are common practises used to induce the mechanical stability of a coating. This process is known as surface functionalisation [74, 252, 253, 254, 255, 271] or modification [4, 6, 240, 263, 264, 272]. Often in the applications, the implant surface is functionalised to enhance mechanical properties and biocompatibility. In that sense, the major advantage of Ti-based implant is that it can easily form an *in-situ* highly adherent TiO_2 film on the surface by only applying a simple anodisation treatment such as AO.

5.1. Techniques to enhance mechanical stability of anodic TiO_2 layer

One of the most important properties of a coating that defines its mechanical stability is wear and corrosion resistance. The present trend in metallic biomaterial coatings is the formation of TiO_2 nanoparticles as a surface structure to protect the implant from corrosion. For instance, to protect an easily degraded biocompatible implant from corrosion, a magnesium based implant has been coated with TiO_2 particles [273, 274, 275].

A slightly different but in line with this current challenge is a recent study reported by Chitsaz-Khoyi et al. [95] on the development of titanium-carbon-nitride (TiC/N) coatings on NiTi surface using a hybrid PEO method with electrophoretic deposition (EPD) in single step AO. The study reported that the anodised Nitinol increased the surface hardness (H) and elastic modulus (E) to values that were almost double the amount of unmodified surface, which were from ca. E = 75 GPa and ca. H = 4 GPA to ca. E = 157 GPa and ca. H = 11 GPas, respectively. A lower porosity and dense structure of the anodised titanium can be achieved by suspending the hydroxyapatite (HAp) nanoparticles in their altered electrolyte [95], which significantly reduces the hardness of the coating (to ca. H = 9 GPa) and the elastic modulus (to ca. E = 131 GPa). Moreover, Chitsaz-Khoyi et al. found that their anodised titanium structurally acts as a barrier layer on NiTi surface and hinder the diffusion of corrosive ions into the surface and subsequently improves the corrosion resistance of NiTi [95]. Therefore, this study shows how easy it is to modify the AO cell and its parameters such as electrolyte formulations (aqueous Hap suspension) and the AO setup (hybrid with EPD) to significantly alter the hardness and elasticity of the coatings and of the materials corrosion resistivity as a whole.

Another study reported by Yang et al. [276] provided further interesting evidence that the alteration of the AO electrolyte has a significant effect on the mechanical stability of anodised titanium. According to this work, there are a multitude of possibilities for altering the PEO electrolytes used in previous studies [276], thereby improving the final mechanical stability of the anodised titanium. The presence of organic molecules to base electrolytes significantly affected the formation of the pore morphology and anti-abrasion films on Ti6Al4V [277, 278]. Silicate-based electrolytes are one of the more common electrolytes in AO used to produce anodised titanium incorporated with inorganic polymer functional groups [211, 276, 277, 278, 279]. The anti-abrasive and anticorrosive ability of the anodised titanium improved with addition of silanes to the mixture [276]. Recently, the oxidation of cp-Ti in sodium silicate (Na_2SiO_3) altered with aminopropyl trimethoxy silane (APS) electrolyte by Yang et al. showed an improvement in the mechanical stability of the anodised titanium and subsequently promoted the crystallisation of TiO_2 while maintaining a smoother and thicker surface morphology of the film [276].

Yang et al. suggested that the improved resistance to corrosive media is attributed to the formation of a finer inner and outer layer of the anodised titanium, which was compact and thus resistant to corrosion [276]. The APS is confirmed to exist on the anodised surfaces and in between film defects due to the adsorption, self-condensation and/or chemical bonding of the oxidised Ti-O-Si group from the altered electrolytes, resulting in increased abrasive and corrosive resistance of the final anodised film [276]. Moreover, Yang et al. showed that the addition

of APS to the silicate-based electrolyte is able to reduce the energy-intensive nature of traditional PEO, without compromising the desirable structures and performance of the final anodised titanium, while at the same time improving the mechanical stability of the coating [276].

Figure 8(a) depicts a cross-section of the common microporous structure of anodised titanium. As can be seen throughout the coating layers, the *in-situ* deposited TiO_2 protruded from the Ti substrate and causes the coalescence of small pores into large, discontinuous but interconnected and elongated ones, creating subsurface layers (Figure 8, ox_1 and ox_2) and pores from the base to the outer surface. The presence of subsurface porosity formation was due to the fact that the only segment in which pore formation can occur is when a consistent microstructure has been established [62]. These coalescing microstructures of anodised titanium make the coating strongly adherent to the oxidised structure in terms of layer-by-layer, which results in excellent corrosion resistance and wear protection against friction [189, 280, 281, 282, 283], subsequently reduced the fretting fatigue of the coated surface [39, 284]. There is no significant evidence to date that the microporous anodically deposited TiO_2 (microstructured anodised titanium) on the titanium-based implant generates a modulus elasticity mismatch between its gradually constructed microporous structure from the base to the surface of the host substrate. At this stage, the structural assumption that the stress shielding effects between anodised titanium and Ti-based implants may not occur. Despite its brittleness, most of the literature on microstructured anodised titanium found that the coating is highly adherent to the substrate with excellent corrosion and wear protection capability [138, 141, 144, 189, 209, 280, 281, 282, 283].

In terms of wear behaviour of anodised titanium in body fluids, Cheraghali et al. confirms that the anodised samples wear more and have a higher tribocorrosion rate than thermally oxidised titanium, but have the highest cell viability [285]. Their study found that the corrosion rate of the anodised samples was significantly lower than that of thermally oxidised titanium, which explains why the mechanical biocompatibility was lower. To overcome this specific issue, a duplex coating has been proposed [285] where before anodisation, the cp-Ti substrate was thermally oxidised. Cheraghali et al. reported that a low capacity for plastic deformation of the oxide phases formed on the surface prevented plastic deformation, and consequently no plastic deformation and no grooves were observed on the surfaces of thermally oxidised/anodised samples.

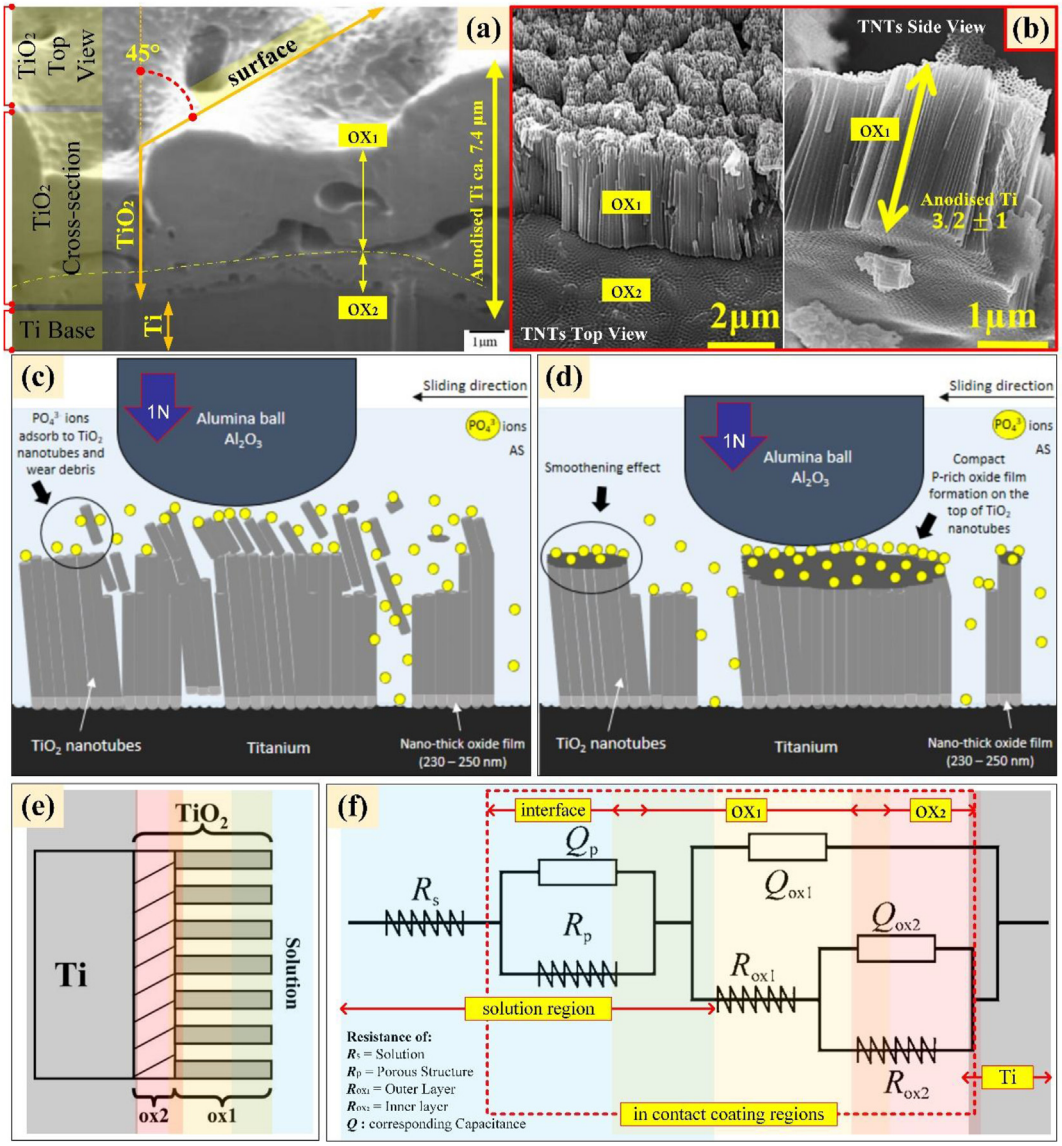

Figure 8. Cross-section of microstructured anodised titanium (a), and titanium nanotubes, TNTs (b), upon tribo-mechanical test (c), with increased mechanical stability (d), and these coating structures could schematically be represented in two-layer model (e), via electrochemical analysis (f) (reillustrated with permission from [50, 62, 286, 287]).

The oxygen's diffusion from thermal oxidation caused a lowering of the active slip systems in titanium, which caused the '*c* to *a*' ratio for hexagonal closed packed (HCP) of the anodised titanium substrate to increase by over 1.588 [285]. The cp-Ti has a lower tribocorrosion rate at different sliding distances of 16–76% when thermally oxidised [285]. Thus, it is possible that passivation of anodised TiO_2 layers on thermally oxidised cp-Ti improved wear resistance of the anodised titanium.

On the contrary, it is well known that the nanotube formed by anodisation of titanium (TNTs) exhibit poor mechanical stability [49, 263, 288] owing to their tubular structures [48, 50, 289] as depicted in Figure 8(b). The granulation, structural degradation, uneven density, and contamination all impede the clinical implementation of TNTs [49, 290, 291]. The apparent presence of discontinuous layers between the metal base to oxide layer (ox_1 to ox_2) and the inhomogeneous lateral attachment between the nanotubes (ox_1) are depicted in Figure 8(b) and these reveal the fragility of the TNTs. These structures relative could be easily detached from Ti-base [48] or suffer fracture between the tubes [292] when its subjected to external force during implantation [291] or by incorrect handling in transport, storage or use [242]. Structurally, these layers of TNTs suffer from weak delamination strength [48, 127]. Prior to the implantation procedures, the coating structure should be able to withstand the premature delamination that potentially yields wear debris on the surface. Debris or loose oxide from the coating could activate the immune system and osteoclasts, causing bone resorption and aseptic implant failure [7, 293, 294].

To resolve these issues of TNTs, Zhao et al. [295] attempted to increase the adhesion strength of the nanostructured anodic layer by using non-protonated polar substances, such as ether/cyclohexane for the AO base electrolyte. The anodising process was conducted in an ethylene glycol/NH_4F system containing 3 vol% H_2O, 0.5 vol% H_3PO_4 and 0.3 wt % NH_4F as electrolyte. It was discovered in their study that the hydrogen-assisted cracking mechanism is the main pathway for oxide layer detachment from the substrate. The cohesion of the nanotubes layer (Figure 8(b): ox_1) and the underlying metal (Figure 8(b): ox_2) was controlled by the protonation at the metal to oxide interface. This proposed mechanism claims that high H_2 solubility in solvents containing ethyl functional groups can eliminate the hydrogen-assisted cracking during AO, subsequently increasing the mechanical stability of TNTs.

In Ti alloys, Renjie et al. [294] proposed that the compaction/reduction of the α-phase and/or increase in the amount of the β-phase was the most important factor in promoting the mechanical biocompatibility of the surface. Recently, Chernozem et al. [296] reported the anodic deposition of TNTs on β-alloy Ti-xNb hybrid composites (x = 5, 25 or 50) and it was observed that there was a significant increase in β-phase elements in the alloy leading to an increase in the surface's elastic modulus after anodisation. The surface load-deformation behaviour of TNTs on Ti-50Nb was reduced by approximately 17% when compared to TNTs structure on Ti-Nb composites with lower wt% Nb and by approximately 23% when compared to cp-T [296]. Regarding Young's modulus, the value obtained for the β-alloy Ti-xNb hybrid composites coated with TNTs was approximately the same as that of bone (ca. 20–30 GPa [265, 292]), suggesting that the nanostructured anodic surface has a beneficial effect and could represent a possible solution to the mechanical mismatch between bone and implant materials [296]. Since anodically grown TNTs on the proposed hybrid composite have reduced length, Chernozem et al. confirmed that the pronounced double-wall nanostructural arrays are enhanced. The brittle nature of TNTs wall recovery was controlled by changing the substrate composition. Based on Chernozem et al. study, it can be concluded that the voltage applied during the controlled anodisation process and the alloying element content affect the total performance of the resulting anodised TNT layers. Owing to the different morphologies and crystal structures of the TNTs, the resulting mechanical properties varied. Other previous studies reached similar conclusions on the mechanical stability of TNTs [180, 292, 297, 298].

Regarding the surface of the implant, recent developments have included materials that imitate natural materials and are often cited as "biomimetic" [162, 299, 300, 301, 302] or "bioinspiring" [252, 253] interfaces. However, few details have been provided on the mechanical stability of these biomimetic structures. Future research needs to discuss their tribo-mechanical (dry/wet-contact performance [303, 304]) behaviour that complements the surface integrity of the engineered implants [22, 257, 305]. The bone crystal nanostructure, for instance, was an inspiration for the design of TNTs [4]. To mitigate the material plastic deformation owing to its amorphous structure, Bartmanski et al. [292] coated the nanoparticle of Hap and Cu on top of the TNT surface. The findings show that when TNT is altered to incorporate bioactive nanoparticles, this results in improved nanomechanical coating properties, which is significant as they decrease from 0.42 to only 0.007 $H^2/E^3 \times 10^3$ GPa. In comparison to the uncoated TNTs or unmodified Ti surfaces, the procedure upgrades the nano-hardness (ca. 0.21 GPa) and Young's modulus (ca. 28.49 GPa) of the coated structure, having mechanical property at dry-contact close to human bone [265, 292]. Unfortunately, they did not perform any tests on wet-contact performances (fluid contacting/corrosion) to simulate design issues in body fluids, and these tests can not be generalised to design issues in body fluids or corrosion in fluids. To guarantee the mechanical integrity of the engineered surface, additional research is required on the mechanical stability of these promising materials.

Alves et al. [287] studied the tribocorrosion behaviour of bio-functionalised TNTs (doped with Ca-P & Zn via reverse anodic polarisation) under two-cycle sliding actions and compared it to conventional TNTs. The growth of the nano-thick oxide film (Figure 8(c)) in the Ti/TNTs interface (Figure 8(b): ox_1 to ox_2) significantly increased the adhesion strength of the anodised films to the substrate and therefore their hardness. In addition, the formation of a P-rich tribofilm (from dissolved Ca-P species and dissociation of PO_4^{3-} ion from Fusayama's saliva) occurs during tribo-electrochemical solicitation, which provides both electrochemical protection and mechanical wear resistance. Figure 8(d) shows the surface modification effects of phosphate ions that reduced the coefficient of friction and improved the surface tribology of TNTs that mechanically mitigates its surrounding micro-movement. A similar mechanism has been proposed by other studies which show that bio-functionalised anodised layers (either macro or nano surfaced) have better resistance to corrosion and wear [209, 280, 292, 306, 307].

With regard to anodic layer performances for clinical translations, a better surface structuring strategy for Ti-based implants has been tested *in vivo* by Lotz et al. [308] and Gehrke et al. [309]. The study confirms that; (i) the micro/nano-structured/hydrophilic implants promotes the increased bone-to-implant contact and removal torque values *in vivo* and increased osteoblastic marker production *in vitro* compared to micro/-hydrophilic or micro/nano-structured/hydrophobic implants, suggesting that osseointegration occurs in osteoporotic animals and that nano-structured surface properties improve the integration rate [308]; and (ii) implants with the new macrogeometry, which included healing chambers embedded within the threads, resulted in a significant increase in osseointegration, thereby facilitating better healing process *ex vivo* [309]. In addition, Yi et al. [310] reported that the treated Ti-implant surface with TNTs of different diameters (30 nm, 50 nm, 70 nm, and 100 nm) showed that the highest mean new bone area and the highest mean of removal torque value were observed in 30 nm experimental group and in 70 nm experimental group at 2 weeks and 6 weeks *in vivo*, respectively. The idea of bridging the gap between anodised titanium and clinical translation by optimising the manufacturing of robust titanium nanostructures on complex implant geometries by Li et al. [290] is therefore feasible and very promising if the results of the studies by Yi et al. [310], Lotz et al. [308], and Gehrke et al. [309] are taken into future design consideration.

Table 3. Common terms, procedures and testing techniques to measure the anodised titanium mechanical stability *in vitro* and *in/ex vivo*.

In vitro			Example in-vitro Studies on Anodised Ti			
Method	Purpose: • to study	Measuring Technique	Sample: • AO parameters*	Procedure	Findings	Ref.
Dry-contact Analysis • done at atmospheric condition [282]	Wear (friction/lubrication)	Sliding Test	Micro-arc anodised cp-Ti, vs • hydrothermal; 130 °C 80 kPa, • heat; 5 °C/min 400 and 600 °C, 1 h	Reciprocate tribometer: WC (Co) ball, ⌀6 mm, 3 N, 1 cm/s, half-amp of 1 mm, 9 m distance.	• One order lower of wear rate difference between hydrothermal and heat threatened anodised layer, • hydrothermal have similar rate with standard anodised Ti.	[282]
		Friction Test	Microstructured composite anodised Ti-10V-2Fe-3Al; • altered $C_4H_4Na_2O_6$ electrolyte with polytetrafluoroethylene (PTFE) nanoparticles	Ball-on-disc rotating: Si_3N_4 ball, ⌀2 mm, roughness ~0.01 mm, 100 g load rotation in ⌀4 mm, 100rpm.	• Worn surface decreases with the increase anodising time, enhanced wear resistance of composite anodised sample with thicker films. • Denser latex particles incorporated in the layer produced less wear loss, thus lubricating on the worn surface, reduced friction coefficient.	[183]
		Tensile Test	Microstructured cp-Ti M4 screws.	Fixture anodised screw to nut (tightened-untightened); torque wrench 2 Nm from initial zero load, I∠300°, Motosh ISO 16047.	• Increased layer thickness decreased the coefficient of friction, COF between 10-40%, depends proof load (max 70%). • COF min. attained at anodising 40V–50V corresponds to 0.14–0.24 μm thickness, above these: COF increased eventually (ca. 0.6 to 0.8 static COF).	[318]
		Wear-life Test	Anodised cp-Ti before and after coated by diamond-like carbon (DLC)	Reciprocated ball-on-plate friction (GCr15 stainless ⌀6 mm), distances 1 N for 100 m &10 N for 1500 m; 0.075 m/s. • Wear-life: represented by wear depth graph and wear rate measured using surface profilometer.	• Friction coefficient of the composite coating and the DLC mono-film was similar under both light & heavy load (composite wear-life: ca. 43% longer than DLC mono-film) • Altered bottom TiO_2 film provided necessary hardness and load support. The wear rate of titanium with protective composite was much lower than Ti with DLC mono-film.	[307]
	Adhesion (detachment/peel/flake-off/delamination)	Scratch Test				
		• Microscratch	PEO Ti6Al14 V at 20–90 min.	Progressive load: 0.3–10 N along 5 mm, scratched using 200μm radius Rockwell C diamond tip.	• No failure produced at 90 min, although coating is more porous and looser than the one produced at 60 min. • An adhesive at the edge and cohesive failure in the inner layer of scratch track occur, produced higher critical load (60 min; failed at ca. 5.3N, cracked at ca. 6.2N & delaminated at ca 6.7N), implied greater adhesion and bonding strength.	[283]
		• Nanoscratch	Micro-arc Anodised cp-Ti, vs • hydrothermal; 130 °C 80 kPa, • heat; 5 °C/min 400 and 600 °C, 1 h	Linear ramp 0–400 mN constant load, 600 mm scratch length, 10 mm/s	• Heat treated anodic film has higher cohesion compared to hydrothermal or standard anodised Ti. • Hydrothermal anodised Ti less brittle and more ductile than standard anodised Ti.	[282]
	Deformation (stress shielding/stiffness)	Indentation Test				
		• Microhardness	Microstructured cp-Ti M4 screws	Vickers hardness 100 gf (1 N) load.	Anodic layer thickness increased exponentially from 0.23μm (60V) to a max. of 3.4 μm (100V), implied an increase in mean surface hardness (ca. 380 to 420).	[318]
			TNTs at single and two-stage AO, with and without heat treatments	Vickers; 10 indentations performed randomly per 3 different samples with load of 0.98 N (0.1 kgf).	• No significant differences in roughness between samples (R_a ca. 130nm) but the hardness for untreated (ca. 240 HV) notably lower than TNTs (ca. 290 HV). • The second anodic treatment and heat treatment led to an increase of hardness, highest value was: group 2 stages AO + heat treatments (ca. 340 HV).	[298]
		• Nanoindenter	Micro-arc Anodised cp-Ti, vs • hydrothermal; 130 °C 80 kPa, • heat; 5 °C/min 400 and 600 °C, 1 h	Oliver and Pharr: loads 0.14400 mN, 10 cycles, Berkovich tips	• H/E ratio (elastic strain to failure) of hydrothermal anodic layer was lowest, reiterates the instability due to cracking left by nanoindenter, means highest wear rate. • Heat treated anodic slightly increases the H/E but still lower compared to standard anodised Ti.	[282]
			TNTs via optimised-AO on commercial dental implants (abutments and screws)	Oliver and Pharr: loading force 10,000 μN, Berkovich tip, depth max.10% of the thickness	• Standard TNTs have compromised the edges of implant threads leading to delamination and fracture. • The optimised TNTs, greatly enhanced elastic modulus (ca. 40–60 GPa), significantly outperformed standard TNTs (ca. 4–8 GPa), while retaining desirable hardness (ca. 2.5 GPa).	[290]

(*continued on next page*)

Table 3 (*continued*)

In vitro			Example in-vitro Studies on Anodised Ti			
Method	Purpose: • to study	Measuring Technique	Sample: • AO parameters*	Procedure	Findings	Ref.
Wet-contact Analysis • done in biomimetic simulated environment [314]	Wear (detachment/debris/ion release)	Tribocorrosion Test				
		Usually using flat tribometer coupled to a potentiostat; tested either in; • Sodium chloride (NaCl) [281]/ • Phosphate buffer saline (PBS) [298]/ • Hank's solutions [189]/ • Fusayama's artificial saliva [287]	CaP MAO microporous-Ti vs acid-etched microporous-Ti • porous Ti having closed and interconnected pores (22 and 37% porosities). • Anodised: MAO 300V, 1 min DC, 200rpm. While control: etched 24 h in Kroll's reagent	NaCl tribo-cell: used pin-on-disc tribometer, working substrate facing upwards, 7 mm zirconia pin spherical end 100 mm radius as counter material, mounted vertically above the exposed area (1.13 cm^2), rotated clockwise. Open circuit potential (OCP, 25 °C) before, during and after sliding stable at ΔE <60 mV h^{-1}, pin loaded then slide unidirectional, track ⌀4 mm, 1 Hz (60 rpm), 30 min (1800 cycles), 3 N load, Hertzian 80.8 MPa. After sliding, pin unloaded and OCP kept on monitoring for 30 min.	• All bio-functionalised samples had higher OCP values before, during, and after sliding (but anodised Ti performed better than acid etched samples), indicating a lower corrosion tendency, not only due to the improved corrosion resistance of the oxide layers formed on the outer and pore surfaces, but also due to their high hardness and thus high wear resistance. • During tribocorrosion, the counter material primarily slides over the protruding anodized surfaces, causing the functionalised surfaces to suffer less mechanical damage. Debris removal from pores also reduced third-body abrasion, resulting in improved tribocorrosion performance. • Anodised Ti outperformed acid etched Ti in general.	[280]
			CaP PEO cp-Ti with and without annealing treatment	PBS tribo-cell: sample counterfaced alumina ball ⌀6-mm, 5 N, 1 mm linear peak-to-peak displacement, 1 Hz; 350 cycles. OCP measured for 1 h, for each normal load tested, the region of sliding was changed.	• Tribocurrent (I_{tcorr}) rose after ca.240 s of sliding began and lowered significantly compared to cp-Ti & cp-Ti before annealing. • For 400V samples, no significant variation, differences in tracks of smashed oxide wear (from the porous outer layer); but compact inner layer sustains the contact load during sliding and minimises exposition of the substrate.	[319]
			TNTs at single and two-stage AO, with and without heat treatments	PBS tribo-cell: OCP with a tribometer of pin-on-plate, WE against alumina ball (⌀10 mm, 1 Hz, 0.5 N, amp 2 mm), 30 min sliding after OCP stabilised 2 h ΔE <60 mV/h. After sliding, the counter material was removed and OCP continued to be recorded for 30 min.	• Coefficient of friction; untreated is the highest (0.7 ± 0.1) followed single AO and two-stage AO (0.6 ± 0.1), and then heat treated AO (0.5 ± 0.1). • Wear tracks: untreated presented parallel ploughing grooves, adhered/oxidised patches, and plastic deformations. • Irregular wear track shapes observed for single AO and two-stage AO (detachment of the TNTs), both presented similar wear features to the substrate. But heat treated groups (heat on single AO va two-stage AO) presented dissimilar behaviour; two-stage AO better where no evidence of detachment at the border of wear tracks nor sliding grooves were observed.	[298]
			Two-stage reverse-polarised-AO TNTs with and without doped elements Ca/P/Zn	Fusayama's tribo-cell: pin- on-disk reciprocated sliding (Al_2O_3 ball ⌀10 mm). OCP conducted during two independent cycles; reciprocating sliding & after each period solicitations, 1800 s followed 2000 s to stabilised. Sliding tests; 1 N, 400 MPa, 1 Hz, linear displacement amplitude is 650 μm.	• TNTs achieved stable OCP around −0.14 V, differs strikingly from TNTs-Ca/P/Zn which stabilised around 0.11–0.12 V. • COF measured during the first & second sliding cycle lasted for 1800 s with no significant differences between samples • Wear volume loss was found significantly higher for TNTs than TNTs-Ca/P/Zn. No detachment observed outside the contact region for these samples and the survival of TNTs was detected even in the border and central regions of their wear tracks. • Formation of the tribofilm during mechanical solicitations might be promoted by their improved wear resistance.	[287]
	Corrosion (pitting/ion release/ fretting/crevice)	Electrochemical Test				
		• Open Circuit Potential (OCP) • Current Density (J) • Cyclic Voltammetry (CV) • Electrochemical Impedance Spectroscopy (EIS)	PEO Ti-13Nb-13Zr in ultrasonically dispersed Zr-nanoparticles + acidic electrolyte	Integral investigations: OCP (20h) & potentiodynamic () perform via Voltalab potentiostat, while EIS using Zennium potentiostart (±10mV, 10m–100M Hz). • Medium; SBF + hydrogen peroxide.	• OCP for PEO samples higher than Ti substrate indicating that PEO coating shows higher resistivity against corrosive attack than the non-coated substrate. • Tafel curves: reduced for more than two orders of magnitude for PEO coating than the uncoated samples; the corrosion currents decrease with increasing current density applied in the PEO treatment. • PEO inner barrier R_i = 1.54 MΩ/cm^2 (untreated 160 kΩ/cm^2) and the outer porous R_p = 162 kΩ cm^2 show that resistance of the inner layer plays a crucial role for the enhanced corrosion resistance.	[209]

(*continued on next page*)

Table 3 (*continued*)

In vitro			Example in-vitro Studies on Anodised Ti			
Method	Purpose: • to study	Measuring Technique	Sample: • AO parameters*	Procedure	Findings	Ref.
					• Theoretical capacitances, CPE roughly deviate by a factor of 10 from the fitted values, indicating the incompleteness of the fitting model.	
			TNTs vs structured-optimised, SO-TNTs via multistage AO	Integral Investigation: OCP ±250mV, 0.3 mV/s at 22 °C CH1660D workstation, 60 min to stabilise, scans 1500s. Tafel curves measured at 0.01 V/s, E(V) = −1 to final E(V) = 0. • Medium: Simulated body fluid (SBF)	• OCP: SO-TNT (ca. −0.06 V) presented lower corrosion tendency than NT (ca. −0.28 V). • Corrosion current density of bare Ti and NT were measured as 0.77 μAcm^{-2} and 14.41 μAcm^{-2}, whereas SO-TNT was 0.07 μAcm^{-2}. Obviously, SO-TNT has significantly reduced the corrosion potential and corrosion current density. • Formation of interfacial layer in SO-TNTs act like a "barrier", which prevents the underlying Ti substrate from erosion.	[320]
In/ex vivo	Example in/ex vivo studies on Anodised Ti					
Histomorphometry [321] • histologically and quantitatively assesses bone cells, growth, tissue remodeling, bone architecture, and repair • both the activity of bone cells and the amount and distribution of bone tissue can be analysed	Bone Implant Contact (BIC) Visualisations (qualitative measure) • usually assisted with μCT [316]	Routine Histological [315] • stained site shows more cellular detail, but underemphasises the mineralised bone • does not permit direct evaluation of BIC or bone neoformation near implant surface upon removal/ damage of mineral content	Micro-arc anodised RBM Ti dental implants, placed in sheep mandible • implanted mandibular site dissected en bloc prior to testing. • implantation period: 4 weeks	Fixed in formalin, dehydrated with ethanol, cleared with xylol and set in $C_5H_8O_2$., then sectioned and glued to plastic slides, polished by silicon carbide, then stained with one part of MacNeal's tetrachrome followed by two parts of toluidine blue.	• No evidence of inflammation or titanium particles found within the tissue. • Untreated surface had large masses of disorganised calcified material filling the thread, appeared to be resorbed bone tissue or residual debris. • Anodised surfaces showed less debris than the control, largely incorporated into new bone, filling the threads. • BIC for anodised surfaces were more than 70% relative to control.	[53]
			Micro-arc anodised Ti inserted into the bone marrow in the femurs' Wistar rats • carbon nanohorn (CNH) electrophoretically deposited on the anodic layer • implantation period: 1 & 4 weeks	Fixed in formaldehyde, decalcified with $C_{10}H_{16}N_2O_8$ acid, set in paraffin & sectioned before stained with haematoxylin and eosin.	• Many osteoblasts with a cuboidal shape were observed aligned on the bone newly-formed on anodised Ti, • Deposited CNH induced newly-generated bones with proteoglycans, drives higher BIC% rate, indicates better "contact osteogenesis".	[59]
			Sand-blasted vs PEO microstructured surface of screw-shaped Ti-6Al-4V implants, drilled in rabbit tibias • implantation period: 8 weeks	Tissue was fixed with plastic, and subjected to Haemotoxylin and Eosin staining.	• No signs of inflammation, both structures were in direct contact with the surrounding cortical bone and bone marrow. • Upon implant removal, amount of newly formed bone around anodised surface was higher than sand-blasted surface. • Overall BIC% no difference but the ratio of new bone created nearby the implant fixture was more than doubled in the anodised sample compared to sand-blasted sample.	[317]
			LENS™ printed CaP coated porous Ti implants (25% porosity); surface modified by depositing TNTs, followed by doping Sr^{2+} and Si^{4+} via SBF • implanted by press fit and the incision was sutured by undyed braided coated VICYRL-polyglactin 910 synthetic surgical suture. • implantation period: 4 & 10 weeks	Fixed in formalin, dehydrated via ethanol series finishing with acetone, embedded into Spurs resin, mounted on glass slides, then stained with modified-Masson Goldner's trichrome [322]	• Osteoid-like new bone formation has been observed even at the 4 weeks' time, with more been noticed after 10 weeks of implantation on specimen's dopants with Sr and Si compared to just TNTs film. • Almost 100 % BIC noticed after 10 weeks in Sr & Si dopants TNTs compared to ca. 60% BIC in control samples. • Strong bone interlocking, confirms by presence of no gaps at the implant interface in the CaP/TNTs-coated implants.	[323]
			Commercial Ti dental implants with surface treated by crystallisedHAp vs sand-blasted/acid-etched vs TNTs; installed in sheep' iliac crest • implantation period: 2 & 4 weeks	Trephined samples fixed in formalin, dehydrated with ethanol, embedded in light-curing resin, stained with Toluidine blue + acid fuchsin	• After 2 weeks: nanostructured surface showed large trabeculae of neoformed bone between threads and islands of bone debris in contact with the trabecular bone. • Sand-blasted/acid-etched microstructured surface present similar degree of bone volume but less extensive trabeculae, bone debris between the threads. • Microstructured anodised surface showed bone trabeculae permeating the implant surface at a lower volume than either other 2 samples but with a similar BIC area.	[324]

(*continued on next page*)

Table 3 (*continued*)

In vitro			Example in-vitro Studies on Anodised Ti			
Method	Purpose: • to study	Measuring Technique	Sample: • AO parameters*	Procedure	Findings	Ref.
					• After 4 weeks, newly formed bone around the implants were clearly apparent with minimum amount of connective tissue was observed in all groups. • Overall BIC higher than 80% with no statistical difference in between groups. • All groups experienced a constant increase in trabecular bone fixation to the implant surface from 2 to 4 weeks.	
			Nano vs macro-threaded anodised Ti implant; • TNTs ⌀30, 50, 70, 100nm inserted into the right & left rat' femur at osteotome sites • implantation period: 2 & 6 weeks	Fixed in formalin, decalcified with EDTA, embedded in paraffin, sections stained with hematoxylin-eosin (H&E)	• New bone formed near cortical bone difficult to differentiate, then the one unsuccessful histomorphometric: within the sponge bone is easy to differentiate therefore is measured. • During implant removal, new interface or severely damaged then difficult to analyse. The results showed higher BIC% in 30nm and 70 nm groups at 2 and 6 weeks	[310]
			Machined cp-Ti implants vs Anodised cp-Ti (TNTs) implants placed in rats' right tibia • implantation period: 7 weeks	Fixed in formaldehyde nondecalcified; dehydrated in ethanol, soaked and inlaid in methyl methacrylate; glued to a plexiglass with acrylate-based adhesive; crushed and polished using silicon carbide, then stained in Stevenel's blue/Alizarin red	• Histologic qualitative analyses showed bone formation in close contact with the implant for both groups. • The histomorphometric analyses showed that cp-Ti machined (BIC 37.89%) had a lower percentage of bone area compared with cp-Ti anodised (58.97%)	[325]
Biomechanical Analysis [326] • quantitative measure for bone cell anchorage • conducted immediately after animal termination on rapidly excised and nondehydrated bone samples	BIC Strengths (qualitative measure)	Pull-out Test	Sand-blasted VS PEO microstructured surface of Screw-shaped Ti-6Al-4V implants, drilled in rabbit tibias • implantation period: 8 weeks	Fixture mounted the implant and the torque meter, fastened to 35 Ncm and connected to a torque meter. Torsional removal value recorded over the reverse-rotation of its placement.	• Average removal torque was 49.7 Ncm for sand-blasted sample and 51.5 Ncm for the anodised sample. • Greater torque rotation forces required to remove the implants anodised surface, suggest higher strengths of osseointegration of the structure.	[317]
			TNTs doped with Si implanted in rat femur • implantation period: 2 weeks	Direct pull-out from implanted site at speed of 1 mm/s. The maximal force was the pull-out force.	The peak pull-out force for S-doped sample was increased by 18% and 54% compared to TNT and Ti screws, respectively	[71]
			Nano vs macro-threaded anodised Ti implant; TNTs ⌀30, 50, 70, 100nm inserted into the right & left rat' femur at osteotome sites • implantation period: 2 & 6 weeks	Fixed implant placed at removal torque test apparatus, connected with conventional digital torque gauge. Installed screw driver connected to implant' upper notch and rotated in an anticlockwise direction. Peak value when broken was recorded	Macro threaded showed higher removal torque than nano threaded. 30nm and 70nm TNTs at 2 weeks and 6 weeks showed the highest value; but no significant difference.	[310]
			Machined cp-Ti vs anodised cp-Ti (TNTs) placed in rats' right tibia • implantation period: 7 weeks	Specimens placed on a workbench, aligned with torque meter. An adapted wrench applied counter clockwise for implant removal	The removal torque analyses showed that the Group cp-Ti machined (1.15 ± 0.01, N/cm) had significantly lower values than the Group cp-Ti anodised (1.44 ± 0.01, N/cm)	[325]
	Implant Stability Quotient (ISQ) [324] • acceptable primary stability with mean ISQ values of above 75 N/cm in humans	Resonance frequency analysis (RFA)	Micro-arc anodised RBM Ti dental implants placed in sheep mandible, implanted site was dissected en bloc prior to testing. • implantation period: 4 weeks	ISQ obtained in pairs at right angles projected RFA to each mandible's buccolingually and mesiodistally	There was no statistically significant difference in RFA mean values or trends measured at surgery to a month healing, showing ISQ values do not correlate with histomorphometric figures.	[53]
			Commercial Ti dental implants with surface treated by crystallisedHAp VS sand-blasted/acid-etched VS AO; installed in sheep' iliac crest • installed two different devices (Osstell® and Penguin®) and two magnetic transductors (SmartPeg® and MulTipeg®) • implantation period: 2 & 4 weeks	magnetic transducers were mounted on each implant and tightened with hand pressure using the metallic (MulTipegs®) VS plastic (SmartPeg®) screwdriver. Penguin® RFA Probe held 1 mm from the transducers to register ISQ	• Higher values of statistical differences recorded using MulTipeg®/Penguin®. MultiPeg® showed higher resonance frequency than SmartPeg®, yet no significant ISQ difference occurred between the implants under the same device. • All samples recorded high levels of insertion torque and primary stability, but no correlation existed between the two, suggesting that a high insertion torque does not necessarily correspond with a high ISQ value	[324]

* Stated if significantly varied the test outcomes.

5.2. Testing techniques to measure the anodic TiO_2 mechanical stability

Titanium-based anodised implants will have a chemically roughened hard TiO_2 oxide layer on the surface (known as anodised titanium; either in microstructured or nano surfaced TNTs, or feasibly both [311, 312]) to improve their durability [3, 4, 313, 6, 16, 53, 87, 120, 240, 263, 264]. The general perspective for mechanical stability of anodised titanium deduced from recent *in vitro* and *in/ex vivo* studies has been summarised in Table 3. Based on the information in the table, it appears that there is an unfortunate lack of evidence to show that recent anodised titanium surfaces were indeed stable in the human clinical trials. The overall findings are consistent with trends in the anodised titanium oxide phases, which is limiting dislocation slips and plastic deformation on the Ti-surfaces, thus increasing the strength and durability of the tested implants in animal models.

Table 3 presents common terms, procedures and testing techniques used for technical understanding in order to measure the mechanical stability of the complete mechanical layer. This review shows that most *in vitro* studies can be classified into two methods of analysis, either dry-contact (testing conducted at atmospheric conditions [282]) or wet-contact (testing conducted in biomimetic simulated environment [314]). It has been reported commonly in the literature that *in vivo* studies of anodised titanium are measured using histomorphometry aided by micro-CT and image processing analysis [315, 316], which are quantitatively validated by *ex vivo* study on stained specimens complemented with biomechanical analysis [71, 317].

In the testing strategy of an implant coating, it is imperative that specific problems of the engineered surface be identified, which then act as a focal point for further research efforts. The testing strategy stimulates an *in vitro* design optimisation that could be mitigated by an *in/ex vivo* study to help bridge the gap in clinical translation [290]. Recent advancements in the testing strategy were pivotal in the analysis of surface reactions with body's fluids, where tribology test is a study of wear and the electrochemical test determines the surface corrosion.

Simultaneous testing of wear and corrosion in one test system is known as a tribocorrosion test (*currently using various unstandardised design/setup of tribometer*) [280, 287, 304] or biotribology test [256, 327], all of which were conducted in a wet-contact environment between the sample and the test system (*tribometer*). To date, most of the reported trials of the anodised titanium tribocorrosion properties have been able to estimate the mechanical stability of the coating as a whole once it has been in contact with the bodily fluids [256, 280, 287, 304, 327]. Despite the limited literature, development of standards and test protocols for testing the tribocorrosion properties of anodic TiO_2 layers is lacking. To date, there were no international standards on how the tribo-electrochemical technique was performed, which is why the perceptions of the mechanical stability of the coating especially that of a complex porous structure like anodised titanium (Table 3) vary from one literature source to the other [189, 280, 281, 282, 283, 328, 329]. The clinical translation of tribocorrosion properties is not possible currently, as the prevalent *in/ex vivo* test used is not standardised and varies significantly in terms of time of implantation [15, 298, 319].

Another interesting issue worth tackling here is the precision of the anodised titanium corrosion properties measured by electrochemical tests. According to Menini et al. [286] and Doulache et al. [330], the electrochemical test is subject to four consecutive processes of parametrisation, resulting in the final corrosion properties of the surface being studied. The first begins with the corrosion current density obtained via simulated Tafel curves, and then the corrosion potential derived from the surface's open circuit potentials (OCPs), followed by observed pitting resistance in the electrochemical cell through cyclic-voltammetry, and finally, an electronic fitting (Figure 8(f)) that structurally represents the coating impedance properties on the substrate (Figure 8(e)) via electrochemical impedance spectroscopy (EIS)/-Mott–Scotty analysis.

However, throughout previous studies [138, 141, 144, 189, 209, 214, 331, 332], it can be seen that the building blocks (interconnected coalesced subsurface layers adjacent to the electrolyte interfaces) that create windows (pore walls to electrolyte interfaces) in electrode/electrolyte interfaces circuitry are rarely considered to be double-layer structure of porous anodised titanium, as shown in Figure 8(e) [286] (*similar illustration was found elsewhere* [39, 333]). As a result, studies have produced higher statistical functions (χ^2) in their electronic fittings [306], yet the issue is that some of the tests did not report their χ^2 fitting accuracy [138, 189, 209], and thus it is hard to be certain that the integrity of their circuit fitting prior to the EIS calibration of the testing being optimised. This function is important to the surface' electrochemical analysis because for instance, χ^2 in the order of 10^{-3} [306] is considered higher than that in the order of 10^{-5} [286], which then would compromise the accuracy of the proposed final fitting model [138, 189, 209]. Hence based on the literature, the EIS analysis proposed by Menini et al. [286] is seen to be more suitable for representing the fitting electronic model of the porous anodised structures (Figure 8(e)) as illustrated in Figure 8(f).

To date, considering the growth of the nano-thick oxide film (Figure 8(c)) in the Ti/TNTs interface (Figure 8(b): ox_1 to ox_2, as observed elsewhere [290, 320, 334]) together with the existence of tribofilm-laminated porous walls on top of the TNTs (Figure 8(d)), the fitting model as shown in Figures 8(e) and 8(f) has been shown to be the most appropriate electronic fitting (lowest accuracy) ever reported for the anodised titanium [144, 286, 330, 332].

The anodised titanium is a structurally an advanced semiconductor [87, 167, 332, 335, 336]. Precise electronic fitting of its electrochemical characteristics, which could reduce the high-sensitivity of χ^2, could result in improved analysis of the porous anodic properties of the crystallised TiO_2 semiconductor, validating the measured surface stability in the electrochemical circuit, which was neglected in other studies [138, 141, 144, 189, 209, 214, 331, 332, 333]. From most of these corrosion studies, the increase of current density in the passive region of TiO_x was owing to the formation of metastable oxides such as Ti_3O in the anodised layers, which were transformed to a more stable titanium oxide, i.e., TiO_2 when the voltage in the test circuit was increased. As a result, the occurrence of oxidation reactions generates excited electrons due to the charge transfer in the double layer and therefore, a higher current density in the anodic branch results. Given that this mechanism is about to take place in an EIS electrochemical cell, finding an optimised electronic fitting model for an anodic TiO_2 layer is crucial to the analysis. Prior to testing, once the fitting function has been optimised (as low a value for χ^2 as possible based on the EIS parameterisations during experiment [286, 330]), the test measure will be more accurate for comparison.

Another concern is the limited progress of novel surface morphologies that have been proven *in vitro* to have an excellent biocompatibility with no evidence of its mechanical stability, [44, 70, 90, 91, 245, 337]. Wang et al. [338] provided data complementary to literature on the corrosion rate of microporous anodised titanium produced in silicate-based electrolytes versus CaP-based ones. They proved that with an increase of positive voltage, the MAO coatings obtained from the CaP-based electrolytes show good surface stability, and the micro-morphology of the coatings is smoother than that obtained from the silicate-based electrolytes [338]. As for TNTs, recent comprehensive study Çaha et al. [298] clarified that the fabrication of a mechanically stable TNTs via multilayer anodising process is highly demanding, but their proposed AO double-stage route is facile and the optimised TNTs stability was tested using reliable techniques without compromising the integrity of the coating. Their proposed TNTs stability enhancements was confirmed to be significant based on data from coating adhesion, hardness and corrosion complemented with tribo-mechanical performances [298], whereas similar findings were reported elsewhere [287, 290, 314]. Overall, Figure 9 represents the recent optimised design of anodised titanium as a coating on commercial implants, which is biocompatible and mechanically stable with increased bioactivity *in vitro* and *in/ex vivo*

compared to other comparable coating structure such as sandblasted and acid-etched Ti surfaces [317, 324].

For optimised design of anodised titanium on commercial implants, most *in/ex vivo* studies estimate the implant osseointegration rate using a percentage of bone to implant contact (BIC%) in histomorphometric analysis (assisted with image processing on stained samples), but some others have proposed bone area fraction occupancy (BAFO% [309, 324]) or amount of newly formed bone around the surface (new bone formation rate % [317]). These figures were used to represent the quantitative measures that complement the histomorphometry in defining the osseointegration rate on implant surface. Another quantitative score i.e., implant stability quotient (ISQ; score for stiffness of the bone–implant union measured usually via sensor of resonance frequency analysis (RFA) [324]) was observed to be less sensitive, which was owing to insufficient resolution to detect biomechanical changes *ex vivo* [53]. Another similar study also found that ISQ score for all significantly different specimens do not show statistical difference in scores between groups [309]. Duncan et al. reported that ISQ values at the start of the loading period were not predictive of implant loss during loading, suggesting that caution should be adopted when using RFA analysis to evaluate the success of implantation based on ISQ scores [53]. Moreover, varying the device or transducer in the RFA testing procedures does not have a major effect on the ISQ sensitivity, which could explain the existence of more conflicting results *in vivo* [324] relative to *ex vivo* [339]. Sartoretto et al. reasoned that RFA should be done during *in vivo* not *ex vivo* to limit any kind of damage caused by the insertion torque of the transductors into the implant. This can avoid impairing the histological and histomorphometric evaluations of the implant–bone interface [324].

In the histomorphometry study, different staining procedures were used to semi-quantitatively estimate the rate of bone cell osseointegration *ex vivo*. However, it was reported that most of these procedures caused BIC damage [310, 315], thus Kunrath et al. proposed an enhanced bone preservation protocol for better histological study of implants [315]. The proposed mineralised bone preservation technique by Kunrath et al. shows that the *in situ* mounted specimen provide clear mineralised bone structure *ex vivo* without compromising the significant cellular details [315]. The significant contribution of this newly proposed protocol was the exclusion of staining step in the histomorphometry procedure while permitting surface analysis without implant removal or damage to BIC. This promising protocol needs more attention in the surface histomorphometric analysis in future studies, especially for anodised titanium implant because so far no other study has reported the feasibility of this protocol on AO surface in the current literature.

This review study also envisioned that another possible solution to the subjectivity of routine histomorphometry through the inclusion of autoradiography, which can help to visualise radioactivity in mineralised and cellular specimens *in vivo* and the tissue distributions of radiolabelled compounds can be traced *ex vivo* [340]. Further study of this autoradiography is therefore recommended for the further advancing the reliability and accuracy of the histomorphometry method.

Despite the lack of confirmation of the destruction of the TiO_2 anodic layer in the *ex vivo* study (Table 3), the microrupture test of an anodised layer that can trigger an immune-inflammatory response remains underexplored. Hirakata et al. [155] proposed the stress-based fracture model considering graded, porous and discrete structures of the nanotube arrays of TNTs together with the phenomenological densification model to describe the apparent stress–strain relationship of the indented regions and showed that this could mitigate the microrupture phenomenon. For anodised titanium, this microrupture is directly correlated to the coating brittleness (fracture is likely due to low tensile strength and low fracture toughness) and the fabrication of a crack-free anodic TiO_2 layer is still a huge challenge [155, 285].

5.3. Real-time/in-situ detection methods for surface reactions

The interpretation of findings from real-time or *in situ* study to detect engineered surface reactions in an implanted environment has been very limited. Most studies have used a combination of electrochemical and tribocorrosion analysis to simulate the *in vitro* test environment by mimicking the body's fluid reactions on the proposed surface [209, 280, 287, 298, 319, 320]. A surface profilometer has rarely been used in tribocorrosion analysis to calculate how much wear was produced using a tribology test [307]. The profiling technique was used to measure the dimensions of the *ex situ* wear track. Based on the surface profiler, the loss of volume of each sample tested was the product of the length of the wear track with the cross-section of the wear track, where the rate of sample wear is the fraction of the loss of wear volume over the product of applied force with the sliding distance of the tribo-ball. The results of this quantitative measure appear to be reliable and therefore can complement the surface response analysis. It is recommended that this *ex situ* profiling technique be integrated with *in situ* tribocorrosion test in the future.

Another *in situ* method worth exploring, is a combined chemical analysis using the Pourbaix diagram and X-ray photoelectron spectroscopy (XPS) that has shown that the passivation of titanium and aluminium to form TiO_2 and Al_2O_3 can trigger the dissolution of aluminium as a solvent ion in its implanted environment [341]. On the other study, the quantification of Ti released during the insertion of three different implants was performed *ex vivo* by Pettersson et al.' study [342]. In their trials, a pig bone jaw was used as an implant model and inductively coupled plasma atomic emission spectroscopy (ICP-AES) was used *in situ* for the analysis of Ti released from the implant. Ti was abraded in the surrounding bone when a dental implant was inserted and the surface roughness of the implant increased the amount of Ti detected. Via ICP-AES analysis, this study was able to conclude that the diameter and overall area of the implant were less important to the Ti release relative to the variations in surface roughness of the implant.

A smart trial to detect the Ti surface response towards its implanted environment is credited to the use of real time implementation of quartz crystal microbalance (QCM). This crystal is an advanced sensor that can be used to quantitatively measure the initial adsorption of contacted-matter on the surface, to determine whether biomolecules, such as proteins interact, and to identify the products, and quantify those interactions with the built-in sensor surface in real time. However, there have been only a small number of QCM studies done on Ti implants, and none on anodised titanium. Prior research has demonstrated the efficacy of quantifying mesenchymal proteins and bone-derived cells in surface-treated Ti implants [343], as inspired by the initial design of QCM system that mimics the denture materials which can quantify the amount of protein adsorbed to the engineered surface [344]. Their extended recent work demonstrates that QCM is a promising tool for measuring the nanogram level of protein and bone marrow cells attached to titanium surfaces in real time [345]. The results of QCM measurements revealed that surface treatment improved the adhesion of both proteins and bone marrow cells. This series has verified that QCM is an effective method for the analysis of the initial implant anchorage to bone cell *in situ*/real time. Therefore, more studies of QMC are recommended to verify the efficacy of anodised titanium as implant coating materials in future research.

5.4. Cost-efficiency and safety of TiO_2 anodic layers as implant's coating materials

It is of utmost importance that the safety of the materials be assured in relation to the costs [346, 347, 348]. In the case of osseointegration implants, if the level of safety of the materials is similar to that of titanium as the base material, then the cost of production will be a

comparison point. With regard to the safety of implants, Apostu et al. [3] showed that the surgeon's experience in managing pre/intra/postoperative protocols for uncemented total hip arthroplasty is the most important variable in the implant survival. Ravida et al. [349] suggested that the survival of the implant is primarily determined by the intra-operative protocols of surgical technique (which influence the severity of bone loss at the time of treatment) and not by peri-implant therapeutic or implantoplasty procedures.

Eliaz et al. [15] reviewed the requirements for orthopaedic and dental implants, i.e. properties, methods and standards for CaP-based bone prosthesis. Based on the report, to date, there are no clear international standards for surface coverage of implants in terms of animal and clinical studies that could be used to govern the commercial translation of the proposed engineered surfaces. For instance, various commercial implants studied by Penha et al. [350] were found to contain impurities, which if tested would be expected to have an adverse effect on the implant integrity and its rate of survival. As such, the survival of the implant is still assured solely by the experience of the surgeon [3, 349]; however, researchers need to ensure that the proposed surface is safe [351], but it is not clear which standards are to be followed [15]. Since there is no standard of testing procedures, the safety of the engineered surfaces remains a matter of urgency.

Despite their importance for commercialisation, standardised testing of materials is a costly component when implemented. That is why most of the proposed medical materials fall into the 'valley of death.' This death valley is an interesting recent term coined by Martinez-Marquez et al. [256] for the life-cycle product development of medical devices and shows that the majority of products failed due to the large investment needed for pre-clinical and clinical trials, subsequently limiting the clinical translation and commercialisation. An improved setting of anodic oxidation (optimised AO [69, 95, 334]) is now regarded as the industry front-runner when compared to other techniques in terms of simplicity and low-cost surface processing. The optimised AO is capable of lowering coating production costs while also providing adequate design biocompatibility for Ti-based implants. This improved AO is thought to be capable of lowering production costs and reducing the future impact of this 'valley of death' on Ti-based implants.

A machine (AC/DC) for AO is also used for executing it counter process named as electrophoretic deposition (EPD) [62, 352]. Investing in an AO machine could enable a hybrid process that combines AO and EPD in a single optimised setup that is simple to use and has recently been proven to produce excellent coatings [95]. So, the cost of surface modification via this electrochemical process is considered the most economic for the engineering and design of products, processes, and systems. Undoubtedly, to produce titanium from raw materials is expensive [353], so a multifunction and flexible surface modification technique can have reduce the cost of implant production; AO is seen to fit this description. In AO, changing electrolyte formulation and cell setup [95, 277, 278, 334] can help to vary the processing parameters and increased cost-effectiveness.

Optimising the production process could lead to cost minimisation, subsequently increasing the cost effectiveness of the products. In literature, AO is proven to be highly flexible and its process optimisation is feasible. As for a single-step anodisation, the setup for an AO cell can be altered [334] or converted to a hybrid simultaneously [95] without compromising the performance of the final coatings [290]. The hybrid between AO and EPD in single process is proposed to be the most cost effective in producing highly biocompatible and mechanically stable composite coatings. As for the Ti-based implant, via AO, the need for surface pre-treatments is not necessary [290].

Moreover, the discoveries of new, low-cost but stable and biocompatible alloying elements for titanium is progressing and trust for its clinical translation is promising for years to come [257, 290]. Optimised outcomes of anodised titanium as implant coatings can be successfully translated onto the complex geometries characteristic of the current implant market, including dental implant abutments and screws, but also to a wider implant market including orthopaedics [290]. For Ti-based implant, the polishing pre-treatment is not important once the surface was subjected to electrochemical anodisation [290]. During the anodisation process, higher local temperatures (usually more than 600 °C [12]) will remove any adverse biologically molecules [354]. If there are any foreign particles, it appears to not have any significant effect on the implant performances. This is evident from commercialised Ti implants which are contaminated by foreign elements that affect its purity [350] but still show high survival rates upon post implantation [4, 257]. Ormellese et al. discovered an *in situ* and simple recovery procedure after anodic layer damage, recommending either 72 h of anodic layer exposure to NaOH or 6 h of H_2O_2 at room temperature [242]. Their study proving the AO coatings can be restored using simple but reliable cost of oxidation in the process.

6. Future trend of the anodised titanium in the implant's coating evolutions

The production process of anodised titanium via two-step AO is now common practice in order to produce a bio-functionalised and reliable passivation of TiO_2 with higher degrees of mechanical stability [92, 93, 164, 298, 320, 355, 356].

Bartkowiak et al. [355] suggested a U-shaped layering of TNTs derived from two-step anodisation produced a highly adherent TNTs to the substrate. The proposed nanotubes were the second stage anodised passivation of TiO_2, which was guided by nanopit-imprints produced from the first stage of anodisation. As a result, the crystalline nanoporous U-shaped structure of anodised titanium has a scratch resistance that was twice as high compared to the brittle nanotubes produced by single-step AO [355]. Similar procedures were applied to produce the optimised TNTs [320]. The engineered thick interfacial bonding between Ti-base and the nanotubes increased the contact area of the tube bottoms and this characteristic helps to overcome shear forces and bore loadings applied on TNTs [320].

The functionality of TNTs is highly tuneable [77, 78, 79, 162], which fits the optimal design of micro/nano structure for ‘neck & body’ of implants [311], and it can also fit the cell-size microhole array [206] via the narrow window cell growth of TNTs [251]. As for the micro-structured anodised titanium, a superhydrophilic triple hierarchical anodic TiO_2 layer (macro/micro/nano topography [92]) and anti-spalling & well-adhered HAp/TiO_2 coating [93] were also fabricated via two-step AO, all of which were proven mechanically stable and biocompatible.

On the other hand, a study of AO [2] has shown that this electrochemical process is highly flexible [69, 334] and easy to conduct [70, 95], offering wide variety of anodic TiO_2 layer properties including excellent biocompatibility [8, 271] good mechanical stability [16, 314], through multifunctional nanostructured films [11, 49], nano-morphologies [44, 79, 162], complex hierarchical topographies [35, 45, 92, 248], and surface biofunctionalisation [73, 74, 280, 314], whereas all of which were feasible to be implemented as implant coatings [72, 290, 311] and with an economical scale-up or optimised fabrication [69, 95, 256, 334].

However, most of these studies report that anodised titanium has been grown on the block/sheet substrate of cp-Ti and there has been limited analysis of the effect of alloy elements on anodised layers grown from other titanium substrates [297], such as Ti-substrate with an α-dense structure [294], a free loose molten oxide of 3D-printed scaffold [357] or ultrafine-grained Ti [16, 358] before and after AO. Nano-structured films comprised of concurrent regions of tubes and laminar structures have not been documented among the highly promising properties and characteristics of anodised titanium today. In Ti-alloying, the biocompatible beta alloys made up of non-toxic elements (Nb, Ta, and Mo) have outstanding mechanical properties and corrosion resistance [211, 296, 298], making the β-phase titanium alloys as good candidates

for replacing pure Ti and Ti-Al-V alloys in biomedical applications [297], but to validate their clinical translation, more research is required on these topics. Henceforth, this review envisioned that the trend of research for anodised titanium in the future should focus on substrate pre-processing and have more variety of Ti-substrates alloyed with β-elements tested and then anodised to broaden the functionality of the anodised titanium for implant coatings.

In the area of implant surface coating and technology, systemic strategies to test the integrity of the engineered surface coupled with a translated understanding of enhanced biocompatibility and adequate mechanical stability for clinical applications is necessary [6]. An adequate study should focus on comprehensive studies to confirm the chemical composition, followed by assessment of topography suitability for the applications, comparison of different surface morphologies in terms of which coating interfaces having better performance in biological response while displaying reliable mechanical biocompatibility, when tested in dry/wet-contact environments *in vitro* or *in vivo*.

As the implant coating evolves, the versatility of anodised oxidation (AO) as a surface modification/functionalisation technique for the production of multifunctional anodised TiO_2 layer, which is porous in structure from micro to nanoscale, is remarkable. Another feature of AO, is the flexibility of processing that has proved to be easy to set up in a variety of optimised configurations [69, 75, 95, 334]. The low-cost AO as a surface modification technique promotes its feasibility in the industry [69], making it evolve into a variety of applications [308, 309]. As far as anodised titanium is concerned, its distinctive topography, either in micro or nanostructure, is a beneficial interface that acts as a template for other organic/inorganic biomaterials to form multifunctional biocomposite coatings [237, 306, 359] that have been shown to be highly biocompatible and mechanically stable [59, 271, 297, 306, 307, 316, 355]. Figure 10 shows how anodised titanium can be used as a template in a variety of composite coatings, as reported in most current literature [56, 355]. This specialised and specific range of functions makes anodised titanium the most promising coating structure for implants today and in the near future.

Having HAp coatings on non-planar substrates and patterned cathodic surface is not foreign to electrophoretic deposition. Highly ordered microporous bioactive ceramics have been prepared by EPD using a patterned substrate [359] acting as a template. Khanmohammadi et al. [56] produced a patterned substrate capable of providing a strong mechanical interlock in the biocomposite deposit on a metal surface that is mechanically stable compared to other bonding mechanisms such as electrostatic, physical adsorption or chemical bonding. By coating the surface anodised titanium with a suspended composite, an EPD-shaped cathode capable of producing complex deposition layers, which has been shown to have the power to use all of these bonding mechanisms in its deposition and which forms a highly adhesive, dense and mechanically stable biocomposite coatings [56, 59, 95]. Recently, Keceli et al.

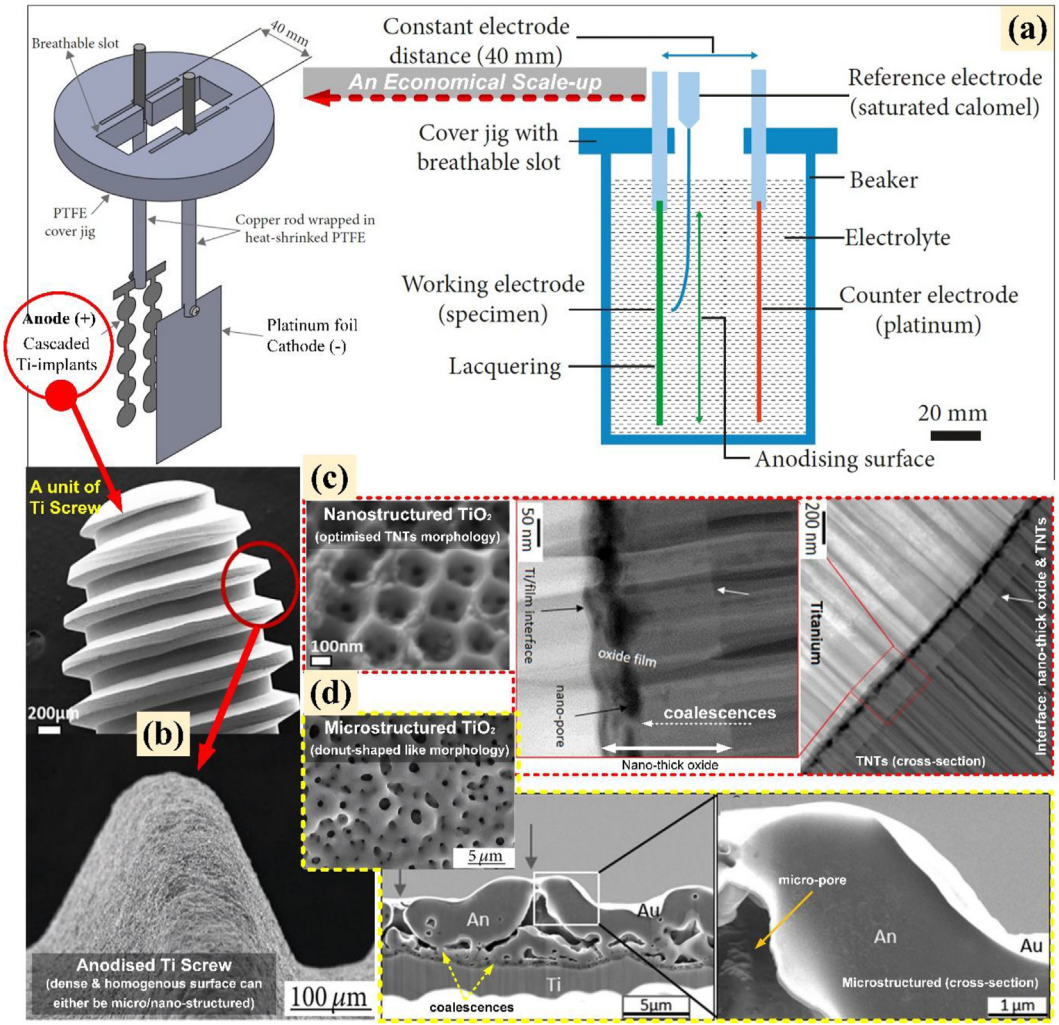

Figure 9. The optimised design of AO cell for commercial fabrication in economical scale-up (a). Ti implants like Ti screw can be anodised simultaneously via cascaded anode. The anodised Ti screw appears to have dense & homogenous surfaces (b), facile fabrication of both nano-(c)/micro-(d) structured morphologies, which have high biocompatibility and mechanical stability. (with permission, images/micrographs were taken and reillustrated from [53, 59, 69, 290, 334]).

[58] used anodised titanium as a template stencil for depositing silk fibroin by electrospinning, while Niu et al. [57] deposited drugs and antimicrobial polymers on anodised titanium using polymerisation, where all of these exhibited stronger biofunctionalised composite coating [61], subsequently strengthening the structure of anodised titanium [60]. These include deposition of carbon nanohorns on the surface of microstructured anodised titanium [59] and chitosan on TNTs [306]. All of these recent studies, prove that the anodised titanium is a great template for producing mechanically stable biocomposite structure, subsequently improving the mechanical biocompatibility.

7. Conclusions

Anodised oxidation (AO) is a method that can substitute the native oxide layer of titanium with a thick crystalline oxide layer engineered to different forms and functionalities that are highly dependent on the type and concentration of electrolyte, cell processing setup and also the processing parameters, such as anodising time and voltage. The evolution of the engineered oxidised structures of TiO_2 anodic layer begins with the attempt to dope Ca and P ions in an anodised matrix, which is evolved into the nanotubes for therapeutic drug delivery and release in implant nanocontainer technology.

In addition, demands for a better implant coating structure has driven the development of anodised titanium into a complex hierarchical coating topography blended with the micromagnetism of CaP-based components, whereas AO requires additional pre-or post-treatments that adds to is processing complexity. However, recent trends of AO were able to optimise the processing design via hybrid AO setup and the formulation of altered electrolytes to produce highly biofunctionalised composite coatings with remarkable mechanical stability, whereas anodised titanium acts as a template stencil upon coating depositions.

In its applications as template stencil for biocomposite coatings, the anodised surfaces have been proven to provide higher mechanical interlocking on the bonding mechanism between organic and inorganic elements. On the other hand, most recent *in/ex vivo* studies have shown that this hybrid topography reinforces cell attachment and rapid new bone development with increased mechanical stability, suggesting that using anodised titanium as template stencil for the fabrication of biocomposite coating is currently a potential application of AO in the future design of implant coatings. With regard to the broad research on

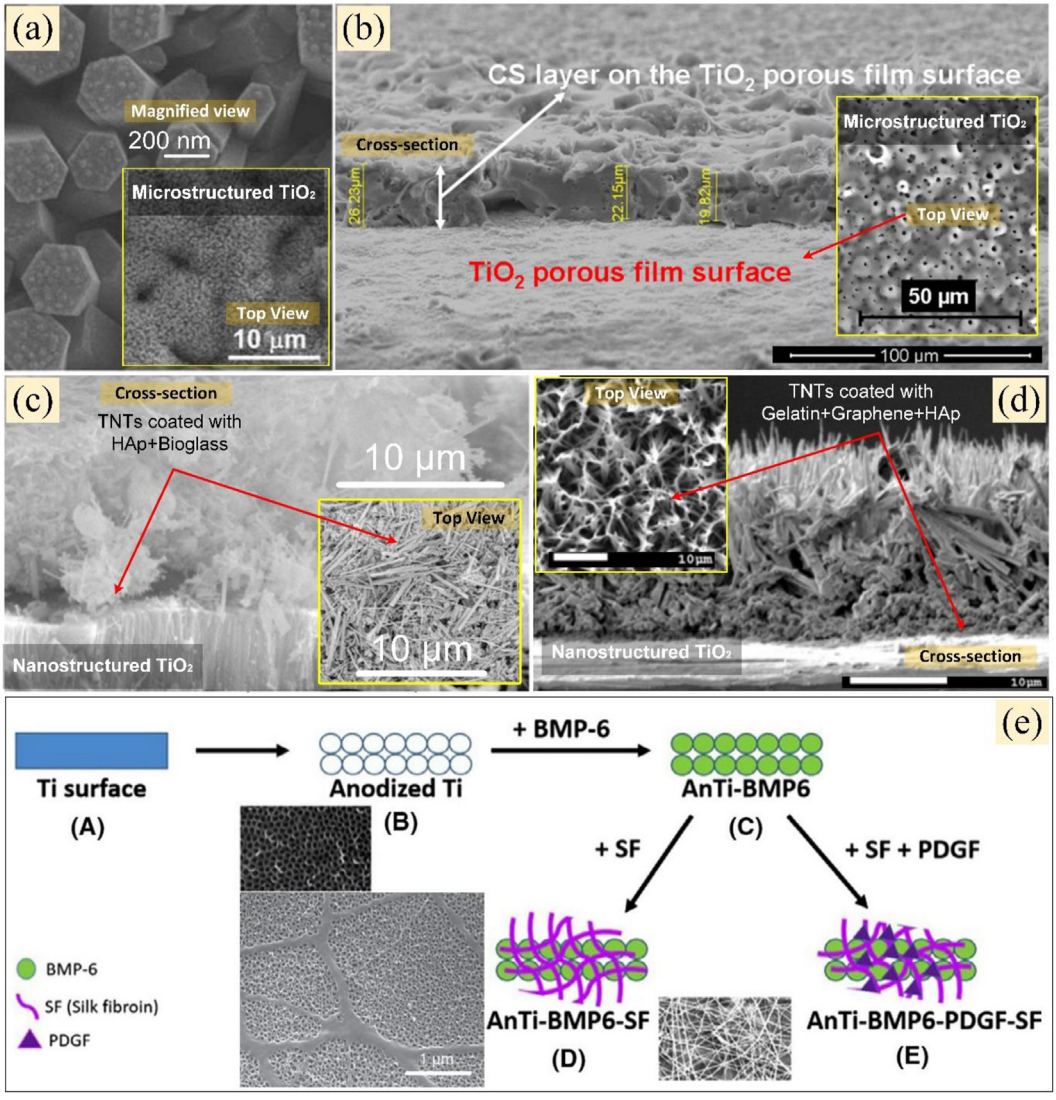

Figure 10. CaP micro-arc anodised titanium used as template to; (a) growth of magnetic nanorod [246], and deposition, (b) chitosan-based biocomposite coatings [360]. While nanocomposite coatings were successfully deposited on TNTs; via electrophoretic deposition (EPD) for (c) HAp/Bioglass [56], and (d) Gelatin/Graphene oxide/HAp [61], meanwhile (e) the process of utilising TNTs as template to deposit electrospinned silk fibroin [58] (reillustrated and taken with permission from [56, 58, 61, 246, 360]).

anodised titanium, there are still lack of clinical studies in literature. To date, there is no standard to govern the coating surface coverage and the period of *in vivo* implantation studies either in animal or clinical trials. Similar to the perspective of anodised titanium mechanical stability, various testing methods and procedures have been proposed but there are no clear international standards, especially in terms of surface biotribology to ensure the testing validity both in dry and wet contact. All of these challenges have become key issues that have affected the understanding and augmenting the integrity of the engineered coating towards optimised clinical translations. Accordingly, this review concludes that any potential trials on anodised titanium should be conducted beyond the *in vitro* assay, as their *in vivo* response is largely unknown for many novel structures.

Declarations

Author contribution statement

All authors listed have significantly contributed to the development and the writing of this article.

Funding statement

This work was supported by Universiti Tun Hussein Onn Malaysia and the Ministry of Higher Education, Malaysia (FRGS/1/2018/TK05/UTHM/03/8 (FRGS K907)).

Data availability statement

Data included in article/supplementary material/referenced in article.

Declaration of interests statement

The authors declare no conflict of interest.

Additional information

No additional information is available for this paper.

References

[1] R. Brånemark, P.-I. Brånemark, B. Rydevik, R.R. Myers, Osseointegration in skeletal reconstruction and rehabilitation, J. Rehabil. Res. Dev. 38 (2001) 175–181.
[2] M.R. Kaluđerović, J.P. Schreckenbach, H.L. Graf, Titanium dental implant surfaces obtained by anodic spark deposition – from the past to the future, Mater. Sci. Eng. C 69 (2016) 1429–1441.
[3] D. Apostu, O. Lucaciu, C. Berce, D. Lucaciu, D. Cosma, Current methods of preventing aseptic loosening and improving osseointegration of titanium implants in cementless total hip arthroplasty: a review, J. Int. Med. Res. 46 (2018) 2104–2119.
[4] A. Civantos, E. Martínez-Campos, V. Ramos, C. Elvira, A. Gallardo, A. Abarrategi, Titanium coatings and surface modifications: toward clinically useful bioactive implants, ACS Biomater. Sci. Eng. 3 (2017) 1245–1261.
[5] J. Jeong, J.H. Kim, J.H. Shim, N.S. Hwang, C.Y. Heo, Bioactive calcium phosphate materials and applications in bone regeneration, Biomater. Res. 23 (2019).
[6] R.S. Liddell, E. Ajami, Y. Li, E. Bajenova, Y. Yang, J.E. Davies, The influence of implant design on the kinetics of osseointegration and bone anchorage homeostasis, Acta Biomater. (2020).
[7] F.A. Shah, P. Thomsen, A. Palmquist, Osseointegration and current interpretations of the bone-implant interface, Acta Biomater. 84 (2019) 1–15.
[8] R. Trindade, T. Albrektsson, S. Galli, Z. Prgomet, P. Tengvall, A. Wennerberg, Osseointegration and foreign body reaction: titanium implants activate the immune system and suppress bone resorption during the first 4 weeks after implantation, Clin. Implant Dent. Relat. Res. 20 (2018) 82–91.
[9] A. Rothschild, F. Edelman, Y. Komem, F. Cosandey, Sensing behavior of TiO_2 thin films exposed to air at low temperatures, Sensor. Actuator. B Chem. 67 (2000) 282–289.
[10] J. Rouquerol, K.S.W. Sing, P. Llewellyn, Adsorption by metal oxides, in: Adsorpt. By Powders Porous Solids Princ. Methodol. Appl, second ed., 2013, pp. 393–465.
[11] D.V. Shtansky, E.A. Levashov, I.V. Sukhorukova, Multifunctional bioactive nanostructured films, in: Hydroxyapatite Biomed. Appl., 2015, pp. 159–188.
[12] D.A.H. Hanaor, C.C. Sorrell, Review of the anatase to rutile phase transformation, J. Mater. Sci. 46 (2011) 855–874.
[13] C. Ning, P. Yu, Y. Zhu, M. Yao, X. Zhu, X. Wang, Z. Lin, W. Li, S. Wang, G. Tan, Y. Zhang, Y. Wang, C. Mao, Built-in microscale electrostatic fields induced by anatase–rutile-phase transition in selective areas promote osteogenesis, NPG Asia Mater. 8 (2016) 243.
[14] H.H. Park, I.S. Park, K.S. Kim, W.Y. Jeon, B.K. Park, H.S. Kim, T.S. Bae, M.H. Lee, Bioactive and electrochemical characterization of TiO_2 nanotubes on titanium via anodic oxidation, Electrochim. Acta 55 (2010) 6109–6114.
[15] N. Eliaz, N. Metoki, Calcium Phosphate Bioceramics: a review of their history, structure, properties, coating technologies and biomedical applications, Matrials MDPI 10 (2017) 2–104.
[16] C.N. Elias, D.J. Fernandes, F.M. De Souza, E.D.S. Monteiro, R.S. De Biasi, Mechanical and clinical properties of titanium and titanium-based alloys (Ti G2, Ti G4 cold worked nanostructured and Ti G5) for biomedical applications, J. Mater. Res. Technol. 8 (2019) 1060–1069.
[17] X. Liu, P.K. Chu, C. Ding, Surface modification of titanium, titanium alloys, and related materials for biomedical applications, Mater. Sci. Eng. R Rep. 47 (2004) 49–121.
[18] T.C. Lee, H.Z. Abdullah, P. Koshy, M.I. Idris, Ultraviolet-assisted biomimetic coating of bone-like apatite on anodised titanium for biomedical applications, Thin Solid Films 660 (2018) 191–198.
[19] N.R. Patel, P.P. Gohil, A review on biomaterials: scope, applications & human anatomy significance, in: Int. J. Emerg. Technol. Adv. Eng., 2012. www.ijetae.com. (Accessed 2 February 2019).
[20] International Titanium Association (ITA), Medical technology, Int. Titan. Assoc. (2019). https://titanium.org/page/MedicalTechnology. (Accessed 26 December 2019).
[21] S. Najeeb, M.S. Zafar, Z. Khurshid, S. Zohaib, S.M. Hasan, R.S. Khan, Bisphosphonate releasing dental implant surface coatings and osseointegration: a systematic review, J. Taibah Univ. Med. Sci. 12 (2017) 369–375.
[22] R. Osman, M. Swain, A critical review of dental implant materials with an emphasis on titanium versus zirconia, Materials 8 (2015) 932–958.
[23] T.A. El Awadly, G. Wu, M. Ayad, I.A.W. Radi, D. Wismeijer, H. Abo El Fetouh, R.B. Osman, A histomorphometric study on treated and untreated ceramic filled PEEK implants versus titanium implants: preclinical in vivo study, Clin. Oral Implants Res. 31 (2020) 246–254.
[24] L. Wang, X. Hu, X. Ma, Z. Ma, Y. Zhang, Y. Lu, X. Li, W. Lei, Y. Feng, Promotion of osteointegration under diabetic conditions by tantalum coating-based surface modification on 3-dimensional printed porous titanium implants, Colloids Surf. B Biointerfaces 148 (2016) 440–452.
[25] F. Ordikhani, E. Tamjid, A. Simchi, Characterization and antibacterial performance of electrodeposited chitosan-vancomycin composite coatings for prevention of implant-associated infections, Mater. Sci. Eng. C 41 (2014) 240–248.
[26] S. Ferraris, S. Spriano, Antibacterial titanium surfaces for medical implants, Mater. Sci. Eng. C 61 (2016) 965–978.
[27] M. Croes, S. Bakhshandeh, I.A.J. van Hengel, K. Lietaert, K.P.M. van Kessel, B. Pouran, B.C.H. van der Wal, H.C. Vogely, W. Van Hecke, A.C. Fluit, C.H.E. Boel, J. Alblas, A.A. Zadpoor, H. Weinans, S. Amin Yavari, Antibacterial and immunogenic behavior of silver coatings on additively manufactured porous titanium, Acta Biomater. 81 (2018) 315–327.
[28] S. Saidin, M.A. Jumat, N.A.A. Mohd Amin, A.S. Saleh Al-Hammadi, Organic and inorganic antibacterial approaches in combating bacterial infection for biomedical application, Mater. Sci. Eng. C 118 (2021) 111382.
[29] C. Gao, C. Li, C. Wang, Y. Qin, Z. Wang, F. Yang, H. Liu, F. Chang, J. Wang, Advances in the induction of osteogenesis by zinc surface modification based on titanium alloy substrates for medical implants, J. Alloys Compd. 726 (2017) 1072–1084.
[30] M. Kulkarni, A. Mazare, E. Gongadze, Perutkova, V. Kralj-Iglic, I. Milošev, P. Schmuki, A. Iglič, M. Mozetič, Titanium nanostructures for biomedical applications, Nanotechnology 26 (2015).
[31] C. Domínguez-Trujillo, E. Peón, E. Chicardi, H. Pérez, J.A. Rodríguez-Ortiz, J.J. Pavón, J. García-Couce, J.C. Galván, F. García-Moreno, Y. Torres, Sol-gel deposition of hydroxyapatite coatings on porous titanium for biomedical applications, Surf. Coating. Technol. 333 (2018) 158–162.
[32] W. Zhang, J. Gu, C. Zhang, Y. Xie, X. Zheng, Preparation of titania coating by induction suspension plasma spraying for biomedical application, Surf. Coating. Technol. 358 (2019) 511–520.
[33] H.Z. Abdullah, P. Koshy, C.C. Sorrell, Gel oxidation of titanium for biomedical application, in: Adv. Mater. Res., 2013, pp. 122–126.
[34] Y.S. Cho, L.K. Liao, C.H. Hsu, Y.H. Hsu, W.Y. Wu, S.C. Liao, K.H. Chen, P.W. Lui, S. Zhang, S.Y. Lien, Effect of substrate bias on biocompatibility of amorphous carbon coatings deposited on Ti6Al4V by PECVD, Surf. Coating. Technol. 357 (2019) 212–217.
[35] A.M. Vilardell, N. Cinca, N. Garcia-Giralt, C. Müller, S. Dosta, M. Sarret, I.G. Cano, X. Nogués, J.M. Guilemany, In-vitro study of hierarchical structures: anodic oxidation and alkaline treatments onto highly rough titanium cold gas spray coatings for biomedical applications, Mater. Sci. Eng. C 91 (2018) 589–596.
[36] C.-C. Ma, E.M.J. Peres, Corrosion resistance of anodized and unanodized titanium; Effect of common mineral acid solutions, Ind. Eng. Chem. 43 (1951) 675–679. https://pubs.acs.org/sharingguidelines. (Accessed 14 February 2021).

[37] M.V. Diamanti, B. Del Curto, M. Pedeferri, Anodic oxidation of titanium: from technical aspects to biomedical applications, J. Appl. Biomater. Biomech. 9 (2011) 55–69.

[38] T. Mi, B. Jiang, Z. Liu, L. Fan, Plasma formation mechanism of microarc oxidation, Electrochim. Acta 123 (2014) 369–377.

[39] L.M. Muresan, Corrosion protective coatings for Ti and Ti alloys used for biomedical implants, in: Intell. Coatings Corros. Control, Elsevier, 2015, pp. 585–602.

[40] X. Wang, B. Li, L. Zhou, J. Ma, X. Zhang, H. Li, C. Liang, S. Liu, H. Wang, Influence of surface structures on biocompatibility of TiO_2/HA coatings prepared by MAO, Mater. Chem. Phys. 215 (2018) 339–345.

[41] W.H. Song, Y.K. Jun, Y. Han, S.H. Hong, Biomimetic apatite coatings on micro-arc oxidized titania, Biomaterials 25 (2004) 3341–3349.

[42] T.C. Lee, M.H.H. Mazlan, M.I. Abbas, H.Z. Abdullah, M.I. Idris, Effect of bath temperature on surface properties of anodised titanium for biomedical application, Mater. Sci. Forum 840 (2016) 175–179.

[43] T.C. Lee, H.Z. Abdullah, P. Koshy, M.I. Idris, Deposition of novel bioactive nanoflower-like sodium titanate on TiO_2 coating via anodic oxidation for biomedical applications, Mater. Lett. 216 (2018) 256–260.

[44] D.J. Lin, L.J. Fuh, W.C. Chen, Nano-morphology, crystallinity and surface potential of anatase on micro-arc oxidized titanium affect its protein adsorption, cell proliferation and cell differentiation, Mater. Sci. Eng. C 107 (2020) 110204.

[45] W.-C. Lan, C.-H. Wang, B.-H. Huang, Y.-C. Cho, T. Saito, C.-C. Huang, M.-S. Huang, Fabrication of a promising hierarchical porous surface on titanium for promoting biocompatibility, Appl. Sci. 10 (2020) 1363.

[46] A.A. Ayon, M. Cantu, K. Chava, C.M. Agrawal, M.D. Feldman, D. Johnson, D. Patel, D. Marton, E. Shi, Drug loading of nanoporous TiO_2 films, Biomed. Mater. 1 (2006) L11–L15.

[47] G. Eaninwene, C. Yao, T.J. Webster, T.J. Webster, Enhanced osteoblast adhesion to drug-coated anodized nanotubular titanium surfaces, Int. J. Nanomed. 3 (2008) 257–264. http://www.ncbi.nlm.nih.gov/pubmed/18686785. (Accessed 19 February 2019).

[48] E. Zalnezhad, S. Baradaran, A.R. Bushroa, A.A.D. Sarhan, Mechanical property enhancement of Ti-6Al-4V by Multilayer thin solid film Ti/TiO_2 nanotubular array coating for biomedical application, Metall. Mater. Trans. A Phys. Metall. Mater. Sci. 45 (2014) 785–797.

[49] T. Li, K. Gulati, N. Wang, Z. Zhang, S. Ivanovski, Understanding and augmenting the stability of therapeutic nanotubes on anodized titanium implants, Mater. Sci. Eng. C 88 (2018) 182–195.

[50] M. Mansoorianfar, A. Khataee, Z. Riahi, K. Shahin, M. Asadnia, A. Razmjou, A. Hojjati Najafabadi, C. Mei, Y. Orooji, D. Li, Scalable fabrication of tunable titanium nanotubes via sonoelectrochemical process for biomedical applications, Ultrason. Sonochem. (2019) 104783.

[51] H. Ishizawa, M. Ogino, Formation and characterization of anodic titanium oxide films containing Ca and P, J. Biomed. Mater. Res. 29 (1995) 65–72.

[52] H. Ishizawa, M. Ogino, Characterization of thin hydroxyapatite layers formed on anodic titanium oxide films containing Ca and P by hydrothermal treatment, J. Biomed. Mater. Res. 29 (1995) 1071–1079.

[53] W.J. Duncan, M.H. Lee, T.S. Bae, S.J. Lee, J. Gay, C. Loch, Anodisation increases integration of unloaded titanium implants in sheep mandible, BioMed Res. Int. 2015 (2015).

[54] K. Gulati, M. Kogawa, M. Prideaux, D.M. Findlay, G.J. Atkins, D. Losic, Drug-releasing nano-engineered titanium implants: therapeutic efficacy in 3D cell culture model, controlled release and stability, Mater. Sci. Eng. C 69 (2016) 831–840.

[55] Y. Li, Y. Yang, R. Li, X. Tang, D. Guo, Y. Qing, Y. Qin, Enhanced antibacterial properties of orthopedic implants by titanium nanotube surface modification: a review of current techniques, Int. J. Nanomed. 14 (2019) 7217–7236.

[56] S. Khanmohammadi, M. Ojaghi-Ilkhchi, M. Farrokhi-Rad, Development of bioglass coating reinforced with hydroxyapatite whiskers on TiO_2 nanotubes via electrophoretic deposition, Ceram. Int. 47 (2021) 1333–1343.

[57] Z. Li, T. Du, C. Ruan, X. Niu, Bioinspired mineralized collagen scaffolds for bone tissue engineering, Bioact. Mater. 6 (2021) 1491–1511.

[58] H.G. Keceli, C. Bayram, E. Celik, N. Ercan, M. Demirbilek, R.M. Nohutcu, Dual delivery of platelet-derived growth factor and bone morphogenetic factor-6 on titanium surface to enhance the early period of implant osseointegration, J. Periodontal. Res. 55 (2020) 694–704.

[59] S. Takada, E. Hirata, M. Sakairi, E. Miyako, Y. Takano, N. Ushijima, M. Yudasaka, S. Iijima, A. Yokoyama, Carbon nanohorn coating by electrodeposition accelerate bone formation on titanium implant, Artif. Cells, Nanomedicine, Biotechnol. 49 (2021) 20–29.

[60] A. Kamyar, M. Khakbiz, A. Zamanian, M. Yasaei, B. Yarmand, Synthesis of a novel dexamethasone intercalated layered double hydroxide nanohybrids and their deposition on anodized titanium nanotubes for drug delivery purposes, J. Solid State Chem. 271 (2019) 144–153.

[61] Y. Yan, X. Zhang, H. Mao, Y. Huang, Q. Ding, X. Pang, Hydroxyapatite/gelatin functionalized graphene oxide composite coatings deposited on TiO_2 nanotube by electrochemical deposition for biomedical applications, Appl. Surf. Sci. 329 (2015) 76–82.

[62] H.Z. Abdullah, Titanium Surface Modification by Oxidation for Biomedical Application, University of New South Wales, 2010. http://eprints.uthm.edu.my/2701/. (Accessed 6 February 2019).

[63] Y.K. Pan, C.Z. Chen, D.G. Wang, Z.Q. Lin, Preparation and bioactivity of micro-arc oxidized calcium phosphate coatings, Mater. Chem. Phys. 141 (2013) 842–849.

[64] G. Tang, R. Zhang, Y. Yan, Z. Zhu, Preparation of porous anatase titania film, Mater. Lett. 58 (2004) 1857–1860.

[65] M.P. Neupane, I.S. Park, T.S. Bae, M.H. Lee, Sonochemical assisted synthesis of nano-structured titanium oxide by anodic oxidation, J. Alloys Compd. 581 (2013) 418–422.

[66] Y. Han, S.H. Hong, K. Xu, Structure and in vitro bioactivity of titania-based films by micro-arc oxidation, Surf. Coating. Technol. 168 (2003) 249–258.

[67] H. Yong, W. Yingjun, N. Chengyun, N. Kaihui, H. Yong, Preparation and properties of a cerium-containing hydroxyapatite coating on commercially pure titanium by micro-arc oxidation, Rare Met. 27 (2008) 257–260.

[68] C.S. Chen, Y.L. Tsao, D.J. Wang, S.F. Ou, H.Y. Cheng, Y.C. Chiang, K.L. Ou, Research on cell behavior related to anodized and hydrothermally treated titanium surface, Appl. Surf. Sci. 271 (2013) 1–6.

[69] J.S. Khaw, M. Curioni, P. Skeldon, C.R. Bowen, S.H. Cartmell, Y. Li, A novel methodology for economical scale-Up of TiO_2 nanotubes fabricated on Ti and Ti alloys, J. Nanotechnol. Hindawi 20 (2019) 1–13.

[70] Y. Li, W. Wang, F. Yu, D. Wang, S. Guan, Y. Li, M. Qi, Characterization and cytocompatibility of hierarchical porous TiO_2 coatings incorporated with calcium and strontium by one-step micro-arc oxidation, Mater. Sci. Eng. C 109 (2020) 110610.

[71] X. Zhao, T. Wang, S. Qian, X. Liu, J. Sun, B. Li, Silicon-doped titanium dioxide nanotubes promoted bone formation on titanium implants, Int. J. Mol. Sci. 17 (2016) 292.

[72] C.I. Fernando de Almeida Barros Mourão, V.I. Senna Diniz, P. Cesar Silva III, L.I. Meirelles, E. V Santos Junior, A.V. Schanaider, In-vivo bone response to titanium screw implants anodized in sodium sulfate Flávio Alexandre Lima Pinheiro, Acta Cir. Bras. 29 (2014) 2014–2377.

[73] A. Roguska, M. Pisarek, A. Belcarz, L. Marcon, M. Holdynski, M. Andrzejczuk, M. Janik-Czachor, Improvement of the bio-functional properties of TiO_2 nanotubes, Appl. Surf. Sci. 388 (2016) 775–785.

[74] Y. Wang, S.E. Naleway, B. Wang, Biological and bioinspired materials: structure leading to functional and mechanical performance, Bioact. Mater. 5 (2020) 745–757.

[75] J.J. Jasinski, Investigation of bio-functional properties of titanium substrates after hybrid oxidation, Arch. Metall. Mater. 65 (2020) 141–149.

[76] Y. Zhang, D. Yu, M. Gao, D. Li, Y. Song, R. Jin, W. Ma, X. Zhu, Growth of anodic TiO_2 nanotubes in mixed electrolytes and novel method to extend nanotube diameter, Electrochim. Acta 160 (2015) 33–42.

[77] E. Feschet-Chassot, V. Raspal, Y. Sibaud, O.K. Awitor, F. Bonnemoy, J.L. Bonnet, J. Bohatier, Tunable functionality and toxicity studies of titanium dioxide nanotube layers, Thin Solid Films 519 (2011) 2564–2568.

[78] V.C. Anitha, D. Menon, S.V. Nair, R. Prasanth, Electrochemical tuning of titania nanotube morphology in inhibitor electrolytes, Electrochim. Acta 55 (2010) 3703–3713.

[79] N.S. Peighambardoust, F. Nasirpouri, Manipulating morphology, pore geometry and ordering degree of TiO_2 nanotube arrays by anodic oxidation, Surf. Coating. Technol. 235 (2013) 727–734.

[80] G. Wang, Y. Wan, B. Ren, Z. Liu, Bioactivity of micropatterned TiO_2 nanotubes fabricated by micro-milling and anodic oxidation, Mater. Sci. Eng. C 95 (2019) 114–121.

[81] K. Kyo-Han, N. Ramaswamy, Electrochemical Surface Modification of Titanium in Dentistry, 2009.

[82] E.J. Park, Y.H. Song, M.J. Hwang, H.J. Song, Y.J. Park, Surface characterization and osteoconductivity evaluation of micro/nano surface formed on titanium using anodic oxidation combined with H_2O_2 etching and hydrothermal treatment, J. Nanosci. Nanotechnol. 15 (2015) 6133–6136.

[83] D. He, P. Wang, P. Liu, X. Liu, F. Ma, W. Li, X. Chen, J. Zhao, H. Ye, Preparation of hydroxyapatite-titanium dioxide coating on Ti6Al4V substrates using hydrothermal-electrochemical method, J. Wuhan Univ. Technol.-Materials Sci. Ed. 31 (2016) 461–467.

[84] S.F. Ou, H.H. Chou, C.S. Lin, C.J. Shih, K.K. Wang, Y.N. Pan, Effects of anodic oxidation and hydrothermal treatment on surface characteristics and biocompatibility of Ti-30Nb-1Fe-1Hf alloy, Appl. Surf. Sci. 258 (2012) 6190–6198.

[85] R. Rodriguez, K. Kim, J.L. Ong, In vitro osteoblast response to anodized titanium and anodized titanium followed by hydrothermal treatment, J. Biomed. Mater. Res. 65A (2003) 352–358.

[86] A. Rajendran, S. Sugunapriyadharshini, D. Mishra, D.K. Pattanayak, Role of calcium ions in defining the bioactivity of surface modified Ti metal, Mater. Sci. Eng. C 98 (2019) 197–204.

[87] I. González Morán, F. Fernández Martínez, M. del Río Merino, M.V. Diamanti, M.P. Pedeferri, X. Chen, Photocatalytic behaviour of anodised titanium using different cathodes, Surf. Eng. 35 (2019) 46–53.

[88] J. Lausmaa, Mechanical, thermal, Chemical and Electrochemical Surface Treatment of Titanium, 2001, pp. 231–266.

[89] T.C. Lee, P. Koshy, H.Z. Abdullah, M.I. Idris, Precipitation of bone-like apatite on anodised titanium in simulated body fluid under UV irradiation, Surf. Coating. Technol. 301 (2016) 20–28.

[90] D.J. Lin, L.J. Fuh, C.Y. Chen, W.C. Chen, J.H.C. Lin, C.C. Chen, Rapid nano-scale surface modification on micro-arc oxidation coated titanium by microwave-assisted hydrothermal process, Mater. Sci. Eng. C 95 (2019) 236–247.

[91] Y. Li, W. Wang, H. Liu, J. Lei, J. Zhang, H. Zhou, M. Qi, Formation and in vitro/in vivo performance of "cortex-like" micro/nano-structured TiO_2 coatings on titanium by micro-arc oxidation, Mater. Sci. Eng. C 87 (2018) 90–103.

[92] Y. Li, W. Wang, J. Duan, M. Qi, A super-hydrophilic coating with a macro/micro/nano triple hierarchical structure on titanium by two-step micro-arc oxidation treatment for biomedical applications, Surf. Coating. Technol. 311 (2017) 1–9.

[93] B.L. Pereira, G. Beilner, C.M. Lepienski, E.S. Szameitat, B.S. Chee, N.K. Kuromoto, L.L. dos Santos, I. Mazzaro, A.P.R.A. Claro, M.J.D. Nugent, Oxide coating containing apatite formed on Ti-25Nb-25Ta alloy treated by two-step plasma electrolytic oxidation, Surf. Coating. Technol. 382 (2020).

[94] K. Indira, U.K. Mudali, T. Nishimura, N. Rajendran, A review on TiO_2 nanotubes: influence of anodization parameters, formation mechanism, properties, corrosion behavior, and biomedical applications, J. Bio- Tribo-Corrosion. 1 (2015).

[95] L. Chitsaz-Khoyi, J. Khalil-Allafi, A. Motallebzadeh, M. Etminanfar, The effect of hydroxyapatite nanoparticles on electrochemical and mechanical performance of TiC/N coating fabricated by plasma electrolytic saturation method, Surf. Coating. Technol. 394 (2020) 125817.

[96] E. Marin, M.V. Diamanti, M. Boffelli, M. Sendoh, M.P. Pedeferri, A. Mazinani, M. Moscatelli, B. Del Curto, W. Zhu, G. Pezzotti, R. Chiesa, Effect of etching on the composition and structure of anodic spark deposition films on titanium, Mater. Des. 108 (2016) 77–85.

[97] O. Oleshko, V. Deineka, Y. Husak, V. Korniienko, B. Dryhval, J. Dudko, O. Solodovnyk, W. Simka, J. Michalska, O. Mishchenko, K. Grundsteins, M. Pogorielov, Plasma electrolytic oxidation of TiZr alloy in ZnONPs-contained solution: structural and biological assessment, in: Springer Proc. Phys., Springer Science and Business Media Deutschland GmbH, 2020, pp. 75–82.

[98] V.A. Nadolinny, I.B. Kireenko, EPR of transition metal ions in microplasma coatings on the surface of Ti−0,3al and Ti−6Al−4V titanium alloys, Surf. Coating. Technol. 325 (2017) 333–337.

[99] A.A. Voevodin, A.L. Yerokhin, V.V. Lyubimov, M.S. Donley, J.S. Zabinski, Characterization of wear protective Al-Si-O coatings formed on Al-based alloys by micro-arc discharge treatment, Surf. Coating. Technol. 86–87 (1996) 516–521.

[100] V.M. Frauchiger, M. Textor, F. Schlottig, B. Gasser, N.D. Spencer, Anodic plasma-chemical treatment of titanium implant surfaces, in: Eur. Cells Mater., 2001, p. 26.

[101] A.L. Yerokhin, X. Nie, A. Leyland, A. Matthews, S.J. Dowey, Plasma electrolysis for surface engineering, Surf. Coating. Technol. 122 (1999) 73–93.

[102] J.L. Delplancke, M. Degrez, A. Fontana, R. Winand, Self-colour anodizing of titanium, Surf. Technol. 16 (1982) 153–162.

[103] D. Ellerbrock, D.D. MacDonald, Passivity of titanium, part 1: film growth model diagnostics, J. Solid State Electrochem. 18 (2014) 1485–1493.

[104] D. Regonini, C.R. Bowen, A. Jaroenworaluck, R. Stevens, A review of growth mechanism, structure and crystallinity of anodized TiO_2 nanotubes, Mater. Sci. Eng. R Rep. 74 (2013) 377–406.

[105] S. Minagar, C.C. Berndt, J. Wang, E. Ivanova, C. Wen, A review of the application of anodization for the fabrication of nanotubes on metal implant surfaces, Acta Biomater. 8 (2012) 2875–2888.

[106] J. Choi, R.B. Wehrspohn, J. Lee, U. Gösele, Anodization of nanoimprinted titanium: a comparison with formation of porous alumina, Electrochim. Acta 49 (2004) 2645–2652.

[107] T.J. Webster, C. Yao, Anodization: a promising nano modification technique of titanium-based implants for orthopedic applications, in: Surg. Tools Med. Devices, second ed., 2016, pp. 55–80.

[108] Y. Li, Q. Ma, J. Han, L. Ji, J. Wang, J. Chen, Y. Wang, Controllable preparation, growth mechanism and the properties research of TiO_2 nanotube arrays, Appl. Surf. Sci. 297 (2014) 103–108.

[109] W.F. Oliveira, I.R.S. Arruda, G.M.M. Silva, G. Machado, L.C.B.B. Coelho, M.T.S. Correia, Functionalization of titanium dioxide nanotubes with biomolecules for biomedical applications, Mater. Sci. Eng. C 81 (2017) 597–606.

[110] S. Kim, M. Seong, J. Choi, Rapid breakdown anodization for the preparation of titania nanotubes in halogen-free acids, J. Electrochem. Soc. 162 (2015) C205–C208.

[111] C. Arunchandran, S. Ramya, R.P. George, U. Kamachi Mudali, Corrosion inhibitor storage and release property of TiO_2 nanotube powder synthesized by rapid breakdown anodization method, Mater. Res. Bull. 48 (2013) 635–639.

[112] R. Hahn, J.M. Macak, P. Schmuki, Rapid anodic growth of TiO_2 and WO_3 nanotubes in fluoride free electrolytes, Electrochem. Commun. 9 (2007) 947–952.

[113] C. Richter, E. Panaitescu, R. Willey, L. Menon, Titania nanotubes prepared by anodization in fluorine-free acids, J. Mater. Res. 22 (2007) 1624–1631.

[114] R.P. Antony, T. Mathews, A. Dasgupta, S. Dash, A.K. Tyagi, B. Raj, Rapid breakdown anodization technique for the synthesis of high aspect ratio and high surface area anatase TiO_2 nanotube powders, J. Solid State Chem. 184 (2011) 624–632.

[115] S. Ali, H. Granbohm, J. Lahtinen, S.P. Hannula, Titania nanotubes prepared by rapid breakdown anodization for photocatalytic decolorization of organic dyes under UV and natural solar light, Nanoscale Res. Lett. 13 (2018).

[116] T.C. Lee, In Vitro Bioactivities of Anodised Titanium in Mixture of β-glycerophosphate and Calcium Acetate for Biomedical Application, University Tun Hussein Onn Malaysia, 2016. http://eprints.uthm.edu.my/9216/1/Lee_Te_Chuan.pdf. (Accessed 3 February 2019).

[117] G. Napoli, M. Paura, T. Vela, A. Di Schino, Colouring titanium alloys by anodic oxidation, Metalurgija 57 (2018) 111–113. https://hrcak.srce.hr/189377.

[118] Y.T. Sul, C.B. Johansson, Y. Jeong, T. Albrektsson, The electrochemical oxide growth behaviour on titanium in acid and alkaline electrolytes, Med. Eng. Phys. 23 (2001) 329–346.

[119] T.C. Lee, M.I. Idris, H.Z. Abdullah, C.C. Sorrell, Effect of electrolyte concentration on anodised titanium in mixture of β-glycerophosphate (β-GP) and calcium acetate (CA), Adv. Mater. Res. 1087 (2015) 116–120.

[120] Y.T. Sul, C.B. Johansson, K. Röser, T. Albrektsson, Qualitative and quantitative observations of bone tissue reactions to anodised implants, Biomaterials 23 (2002) 1809–1817.

[121] V. Zwilling, M. Aucouturier, E. Darque-Ceretti, Anodic oxidation of titanium and TA6V alloy in chromic media. An electrochemical approach, Electrochim. Acta 45 (1999) 921–929.

[122] V. Zwilling, E. Darque-Ceretti, A. Boutry-Forveille, D. David, M.Y. Perrin, M. Aucouturier, Structure and physicochemistry of anodic oxide films on titanium and TA6V alloy, Surf. Interface Anal. 27 (1999) 629–637.

[123] H. Jha, R. Hahn, P. Schmuki, Ultrafast oxide nanotube formation on TiNb, TiZr and TiTa alloys by rapid breakdown anodization, Electrochim. Acta 55 (2010) 8883–8887.

[124] Q.A. Nguyen, Y.V. Bhargava, T.M. Devine, Titania nanotube formation in chloride and bromide containing electrolytes, Electrochem. Commun. 10 (2008) 471–475.

[125] E. Panaitescu, C. Richter, L. Menon, A study of titania nanotube synthesis in chloride-ion-containing media, J. Electrochem. Soc. 155 (2008) E7.

[126] A. Pawlik, M. Jarosz, K. Syrek, G.D. Sulka, Co-delivery of ibuprofen and gentamicin from nanoporous anodic titanium dioxide layers, Colloids Surf. B Biointerfaces 152 (2017) 95–102.

[127] D. Losic, M.S. Aw, A. Santos, K. Gulati, M. Bariana, Titania nanotube arrays for local drug delivery: recent advances and perspectives, Expet Opin. Drug Deliv. 12 (2015) 103–127.

[128] M.F. Kunrath, R. Hubler, R.S.A. Shinkai, E.R. Teixeira, Application of TiO_2 nanotubes as a drug delivery system for biomedical implants: a critical overview, ChemistrySelect 3 (2018) 11180–11189.

[129] N. Çalişkan, C. Bayram, E. Erdal, Z. Karahaliloğlu, E.B. Denkbaş, Titania nanotubes with adjustable dimensions for drug reservoir sites and enhanced cell adhesion, Mater. Sci. Eng. C 35 (2014) 100–105.

[130] L. Shi, H. Xu, X. Liao, G. Yin, Y. Yao, Z. Huang, X. Chen, X. Pu, Fabrication of two-layer nanotubes with the pear-like structure by an in-situ voltage up anodization and the application as a drug delivery platform, J. Alloys Compd. 647 (2015) 590–595.

[131] M. Jarosz, A. Pawlik, M. Szuwarzyński, M. Jaskuła, G.D. Sulka, Nanoporous anodic titanium dioxide layers as potential drug delivery systems: drug release kinetics and mechanism, Colloids Surf. B Biointerfaces 143 (2016) 447–454.

[132] W.-T. Kim, K.-H. Na, J.-K. Lee, I. Jang, D.-S. Choi, W.-Y. Choi, Porous TiO_2 nanotube arrays for drug loading and their elution sensing, J. Nanosci. Nanotechnol. 19 (2019) 1743–1748. http://www.ncbi.nlm.nih.gov/pubmed/19280965. (Accessed 15 February 2019).

[133] M. Sinn Aw, M. Kurian, D. Losic, Non-eroding drug-releasing implants with ordered nanoporous and nanotubular structures: concepts for controlling drug release, Biomater. Sci. 2 (2014) 10–34.

[134] A. Santos, M. Sinn Aw, M. Bariana, T. Kumeria, Y. Wang, D. Losic, Drug-releasing implants: current progress, challenges and perspectives, J. Mater. Chem. B. 2 (2014) 6157–6182.

[135] R.B.S.M.N. Mydin, R. Hazan, M.F. FaridWajidi, S. Sreekantan, Titanium dioxide nanotube arrays for biomedical implant materials and nanomedicine applications, in: Titan. Dioxide - Mater. A Sustain. Environ., InTech, 2018.

[136] D. Ionita, D. Bajenaru-Georgescu, G. Totea, A. Mazare, P. Schmuki, I. Demetrescu, Activity of vancomycin release from bioinspired coatings of hydroxyapatite or TiO2 nanotubes, Int. J. Pharm. 517 (2017) 296–302.

[137] L.H. Li, Y.M. Kong, H.W. Kim, Y.W. Kim, H.E. Kim, S.J. Heo, J.Y. Koak, Improved biological performance of Ti implants due to surface modification by micro-arc oxidation, Biomaterials 25 (2004) 2867–2875.

[138] F.Y. Teng, I.C. Tai, M.W. Wang, Y.J. Wang, C.C. Hung, C.C. Tseng, The structures, electrochemical and cell performance of titania films formed on titanium by micro-arc oxidation, J. Taiwan Inst. Chem. Eng. 45 (2014) 1331–1337.

[139] H.J. Song, K.H. Shin, M.S. Kook, H.K. Oh, Y.J. Park, Effects of the electric conditions of AC-type microarc oxidation and hydrothermal treatment solution on the characteristics of hydroxyapatite formed on titanium, Surf. Coating. Technol. 204 (2010) 2273–2278.

[141] S.A. Fadl-allah, Q. Mohsen, Characterization of native and anodic oxide films formed on commercial pure titanium using electrochemical properties and morphology techniques, Appl. Surf. Sci. 256 (2010) 5849–5855.

[142] H.Y. Si, Z.H. Sun, X. Kang, W.W. Zi, H.L. Zhang, Voltage-dependent morphology, wettability and photocurrent response of anodic porous titanium dioxide films, Microporous Mesoporous Mater. 119 (2009) 75–81.

[143] X. Cui, H.-M. Kim, M. Kawashita, L. Wang, T. Xiong, T. Kokubo, T. Nakamura, Preparation of bioactive titania films on titanium metal via anodic oxidation, Dent. Mater. 25 (2009) 80–86.

[144] M. Montazeri, C. Dehghanian, M. Shokouhfar, A. Baradaran, Investigation of the voltage and time effects on the formation of hydroxyapatite-containing titania prepared by plasma electrolytic oxidation on Ti-6Al-4V alloy and its corrosion behavior, Appl. Surf. Sci. 257 (2011) 7268–7275.

[145] S. Abbasi, M.R. Bayati, F. Golestani-Fard, H.R. Rezaei, H.R. Zargar, F. Samanipour, V. Shoaei-Rad, Micro arc oxidized HAp-TiO_2 nanostructured hybrid layers-part I: effect of voltage and growth time, Appl. Surf. Sci. 257 (2011) 5944–5949.

[147] H.C. Hsu, S.C. Wu, S.K. Hsu, Y.C. Chang, W.F. Ho, Fabrication of nanotube arrays on commercially pure titanium and their apatite-forming ability in a simulated body fluid, Mater. Char. 100 (2015) 170–177.

[148] H.C. Hsu, S.K. Hsu, S.C. Wu, W.F. Ho, Formation of nanotubular structure on low-modulus Ti–7.5Mo alloy surface and its bioactivity evaluation, Thin Solid Films 669 (2019) 329–337.

[155] H. Hirakata, K. Ito, A. Yonezu, H. Tsuchiya, S. Fujimoto, K. Minoshima, Strength of self-organized TiO_2 nanotube arrays, Acta Mater. 58 (2010) 4956–4967.

[157] Y. Liu, B. Zhou, J. Li, X. Gan, J. Bai, W. Cai, Preparation of short, robust and highly ordered TiO_2 nanotube arrays and their applications as electrode, Appl. Catal. B Environ. 92 (2009) 326–332.

[158] R. Narayanan, T.Y. Kwon, K.H. Kim, Anodic TiO_2 from stirred Na_2SO_4/NaF electrolytes: effect of applied voltage and stirring, Mater. Lett. 63 (2009) 2003–2006.
[160] J.B. Chen, C.W. Wang, B.H. Ma, Y. Li, J. Wang, R.S. Guo, W.M. Liu, Field emission from the structure of well-aligned TiO_2/Ti nanotube arrays, Thin Solid Films 517 (2009) 4390–4393.
[161] I. Roman, R.D. Trusca, M.L. Soare, C. Fratila, E. Krasicka-Cydzik, M.S. Stan, A. Dinischiotu, Titanium dioxide nanotube films: preparation, characterization and electrochemical biosensitivity towards alkaline phosphatase, Mater. Sci. Eng. C 37 (2014) 374–382.
[162] F. Nasirpouri, I. Yousefi, E. Moslehifard, J. Khalil-Allafi, Tuning surface morphology and crystallinity of anodic TiO2 nanotubes and their response to biomimetic bone growth for implant applications, Surf. Coating. Technol. 315 (2017) 163–171.
[163] J. Kapusta-Kołodziej, K. Syrek, A. Pawlik, M. Jarosz, O. Tynkevych, G.D. Sulka, Effects of anodizing potential and temperature on the growth of anodic TiO_2 and its photoelectrochemical properties, Appl. Surf. Sci. 396 (2017) 1119–1129.
[164] J.V. Pasikhani, N. Gilani, A.E. Pirbazari, The effect of the anodization voltage on the geometrical characteristics and photocatalytic activity of TiO_2 nanotube arrays, Nano-Struct. Nano-Obj. 8 (2016) 7–14.
[166] B.X. Lei, Q.P. Luo, Z.F. Sun, D. Bin Kuang, C.Y. Su, Fabrication of partially crystalline TiO_2 nanotube arrays using 1, 2-propanediol electrolytes and application in dye-sensitized solar cells, Adv. Powder Technol. 24 (2013) 175–182.
[167] C. Lin, S. Chen, L. Cao, Anodic formation of aligned and bamboo-type TiO_2 nanotubes at constant low voltages, Mater. Sci. Semicond. Process. 16 (2013) 154–159.
[169] M. Michalska-Domańska, P. Nyga, M. Czerwiński, Ethanol-based electrolyte for nanotubular anodic TiO_2 formation, Corrosion Sci. 134 (2018) 99–102.
[170] Z. Su, W. Zhou, Formation, morphology control and applications of anodic TiO_2 nanotube arrays, J. Mater. Chem. 21 (2011) 8955–8970.
[171] D. Quintero, O. Galvis, J.A. Calderón, J.G. Castaño, F. Echeverría, Effect of electrochemical parameters on the formation of anodic films on commercially pure titanium by plasma electrolytic oxidation, Surf. Coating. Technol. 258 (2014) 1223–1231.
[172] G.B. de Souza, G.G. de Lima, N.K. Kuromoto, P. Soares, C.M. Lepienski, C.E. Foerster, A. Mikowski, Tribo-mechanical characterization of rough, porous and bioactive Ti anodic layers, J. Mech. Behav. Biomed. Mater. 4 (2011) 796–806.
[173] C. Yue, R. Kuijer, H.J. Kaper, H.C. van der Mei, H.J. Busscher, Simultaneous interaction of bacteria and tissue cells with photocatalytically activated, anodized titanium surfaces, Biomaterials 35 (2014) 2580–2587.
[174] C.A.H. Laurindo, R.D. Torres, S.A. Mali, J.L. Gilbert, P. Soares, Incorporation of Ca and P on anodized titanium surface: effect of high current density, Mater. Sci. Eng. C 37 (2014) 223–231.
[175] H.Z. Abdullah, P. Koshy, C.C. Sorrell, Anodic oxidation of titanium in mixture of β-glycerophosphate (β-GP) and calcium acetate (CA), Key Eng. Mater. 594–595 (2014) 275–280.
[176] H.R. Wang, F. Liu, Y.P. Zhang, D.Z. Yu, F.P. Wang, Preparation and properties of titanium oxide film on NiTi alloy by micro-arc oxidation, Appl. Surf. Sci. 257 (2011) 5576–5580.
[177] S. Durdu, M. Usta, A.S. Berkem, Bioactive coatings on Ti6Al4V alloy formed by plasma electrolytic oxidation, Surf. Coating. Technol. 301 (2016) 85–93.
[178] B. Li, J. Li, C. Liang, H. Li, L. Guo, S. Liu, H. Wang, Surface roughness and hydrophilicity of titanium after anodic oxidation, Rare Met. Mater. Eng. 45 (2016) 858–862.
[179] Y. Wang, Y. Wu, Y. Qin, G. Xu, X. Hu, J. Cui, H. Zheng, Y. Hong, X. Zhang, Rapid anodic oxidation of highly ordered TiO_2 nanotube arrays, J. Alloys Compd. 509 (2011).
[180] G.A. Crawford, N. Chawla, Porous hierarchical TiO_2 nanostructures: processing and microstructure relationships, Acta Mater. 57 (2009) 854–867.
[181] J. Wan, X. Yan, J. Ding, M. Wang, K. Hu, Self-organized highly ordered TiO_2 nanotubes in organic aqueous system, Mater. Char. 60 (2009) 1534–1540.
[182] S. Durdu, Ö.F. Deniz, I. Kutbay, M. Usta, Characterization and formation of hydroxyapatite on Ti6Al4V coated by plasma electrolytic oxidation, J. Alloys Compd. 551 (2013) 422–429.
[183] L. Wu, C. Wen, G. Zhang, J. Liu, K. Ma, Influence of anodizing time on morphology, structure and tribological properties of composite anodic films on titanium alloy, Vacuum 140 (2017) 176–184.
[184] N. Ohtsu, K. Yokoi, Surface structure and photocatalytic performance of an anodic oxide layer fabricated on titanium in a nitrate/ethylene glycol electrolyte with different treatment durations, Surf. Coating. Technol. 294 (2016) 109–114.
[185] B. Munirathinam, L. Neelakantan, Titania nanotubes from weak organic acid electrolyte: fabrication, characterization and oxide film properties, Mater. Sci. Eng. C 49 (2015) 567–578.
[186] S. Komiya, K. Sakamoto, N. Ohtsu, Structural changes of anodic layer on titanium in sulfate solution as a function of anodization duration in constant current mode, Appl. Surf. Sci. 296 (2014) 163–168.
[187] M. Balakrishnan, R. Narayanan, Synthesis of anodic titania nanotubes in Na_2SO_4/NaF electrolyte: a comparison between anodization time and specimens with biomaterial based approaches, Thin Solid Films 540 (2013) 23–30.
[188] Y. Mizukoshi, N. Ohtsu, N. Masahashi, Structural and characteristic variation of anodic oxide on pure Ti with anodization duration, Appl. Surf. Sci. 283 (2013) 1018–1023.
[189] C.K. Lee, Fabrication, characterization and wear corrosion testing of bioactive hydroxyapatite/nano-TiO_2 composite coatings on anodic Ti-6Al-4V substrate for biomedical applications, Mater. Sci. Eng. B Solid-State Mater. Adv. Technol. 177 (2012) 810–818.
[190] T.C. Lee, M.H.H. Mazlan, M.I. Abbas, H.Z. Abdullah, M.I. Idris, Preparation of bioactive titanium film via anodic oxidation in agitation condition, Mater. Sci. Forum 840 (2016) 220–224.
[191] K. Syrek, J. Kapusta-Kołodziej, M. Jarosz, G.D. Sulka, Effect of electrolyte agitation on anodic titanium dioxide (ATO) growth and its photoelectrochemical properties, Electrochim. Acta 180 (2015) 801–810.
[192] R. Liu, W.D. Yang, L.S. Qiang, J.F. Wu, Fabrication of TiO_2 nanotube arrays by electrochemical anodization in an NH_4F/H_3PO_4 electrolyte, Thin Solid Films 519 (2011) 6459–6466.
[193] X. Huang, Z. Liu, Growth of titanium oxide or titanate nanostructured thin films on Ti substrates by anodic oxidation in alkali solutions, Surf. Coating. Technol. 232 (2013) 224–233.
[194] A.F. Yetim, Investigation of wear behavior of titanium oxide films, produced by anodic oxidation, on commercially pure titanium in vacuum conditions, Surf. Coating. Technol. 205 (2010) 1757–1763.
[195] H.D. Traid, M.L. Vera, A.E. Ares, M.I. Litter, Porous titanium dioxide coatings obtained by anodic oxidation for photocatalytic applications, in: Procedia Mater. Sci., 2015, pp. 619–626.
[196] S.K. Lazarouk, D.A. Sasinovich, O.V. Kupreeva, T.I. Orehovskaia, N. Rochdi, F.A. D'Avitaya, V.E. Borisenko, Effect of the electrolyte temperature on the formation and structure of porous anodic titania film, Thin Solid Films 526 (2012) 41–46.
[197] J. Kapusta-Kołodziej, O. Tynkevych, A. Pawlik, M. Jarosz, J. Mech, G.D. Sulka, Electrochemical growth of porous titanium dioxide in a glycerol-based electrolyte at different temperatures, Electrochim. Acta 144 (2014) 127–135.
[198] H.J. Song, M.K. Kim, G.C. Jung, M.S. Vang, Y.J. Park, The effects of spark anodizing treatment of pure titanium metals and titanium alloys on corrosion characteristics, Surf. Coating. Technol. 201 (2007) 8738–8745.
[199] Y. Mizukoshi, N. Masahashi, Fabrication of a TiO_2 photocatalyst by anodic oxidation of Ti in an acetic acid electrolyte, Surf. Coating. Technol. 240 (2014) 226–232.
[200] N.K. Kuromoto, R.A. Simão, G.A. Soares, Titanium oxide films produced on commercially pure titanium by anodic oxidation with different voltages, Mater. Char. 58 (2007) 114–121.
[201] S.S. Saleh, M.R. Yunus, H.Z. Abdullah, Effect of UV rradiation on apatite deposition on anodised TiO_2 coating formed under mixed acid solution, Int. J. Curr. Res. Sci. Eng. Technol. 1 (2018) 88.
[202] H.Z. Abdullah, C.C. Sorrell, Titanium dioxide (TiO_2) films by anodic oxidation in phosphoric acid, in: Adv. Mater. Res., 2012, pp. 223–228.
[203] K. Das, S. Bose, A. Bandyopadhyay, Surface modifications and cell-materials interactions with anodized Ti, Acta Biomater. 3 (2007) 573–585.
[204] M.V. Diamanti, M. Ormellese, M.P. Pedeferri, Alternating current anodizing of titanium in halogen acids combined with anodic spark deposition: morphological and structural variations, Corrosion Sci. 52 (2010) 1824–1829.
[205] I.M. Hamouda, N.A. El-wassefy, H.A. Marzook, A.N.E. A, G.Y. El-awady, Micro-photographic analysis of titanium anodization to assess bio-activation, Eur. J. Biotechnol. Biosci. 1 (2014) 17–26.
[206] J. Liang, R. Song, Q. Huang, Y. Yang, L. Lin, Y. Zhang, P. Jiang, H. Duan, X. Dong, C. Lin, Electrochemical construction of a bio-inspired micro/nano-textured structure with cell-sized microhole arrays on biomedical titanium to enhance bioactivity, Electrochim. Acta 174 (2015) 1149–1159.
[207] A.I. Kociubczyk, M.L. Vera, C.E. Schvezov, E. Heredia, A.E. Ares, TiO_2 coatings in alkaline electrolytes using anodic oxidation technique, in: Procedia Mater. Sci., 2015, pp. 65–72.
[208] I. Han, J.H. Choi, B.H. Zhao, H.K. Baik, I.S. Lee, Micro-arc oxidation in various concentration of KOH and structural change by different cut off potential, Curr. Appl. Phys. 7 (2007).
[209] S. Lederer, P. Lutz, W. Fürbeth, Surface modification of Ti 13Nb 13Zr by plasma electrolytic oxidation, Surf. Coating. Technol. 335 (2018) 62–71.
[210] W. Simka, R.P. Socha, G. Dercz, J. Michalska, A. Maciej, A. Krzakała, Anodic oxidation of Ti-13Nb-13Zr alloy in silicate solutions, Appl. Surf. Sci. 279 (2013) 317–323.
[211] Y.S. Yu, L.S. Xie, M.H. Chen, N. Wang, H. Wang, Surface characteristics and adhesive strength to epoxy of three different types of titanium alloys anodized in NaTESi electrolyte, Surf. Coating. Technol. 280 (2015) 122–128.
[212] D.R.N. Correa, L.A. Rocha, A.R. Ribeiro, S. Gemini-Piperni, B.S. Archanjo, C.A. Achete, J. Werckmann, C.R.M. Afonso, M. Shimabukuro, H. Doi, Y. Tsutsumi, T. Hanawa, Growth mechanisms of Ca- and P-rich MAO films in Ti-15Zr-xMo alloys for osseointegrative implants, Surf. Coating. Technol. 344 (2018) 373–382.
[213] O. Banakh, T. Journot, P.A. Gay, J. Matthey, C. Csefalvay, O. Kalinichenko, O. Sereda, M. Moussa, S. Durual, L. Snizhko, Synthesis by anodic-spark deposition of Ca- and P-containing films on pure titanium and their biological response, Appl. Surf. Sci. 378 (2016) 207–215.
[214] X. Shi, L.L. Xu, Q.L. Wang, Porous TiO_2 film prepared by micro-arc oxidation and its electrochemical behaviors in Hank's solution, Surf. Coating. Technol. 205 (2010) 1730–1735.
[215] P. Zhang, Z. Zhang, W. Li, M. Zhu, Effect of Ti-OH groups on microstructure and bioactivity of TiO_2 coating prepared by micro-arc oxidation, Appl. Surf. Sci. 268 (2013) 381–386.
[216] T.C. Lee, M.H.A. Rashid, M.A. Selimim, H.Z. Abdullah, M.I. Idris, Precipitation of hydroxyapatite on pure titanium substrate via single step anodic oxidation, in: Key Eng. Mater., 2016, pp. 78–82.

[217] B.G. Lee, J.W. Choi, S.E. Lee, Y.S. Jeong, H.J. Oh, C.S. Chi, Formation behavior of anodic TiO_2 nanotubes in fluoride containing electrolytes, Trans. Nonferrous Met. Soc. China (English Ed.) 19 (2009) 842–845.

[218] H.Y. Chang, W.J. Tzeng, S.Y. Cheng, Modification of TiO_2 nanotube arrays by solution coating, Solid State Ionics 180 (2009) 817–821.

[219] R. Narayanan, T.Y. Kwon, K.H. Kim, TiO_2 nanotubes from stirred glycerol/NH_4F electrolyte: roughness, wetting behavior and adhesion for implant applications, Mater. Chem. Phys. 117 (2009) 460–464.

[220] M. Lai, Z. Jin, Z. Su, Surface modification of TiO_2 nanotubes with osteogenic growth peptide to enhance osteoblast differentiation, Mater. Sci. Eng. C 73 (2017) 490–497.

[221] A.P.R. Alves Claro, R.T. Konatu, A.L. do A. Escada, M.C. de Souza Nunes, C.V. Maurer-Morelli, M.F. Dias-Netipanyj, K.C. Popat, D. Mantovani, Incorporation of silver nanoparticles on Ti7.5Mo alloy surface containing TiO_2 nanotubes arrays for promoting antibacterial coating – in vitro and in vivo study, Appl. Surf. Sci. 455 (2018) 780–788.

[222] H. Sopha, K. Tesar, P. Knotek, A. Jäger, L. Hromadko, J.M. Macak, TiO_2 nanotubes grown on Ti substrates with different microstructure, Mater. Res. Bull. 103 (2018) 197–204.

[223] V.S. Saji, H.C. Choe, Electrochemical corrosion behaviour of nanotubular Ti-13Nb-13Zr alloy in Ringer's solution, Corrosion Sci. 51 (2009) 1658–1663.

[224] V.S. Saji, H.C. Choe, W.A. Brantley, An electrochemical study on self-ordered nanoporous and nanotubular oxide on Ti-35Nb-5Ta-7Zr alloy for biomedical applications, Acta Biomater. 5 (2009) 2303–2310.

[225] K.D. Yun, Y. Yang, H.P. Lim, G.J. Oh, J.T. Koh, I.H. Bae, J. Kim, K.M. Lee, S.W. Park, Effect of nanotubular-micro-roughened titanium surface on cell response in vitro and osseointegration in vivo, Mater. Sci. Eng. C 30 (2010) 27–33.

[226] S. Chen, Q. Chen, M. Gao, S. Yan, R. Jin, X. Zhu, Morphology evolution of TiO_2 nanotubes by a slow anodization in mixed electrolytes, Surf. Coating. Technol. 321 (2017) 257–264.

[227] X.F. Xiao, R.F. Liu, Y.Z. Zheng, Characterization of hydroxyapatite/titania composite coatings codeposited by a hydrothermal-electrochemical method on titanium, Surf. Coating. Technol. 200 (2006) 4406–4413.

[228] N. Ohtsu, D. Ishikawa, S. Komiya, K. Sakamoto, Effect of phosphorous incorporation on crystallinity, morphology, and photocatalytic activity of anodic oxide layer on titanium, Thin Solid Films 556 (2014) 247–252.

[229] H. Habazaki, T. Ogasawara, H. Konno, K. Shimizu, S. Nagata, P. Skeldon, G.E. Thompson, Field crystallization of anodic niobia, Corrosion Sci. 49 (2007) 580–593.

[230] A.C. Alves, F. Wenger, P. Ponthiaux, J.P. Celis, A.M. Pinto, L.A. Rocha, J.C.S. Fernandes, Corrosion mechanisms in titanium oxide-based films produced by anodic treatment, Electrochim. Acta 234 (2017) 16–27.

[231] N. Masahashi, Y. Mizukoshi, S. Semboshi, K. Ohmura, S. Hanada, Photo-induced properties of anodic oxide films on Ti6Al4V, Thin Solid Films 520 (2012) 4956–4964.

[232] I.S. Park, H.J. Oh, T.S. Bae, Bioactivity and generation of anodized nanotubular TiO_2 layer of Ti-6Al-4V alloy in glycerol solution, Thin Solid Films 548 (2013) 292–298.

[233] H. Song, K. Cheng, H. Guo, F. Wang, J. Wang, N. Zhu, M. Bai, X. Wang, Effect of ethylene glycol concentration on the morphology and catalytic properties of TiO_2 nanotubes, Catal. Commun. 97 (2017) 23–26.

[234] D. Regonini, Anodised TiO_2 Nanotubes: Synthesis, Growth Mechanism and thermal Stability, University of Bath, 2008. https://purehost.bath.ac.uk/ws/portalfiles/portal/187919095/D_Regonini_Thesis_Anodised_TiO2_Nanotubes.pdf. (Accessed 8 February 2020).

[235] C.N. Elias, J.H.C. Lima, R. Valiev, M.A. Meyers, Biomedical applications of titanium and its alloys, JOM 60 (2008) 46–49.

[236] S.F. Ou, C.S. Lin, Y.N. Pan, Microstructure and surface characteristics of hydroxyapatite coating on titanium and Ti-30Nb-1Fe-1Hf alloy by anodic oxidation and hydrothermal treatment, Surf. Coating. Technol. 205 (2011) 2899–2906.

[237] C. Jaeggi, P. Kern, J. Michler, T. Zehnder, H. Siegenthaler, Anodic thin films on titanium used as masks for surface micropatterning of biomedical devices, Surf. Coating. Technol. 200 (2005) 1913–1919.

[238] S. Mändl, R. Sader, G. Thorwarth, D. Krause, H.F. Zeilhofer, H.H. Horch, B. Rauschenbach, Biocompatibility of titanium based implants treated with plasma immersion ion implantation, in: Nucl. Instruments Methods Phys. Res. Sect. B Beam Interact. with Mater. Atoms, 2003, pp. 517–521.

[239] Y. Wang, H. Yu, C. Chen, Z. Zhao, Review of the biocompatibility of micro-arc oxidation coated titanium alloys, Mater. Des. 85 (2015) 640–652.

[240] A. Manoj, A.K. Kasar, P.L. Menezes, Tribocorrosion of porous titanium used in biomedical applications, J. Bio- Tribo-Corrosion 5 (2019).

[241] W.F. Cui, L. Jin, L. Zhou, Surface characteristics and electrochemical corrosion behavior of a pre-anodized microarc oxidation coating on titanium alloy, Mater. Sci. Eng. C 33 (2013) 3775–3779.

[242] M. Ormellese, D. Prando, D. Nicolis, F. Bolzoni, M.P. Pedeferri, Chemical oxidation as repairing technique to restore corrosion resistance on damaged anodized titanium, Surf. Coating. Technol. 364 (2019) 225–230.

[243] M. Qadir, Y. Li, K. Munir, C. Wen, Calcium phosphate-based composite coating by micro-arc oxidation (MAO) for biomedical application: a review, Crit. Rev. Solid State Mater. Sci. 43 (2018) 392–416.

[244] A. Lugovskoy, S. Lugovskoy, Production of hydroxyapatite layers on the plasma electrolytically oxidized surface of titanium alloys, Mater. Sci. Eng. C 43 (2014) 527–532.

[245] K. Li, F. Dai, T. Yan, Y. Xue, L. Zhang, Y. Han, Magnetic silicium hydroxyapatite nanorods for enhancing osteoblast response in vitro and biointegration in vivo, ACS Biomater. Sci. Eng. 5 (2019) 2208–2221.

[246] L. Zhang, T. Yan, Y. Xue, Y. Han, Magnetic hydroxyapatite nanotubes on micro-arc oxidized titanium for drug loading, Mater. Res. Express 6 (2019).

[247] K. Ohta, H. Monma, S. Takahashi, Adsorption characteristics of proteins on calcium phosphates using liquid chromatography, J. Biomed. Mater. Res. 55 (2001) 409–414.

[248] J. Zhou, B. Li, Y. Han, L. Zhao, The osteogenic capacity of biomimetic hierarchical micropore/nanorod-patterned Sr-HA coatings with different interrod spacings, Nanomed. Nanotechnol. Biol. Med. 12 (2016) 1161–1173.

[249] Y. Han, J. Zhou, S. Lu, L. Zhang, Enhanced osteoblast functions of narrow interligand spaced Sr-HA nano-fibers/rods grown on microporous titania coatings, RSC Adv. 3 (2013) 11169–11184.

[250] L. Peng, A.D. Mendelsohn, T.J. LaTempa, S. Yoriya, C.A. Grimes, T.A. Desai, Long-Term small molecule and protein elution from TiO_2 nanotubes, Nano Lett. 9 (2009) 1932–1936.

[251] J. Park, S. Bauer, P. Schmuki, K. Von Der Mark, Narrow window in nanoscale dependent activation of endothelial cell growth and differentiation on TiO_2 nanotube surfaces, Nano Lett. 9 (2009) 3157–3164.

[252] K. Ishihara, B. Cheng, Bioinspired functionalization of metal surfaces with polymers, in: Met. Biomed. Devices, Elsevier, 2019, pp. 383–403.

[253] Y. Su, C. Luo, Z. Zhang, H. Hermawan, D. Zhu, J. Huang, Y. Liang, G. Li, L. Ren, Bioinspired surface functionalization of metallic biomaterials, J. Mech. Behav. Biomed. Mater. 77 (2018) 90–105.

[254] H. Chouirfa, H. Bouloussa, V. Migonney, C. Falentin-Daudré, Review of titanium surface modification techniques and coatings for antibacterial applications, Acta Biomater. 83 (2019) 37–54.

[255] S. Spriano, S. Yamaguchi, F. Baino, S. Ferraris, A critical review of multifunctional titanium surfaces: new frontiers for improving osseointegration and host response, avoiding bacteria contamination, Acta Biomater. 79 (2018) 1–22.

[256] D. Martinez-Marquez, K. Gulati, C.P. Carty, R.A. Stewart, S. Ivanovski, Determining the relative importance of titania nanotubes characteristics on bone implant surface performance: a quality by design study with a fuzzy approach, Mater. Sci. Eng. C 114 (2020) 110995.

[257] J.M. Cordeiro, V.A.R. Barão, Is there scientific evidence favoring the substitution of commercially pure titanium with titanium alloys for the manufacture of dental implants? Mater. Sci. Eng. C 71 (2017) 1201–1215.

[258] K. Gulati, S. Ivanovski, Dental implants modified with drug releasing titania nanotubes: therapeutic potential and developmental challenges, Expet Opin. Drug Deliv. 14 (2017) 1009–1024.

[259] M. Szymonowicz, A. Kazek-Kęsik, M. Sowa, B. Żywicka, Z. Rybak, W. Simka, On influence of anodic oxidation on thrombogenicity and bioactivity of the Ti-13Nb-13Zr alloy, Acta Bioeng. Biomech. Orig. Pap. 19 (2017).

[260] M. Klein, Y. Kuhn, E. Woelke, T. Linde, C. Ptock, A. Kopp, T. Bletek, T. Schmitz-Rode, U. Steinseifer, J. Arens, J.C. Clauser, In vitro study on the hemocompatibility of plasma electrolytic oxidation coatings on titanium substrates, Artif. Organs 44 (2020) 419–427.

[261] H.T. Shiu, B. Goss, C. Lutton, R. Crawford, Y. Xiao, Formation of blood clot on biomaterial implants influences bone healing, Tissue Eng. B Rev. 20 (2014) 697–712.

[262] G. Wang, Y. Wan, B. Ren, Z. Liu, Fabrication of an orderly micro/nanostructure on titanium surface and its effect on cell proliferation, Mater. Lett. 212 (2018) 247–250.

[263] G.G. de Lima, A.R. da Luz, B.L. Pereira, E.M. Szesz, G.B. de Souza, C.M. Lepienski, N.K. Kuromoto, M.J.D. Nugent, Tailoring surface properties from nanotubes and anodic layers of titanium for biomedical applications, Appl. Nanocomposite Mater. Orthop. (2019) 179–199.

[264] Y. Sasikumar, K. Indira, N. Rajendran, Surface modification methods for titanium and its alloys and their corrosion behavior in biological environment: a review, J. Bio- Tribo-Corrosion. 5 (2019) 1–25.

[265] Q. Chen, G.A. Thouas, Metallic implant biomaterials, Mater. Sci. Eng. R Rep. 87 (2015) 1–57.

[266] N.H. Faisal, A.K. Prathuru, S. Goel, R. Ahmed, M.G. Droubi, B.D. Beake, Y.Q. Fu, Cyclic nanoindentation and nano-impact fatigue mechanisms of functionally graded TiN/TiNi film, Shape Mem. Superelasticity. 3 (2017) 149–167.

[267] F. Sun, K.N. Sask, J.L. Brash, I. Zhitomirsky, Surface modifications of Nitinol for biomedical applications, Colloids Surf. B Biointerfaces 67 (2008) 132–139.

[268] M. Kaur, K. Singh, Review on titanium and titanium based alloys as biomaterials for orthopaedic applications, Mater. Sci. Eng. C 102 (2019) 844–862.

[269] A. Dehghanghadikolaei, H. Ibrahim, A. Amerinatanzi, M. Hashemi, N.S. Moghaddam, M. Elahinia, Improving corrosion resistance of additively manufactured nickel–titanium biomedical devices by micro-arc oxidation process, J. Mater. Sci. 54 (2019) 7333–7355.

[270] M.H. Wong, F.T. Cheng, H.C. Man, Laser oxidation of NiTi for improving corrosion resistance in Hanks' solution, Mater. Lett. 61 (2007) 3391–3394.

[271] M. Wang, T. Tang, Surface treatment strategies to combat implant-related infection from the beginning, J. Orthop. Transl. 17 (2019) 42–54.

[272] B. Ren, Y. Wan, G. Wang, Z. Liu, Y. Huang, H. Wang, Morphologically modified surface with hierarchical micro-/nano-structures for enhanced bioactivity of titanium implants, J. Mater. Sci. 53 (2018) 12679–12691.

[273] P. Amaravathy, S. Sathyanarayanan, S. Sowndarya, N. Rajendran, Bioactive HA/TiO_2 coating on magnesium alloy for biomedical applications, Ceram. Int. 40 (2014) 6617–6630.

[274] V. Hernández-Montes, C. Betancur-Henao, R. Buitrago-Sierra, J.F. Santa-Marín, Modification of ASTM B107 AZ31B magnesium alloy by co-doped TiO_2 for applications in biomaterials, Surf. Interf. 21 (2020) 100623.
[275] A. Kania, W. Pilarczyk, M.M. Szindler, Structure and corrosion behavior of TiO_2 thin films deposited onto Mg-based alloy using magnetron sputtering and sol-gel, Thin Solid Films 701 (2020) 137945.
[276] J. Yang, J. Wang, J. Guan, Morphology, abrasion and corrosion resistance study of the plasma electrolytic oxidation films formed on pure titanium by adding silane in the electrolyte, Appl. Phys. Mater. Sci. Process 126 (2020) 288.
[277] J. Chen, J. Wang, H. Yuan, Morphology and performances of the anodic oxide films on Ti6Al4V alloy formed in alkaline-silicate electrolyte with aminopropyl silane addition under low potential, Appl. Surf. Sci. 284 (2013) 900–906.
[278] J. Wang, Y. Ma, J. Guan, D. Zhang, Characterizations of anodic oxide films formed on Ti6Al4V in the silicate electrolyte with sodium polyacrylate as an additive, Surf. Coating. Technol. 338 (2018) 14–21.
[279] A. Dey, R. Umarani, H.K. Thota, A. Rajendra, A.K. Sharma, P. Bandyopadhyay, A.K. Mukhopadhyay, Nanoindentation study of MAO coatings developed by dual electrolytes, Surf. Eng. 30 (2014) 905–912.
[280] F. Toptan, A.C. Alves, A.M.P. Pinto, P. Ponthiaux, Tribocorrosion behavior of bio-functionalized highly porous titanium, J. Mech. Behav. Biomed. Mater. 69 (2017) 144–152.
[281] A.C. Alves, F. Oliveira, F. Wenger, P. Ponthiaux, J.P. Celis, L.A. Rocha, Tribocorrosion behaviour of anodic treated titanium surfaces intended for dental implants, J. Phys. D Appl. Phys. 46 (2013).
[282] G.G. de Lima, G.B. de Souza, C.M. Lepienski, N.K. Kuromoto, Mechanical properties of anodic titanium films containing ions of Ca and P submitted to heat and hydrothermal treatment, J. Mech. Behav. Biomed. Mater. 64 (2016) 18–30.
[283] S. Durdu, M. Usta, The tribological properties of bioceramic coatings produced on Ti6Al4V alloy by plasma electrolytic oxidation, Ceram. Int. 40 (2014) 3627–3635.
[284] T. Hanawa, Evaluation techniques of metallic biomaterials in vitro, Sci. Technol. Adv. Mater. 3 (2002) 289–295.
[285] B. Cheraghali, H.M. Ghasemi, M. Abedini, R. Yazdi, A functionalized duplex coating on CP-titanium for biomedical applications, Surf. Coating. Technol. 399 (2020) 126117.
[286] R. Menini, M.-J. Dion, S.K.V. So, M. Gauthier, L.-P. Lefebvre, Surface and corrosion electrochemical characterization of titanium foams for implant applications, J. Electrochem. Soc. 153 (2006) B13.
[287] S.A. Alves, A.L. Rossi, A.R. Ribeiro, F. Toptan, A.M. Pinto, T. Shokuhfar, J.P. Celis, L.A. Rocha, Improved tribocorrosion performance of bio-functionalized TiO2 nanotubes under two-cycle sliding actions in artificial saliva, J. Mech. Behav. Biomed. Mater. 80 (2018) 143–154.
[288] A. Ossowska, S. Sobieszczyk, M. Supernak, A. Zielinski, Morphology and properties of nanotubular oxide layer on the "Ti-13Zr-13Nb" alloy, Surf. Coating. Technol. 258 (2014) 1239–1248.
[289] G. Louarn, L. Salou, A. Hoornaert, P. Layrolle, Nanostructured surface coatings for titanium alloy implants, J. Mater. Res. 34 (2019) 1892–1899.
[290] T. Li, K. Gulati, N. Wang, Z. Zhang, S. Ivanovski, Bridging the gap: optimized fabrication of robust titania nanostructures on complex implant geometries towards clinical translation, J. Colloid Interface Sci. 529 (2018) 452–463.
[291] K. Arkusz, M. Nycz, E. Paradowska, Electrochemical evaluation of the compact and nanotubular oxide layer destruction under ex vivo Ti6Al4V ELI transpedicular screw implantation, Materials 13 (2020) 176.
[292] M. Bartmanski, A. Zielinski, M. Jazdzewska, J. Głodowska, P. Kalka, Effects of electrophoretic deposition times and nanotubular oxide surfaces on properties of the nanohydroxyapatite/nanocopper coating on the Ti13Zr13Nb alloy, Ceram. Int. 45 (2019) 20002–20010.
[293] R.A. Gittens, R. Olivares-Navarrete, Z. Schwartz, B.D. Boyan, Implant osseointegration and the role of microroughness and nanostructures: lessons for spine implants, Acta Biomater. 10 (2014) 3363–3371.
[294] R. Ji, H. Wang, B. Wang, H. Jin, Y. Liu, W. Cheng, B. Cai, X. Li, Removing loose oxide layer and producing dense α-phase layer simultaneously to improve corrosion resistance of Ti-6Al-4V titanium alloy by coupling electrical pulse and ultrasonic treatment, Surf. Coating. Technol. 384 (2020).
[295] M. Zhao, J. Li, Y. Li, J. Wang, Y. Zuo, J. Jiang, H. Wang, Gradient control of the adhesive force between Ti/TiO_2 nanotubular arrays fabricated by anodization, Sci. Rep. 4 (2014) 1–7.
[296] R.V. Chernozem, M.A. Surmeneva, V.P. Ignatov, O.O. Peltek, A.A. Goncharenko, A.R. Muslimov, A.S. Timin, A.I. Tyurin, Y.F. Ivanov, C.R. Grandini, R.A. Surmenev, Comprehensive characterization of titania nanotubes fabricated on Ti-Nb alloys: surface topography, structure, physicomechanical behavior, and a cell culture assay, ACS Biomater. Sci. Eng. 6 (2020) 1487–1499.
[297] A.R. Luz, L.S. Santos, C.M. Lepienski, P.B. Kuroda, N.K. Kuromoto, Characterization of the morphology, structure and wettability of phase dependent lamellar and nanotube oxides on anodized Ti-10Nb alloy, Appl. Surf. Sci. 448 (2018) 30–40.
[298] I. Çaha, A.C. Alves, C. Chirico, A.M.P. Pinto, S. Tsipas, E. Gordo, F. Toptan, A promising method to develop TiO_2-based nanotubular surfaces on Ti-40Nb alloy with enhanced adhesion and improved tribocorrosion resistance, Appl. Surf. Sci. 542 (2021) 148658.
[299] B.D. Ratner, S.J. Bryant, Biomaterials: where we have been and where we are going, Annu. Rev. Biomed. Eng. 6 (2004) 41–75.
[300] M.J. Olszta, X. Cheng, S.S. Jee, R. Kumar, Y.Y. Kim, M.J. Kaufman, E.P. Douglas, L.B. Gower, Bone structure and formation: a new perspective, Mater. Sci. Eng. R Rep. 58 (2007) 77–116.
[301] A. Bruinink, M. Bitar, M. Pleskova, P. Wick, H.F. Krug, K. Maniura-Weber, Addition of nano scaled bioinspired surface features: a revolution for bone related implants and scaffolds? J. Biomed. Mater. Res. 102 (2014) 275–294.
[302] M. Nazir, O.P. Ting, T.S. Yee, S. Pushparajan, D. Swaminathan, M.G. Kutty, Biomimetic coating of modified titanium surfaces with hydroxyapatite using simulated body fluid, Ann. Mater. Sci. Eng. 2015 (2015) 8.
[303] L.C. Campanelli, L.T. Duarte, P.S.C.P. da Silva, C. Bolfarini, Fatigue behavior of modified surface of Ti-6Al-7Nb and CP-Ti by micro-arc oxidation, Mater. Des. 64 (2014) 393–399.
[304] Y. Yan, Tribology and tribocorrosion testing and analysis of metallic biomaterials, in: Met. Biomed. Devices, Elsevier, 2019, pp. 213–234.
[305] E.M. Szesz, G.B. de Souza, G.G. de Lima, B.A. da Silva, N.K. Kuromoto, C.M. Lepienski, Improved tribo-mechanical behavior of CaP-containing TiO_2 layers produced on titanium by shot blasting and micro-arc oxidation, J. Mater. Sci. Mater. Med. 25 (2014) 2265–2275.
[306] N. Karimi, M. Kharaziha, K. Raeissi, Electrophoretic deposition of chitosan reinforced graphene oxide-hydroxyapatite on the anodized titanium to improve biological and electrochemical characteristics, Mater. Sci. Eng. C 98 (2019) 140–152.
[307] Z. Chen, X. Ren, L. Ren, T. Wang, X. Qi, Y. Yang, Improving the tribological properties of spark-anodized titanium by magnetron sputtered diamond-like carbon, Coatings 8 (2018) 83.
[308] E.M. Lotz, D.J. Cohen, Z. Schwartz, B.D. Boyan, Titanium implant surface properties enhance osseointegration in ovariectomy induced osteoporotic rats without pharmacologic intervention, Clin. Oral Implants Res. 31 (2020) 374–387.
[309] S.A. Gehrke, J. Aramburú Júnior, L. Pérez-Díaz, T.L.E. Treichel, B.A. Dedavid, P.N. De Aza, J.C. Prados-Frutos, New implant macrogeometry to improve and accelerate the osseointegration: an in vivo experimental study, Appl. Sci. 9 (2019) 3181.
[310] Y.A. Yi, Y.B. Park, H. Choi, K.W. Lee, S.J. Kim, K.M. Kim, S. Oh, J.S. Shim, The evaluation of osseointegration of dental implant surface with different size of TiO_2 nanotube in rats, J. Nanomater. 2015 (2015) 11.
[311] P. Zhou, F. Mao, F. He, Y. Han, H. Li, J. Chen, S. Wei, Screening the optimal hierarchical micro/nano pattern design for the neck and body surface of titanium implants, Colloids Surf. B Biointerfaces 178 (2019) 515–524.
[312] S. Dundar, F. Yaman, A. Bozoglan, T.T. Yildirim, M. Kirtay, M.F. Ozupek, G. Artas, Comparison of osseointegration of five different surfaced titanium implants, J. Craniofac. Surg. 29 (2018) 1991–1995.
[313] K. Kuroda, M. Okido, New approach for controlling osteoconductivity of valve metals based on TiO_2 coatings on Ti substrates, Mater. Technol. 30 (2015) B13–B20.
[314] N.A. Costa, A.L. Rossi, A.C. Alves, A.M.P. Pinto, F. Toptan, L.A. Rocha, Growth mechanisms and tribocorrosion behavior of bio-functionalized ZrO_2 nanoparticles-containing MAO coatings formed on Ti-40Nb alloy, J. Bio- Tribo-Corrosion. 7 (2021) 53.
[315] M.F. Kunrath, R. Hübler, A bone preservation protocol that enables evaluation of osseointegration of implants with micro- and nanotextured surfaces, Biotech. Histochem. 94 (2019) 261–270.
[316] W. He, X. Yin, L. Xie, Z. Liu, J. Li, S. Zou, J. Chen, Enhancing osseointegration of titanium implants through large-grit sandblasting combined with micro-arc oxidation surface modification, J. Mater. Sci. Mater. Med. 30 (2019) 73.
[317] M. Kaseem, H.-C. Choe, Acceleration of bone formation and adhesion ability on dental implant surface via plasma electrolytic oxidation in a solution containing bone ions, Metals 11 (2021) 106.
[318] D.J. Van Vuuren, R.F. Laubscher, Surface friction behaviour of anodized commercially pure titanium screw assemblies, in: Procedia CIRP, Elsevier B.V., 2016, pp. 251–254.
[319] C.A.H. Laurindo, L.M. Bemben, R.D. Torres, S.A. Mali, J.L. Gilbert, P. Soares, Influence of the annealing treatment on the tribocorrosion properties of Ca and P containing TiO_2 produced by plasma electrolytic oxidation, Mater. Technol. 31 (2016) 719–725.
[320] J. Luo, B. Li, S. Ajami, S. Ma, F. Zhou, C. Liu, Growth of TiO_2 nanotube on titanium substrate to enhance its biotribological performance and biocorrosion resistance, J. Bionic Eng. 16 (2019) 1039–1051.
[321] Y.L. Ma, D.B. Burr, R.G. Erben, Bone histomorphometry in rodents, in: Princ. Bone Biol., Elsevier, 2019, pp. 1899–1922.
[322] A. Bandyopadhyay, A. Shivaram, S. Tarafder, H. Sahasrabudhe, D. Banerjee, S. Bose, In vivo response of laser processed porous titanium implants for load-bearing implants, Ann. Biomed. Eng. 45 (2017) 249–260.
[323] S. Bose, D. Banerjee, A. Shivaram, S. Tarafder, A. Bandyopadhyay, W.M. Keck, Calcium phosphate coated 3D printed porous titanium with nanoscale surface modification for orthopedic and dental applications HHS public access, Mater. Des. 151 (2018) 102–112.
[324] S.C. Sartoretto, J. Calasans-Maia, R. Resende, E. Câmara, B. Ghiraldini, F.J. Barbosa Bezerra, J.M. Granjeiro, M.D. Calasans-Maia, The influence of nanostructured hydroxyapatite surface in the early stages of osseointegration: a multiparameter animal study in low-density bone, Int. J. Nanomed. 15 (2020) 8803–8817.
[325] M.C.R. Alves-Rezende, L.C. Capalbo, J.P.J. De Oliveira Limírio, B.C. Capalbo, P.H.J.O. Limírio, J.L. Rosa, The role of TiO_2 nanotube surface on osseointegration of titanium implants: biomechanical and histological study in rats, Microsc. Res. Tech. 83 (2020) 817–823.
[326] M. Dard, Performance studies for dental implants: methodological approach, in: Biocompat. Perform. Med. Devices, Elsevier, 2019, pp. 339–370.
[327] Y. Okazaki, Selection of metals for biomedical devices, in: Met. Biomed. Devices, Elsevier, 2019, pp. 31–94.

[328] M. Fazel, H.R. Salimijazi, M.A. Golozar, M.R. Garsivaz Jazi, A comparison of corrosion, tribocorrosion and electrochemical impedance properties of pure Ti and Ti6Al4V alloy treated by micro-arc oxidation process, Appl. Surf. Sci. 324 (2015) 751–756.
[329] E. Santos, G.B. de Souza, F.C. Serbena, H.L. Santos, G.G. de Lima, E.M. Szesz, C.M. Lepienski, N.K. Kuromoto, Effect of anodizing time on the mechanical properties of porous titania coatings formed by micro-arc oxidation, Surf. Coating. Technol. 309 (2017) 203–211.
[330] M. Doulache, M. Trari, A. Benchettara, The oxidation of titanium thin films in phosphoric medium, Protect. Met. Phys. Chem. Surface 50 (2014) 200–208.
[331] X. ling Shi, Q. liang Wang, F. shun Wang, S. rong Ge, Effects of electrolytic concentration on properties of micro-arc film on Ti6Al4V alloy, Min. Sci. Technol. 19 (2009) 220–224.
[332] S.M. Leal-Marin, H.A. Estupiñán-Duran, EIS, Mott Schottky and EFM analysis of the electrochemical stability and dielectric properties of Ca-P-Ag and Ca-P-Si-Ag coatings obtained by plasma electrolytic oxidation in Ti6Al4V, Rev. Fac. Ing. 2017 (2017) 9–19.
[333] N.A. Al-Mobarak, A.M. Al-Mayouf, A.A. Al-Swayih, The effect of hydrogen peroxide on the electrochemical behavior of Ti and some of its alloys for dental applications, Mater. Chem. Phys. 99 (2006) 333–340.
[334] S.A. Alves, A.L. Rossi, A.R. Ribeiro, J. Werckmann, J.P. Celis, L.A. Rocha, T. Shokuhfar, A first insight on the bio-functionalization mechanisms of TiO_2 nanotubes with calcium, phosphorous and zinc by reverse polarization anodization, Surf. Coating. Technol. 324 (2017) 153–166.
[335] D. Cai, D. Zhang, X. Chen, H. Wu, M. Wang, G. Sang, Y. Li, Influences of pH values' changes on the oxide film of U-0.79 wt.% Ti alloy in aqueous solution—a combined study of traditional electrochemical tests and scanning reference electrode technique, Coatings 9 (2019) 224.
[336] A.M. Schmidt, D.S. Azambuja, E.M.A. Martini, Semiconductive properties of titanium anodic oxide films in McIlvaine buffer solution, Corrosion Sci. 48 (2006) 2901–2912.
[337] S. Guan, M. Qi, Y. Li, W. Wang, Morphology evolution of the porous coatings on Ti–xAl alloys by Al adding into Ti during micro-arc oxidation in $Na_2B_4O_7$ electrolyte, Surf. Coating. Technol. 395 (2020) 125948.
[338] J. Wang, Y. Pan, R. Feng, H. Cui, B. Gong, L. Zhang, Z. Gao, X. Cui, H. Zhang, Z. Jia, Effect of electrolyte composition on the microstructure and bio-corrosion behavior of micro-arc oxidized coatings on biomedical Ti6Al4V alloy, J. Mater. Res. Technol. 9 (2020) 1477–1490.
[339] C. Bural, C. Dayan, O. Geçkili, Initial stability measurements of implants using a new magnetic resonance frequency analyzer with titanium transducers: an ex vivo study, J. Oral Implantol. 46 (2020) 35–40.
[340] J. Karlsson, N. Harmankaya, S. Allard, A. Palmquist, M. Halvarsson, P. Tengvall, M. Andersson, Ex vivo alendronate localization at the mesoporous titania implant/bone interface, J. Mater. Sci. Mater. Med. 26 (2015) 1–8.
[341] S.A. Lone, M. Muck, P. Fosodeder, C.C. Mardare, C. Florian, A. Weth, J. Krüger, C. Steinwender, W. Baumgartner, J. Bonse, J. Heitz, A.W. Hassel, Impact of femtosecond laser treatment accompanied with anodization of titanium alloy on fibroblast cell growth, Phys. Status Solidi 217 (2020) 1900838.
[342] M. Pettersson, J. Pettersson, M. Molin Thorén, A. Johansson, Release of titanium after insertion of dental implants with different surface characteristics – an *ex vivo* animal study, Acta Biomater. Odontol. Scand. 3 (2017) 63–73.
[343] Y. Tashiro, S. Komasa, A. Miyake, H. Nishizaki, J. Okazaki, Analysis of titania nanosheet adsorption behavior using a quartz crystal microbalance sensor, Ann. Mater. Sci. Eng. 2018 (2018).
[344] A. Miyake, S. Komasa, Y. Hashimoto, Y. Komasa, J. Okazaki, Adsorption of saliva related protein on denture materials: an x-ray photoelectron spectroscopy and quartz crystal microbalance study, Ann. Mater. Sci. Eng. 2016 (2016).
[345] T. Matsumoto, Y. Tashiro, S. Komasa, A. Miyake, Y. Komasa, J. Okazaki, Effects of surface modification on adsorption behavior of cell and protein on titanium surface by using quartz crystal microbalance system, Materials (Basel) 14 (2021) 1–16.
[346] T. Micläuş, V. Valla, A. Koukoura, A.A. Nielsen, B. Dahlerup, G.I. Tsianos, E. Vassiliadis, Impact of design on medical device safety, Ther. Innov. Regul. Sci. 54 (2020) 839–849.
[347] D.B. Kramer, Y.T. Tan, C. Sato, A.S. Kesselheim, Ensuring medical device effectiveness and safety: a cross-national comparison of approaches to regulation, Food Drug Law J. 69 (2014) 1, pmc/articles/PMC4091615. (Accessed 28 February 2021).
[348] Consumer Reports, Dangerous medical implants and devices - consumer reports, Consum. Rep. (2012). https://www.consumerreports.org/cro/magazine/2012/04/cr-investigates-dangerous-medical-devices/index.htm. (Accessed 28 February 2021).
[349] A. Ravidà, R. Siqueira, I. Saleh, M.H.A. Saleh, A. Giannobile, H.L. Wang, Lack of clinical benefit of implantoplasty to improve implant survival rate, J. Dent. Res. 99 (2020) 1348–1355.
[350] N. Penha, S. Groisman, J. Ng, O.D. Gonçalves, M.F. Kunrath, Physical-chemical analyses of contaminations and internal holes in dental implants of pure commercial titanium, J. Osseointegr. 10 (2018) 57–63.
[351] W. Khan, E. Muntimadugu, M. Jaffe, A.J. Domb, Implantable medical devices, in: Focal Control. Drug Deliv. Adv. Deliv. Sci. Technol., Springer, Boston, MA, 2014, pp. 33–59.
[352] H.Z. Abdullah, A.R. Boccaccini, Microporous organic-inorganic nanocomposite coatings on stainless steel via electrophoretic deposition for biomedical applications, ECS Trans. 82 (2018) 25–31.
[353] M.O. Bodunrin, L.H. Chown, J.A. Omotoyinbo, Development of low-cost titanium alloys: a chronicle of challenges and opportunities, Mater. Today Proc. 38 (2020) 564–569.
[354] A. Santos-Coquillat, R. Gonzalez Tenorio, M. Mohedano, E. Martinez-Campos, R. Arrabal, E. Matykina, Tailoring of antibacterial and osteogenic properties of Ti6Al4V by plasma electrolytic oxidation, Appl. Surf. Sci. 454 (2018) 157–172.
[355] A. Bartkowiak, A. Zarzycki, S. Kac, M. Perzanowski, M. Marszalek, Mechanical properties of different nanopatterned TiO_2 substrates and their effect on hydrothermally synthesized bioactive hydroxyapatite coatings, Materials 13 (2020) 5290.
[356] M. Jarosz, J. Kapusta-Kołodziej, M. Jaskuła, G.D. Sulka, Effect of different polishing methods on anodic titanium dioxide formation, J. Nanomater. 2015 (2015) 1–10.
[357] N. Soro, N. Saintier, H. Attar, M.S. Dargusch, Surface and morphological modification of selectively laser melted titanium lattices using a chemical post treatment, Surf. Coating. Technol. 393 (2020) 125794.
[358] B.E. Pippenger, M. Rottmar, B.S. Kopf, S. Stübinger, F.H. Dalla Torre, S. Berner, K. Maniura-Weber, Surface modification of ultrafine-grained titanium: influence on mechanical properties, cytocompatibility, and osseointegration potential, Clin. Oral Implants Res. 30 (2019) 99–110.
[359] A.R. Boccaccini, S. Keim, R. Ma, Y. Li, I. Zhitomirsky, Electrophoretic deposition of biomaterials, J. R. Soc. Interface 7 (2010).
[360] L. Benea, J.P. Celis, Reactivity of porous titanium oxide film and chitosan layer electrochemically formed on Ti-6Al-4V alloy in biological solution, Surf. Coating. Technol. 354 (2018) 145–152.